



<https://theses.gla.ac.uk/>

Theses Digitisation:

<https://www.gla.ac.uk/myglasgow/research/enlighten/theses/digitisation/>

This is a digitised version of the original print thesis.

Copyright and moral rights for this work are retained by the author

A copy can be downloaded for personal non-commercial research or study, without prior permission or charge

This work cannot be reproduced or quoted extensively from without first obtaining permission in writing from the author

The content must not be changed in any way or sold commercially in any format or medium without the formal permission of the author

When referring to this work, full bibliographic details including the author, title, awarding institution and date of the thesis must be given

Enlighten: Theses

<https://theses.gla.ac.uk/>  
[research-enlighten@glasgow.ac.uk](mailto:research-enlighten@glasgow.ac.uk)

**CHARACTERISATION OF GLUCOSE TRANSPORT IN RAT AORTIC  
VASCULAR SMOOTH MUSCLE CELLS**

A thesis submitted to the  
FACULTY OF SCIENCE  
For the degree of  
DOCTOR OF PHILOSOPHY

BY

**Jill Margaret Wakefield**

Division of Biochemistry & Molecular Biology  
Institute of Biomedical and Life Sciences  
University of Glasgow  
December 1999

ProQuest Number: 10391328

All rights reserved

INFORMATION TO ALL USERS

The quality of this reproduction is dependent upon the quality of the copy submitted.

In the unlikely event that the author did not send a complete manuscript and there are missing pages, these will be noted. Also, if material had to be removed, a note will indicate the deletion.



ProQuest 10391328

Published by ProQuest LLC (2017). Copyright of the Dissertation is held by the Author.

All rights reserved.

This work is protected against unauthorized copying under Title 17, United States Code  
Microform Edition © ProQuest LLC.

ProQuest LLC.  
789 East Eisenhower Parkway  
P.O. Box 1346  
Ann Arbor, MI 48106 – 1346

GLASGOW  
UNIVERSITY  
LIBRARY

11824 (copy 2)

## ABSTRACT

Cardiovascular disease is the principal cause of death in the Western world.

Atherosclerosis is a major contributor to the progression of cardiovascular disease.

Increased proliferation of vascular smooth muscle cells plays an important role in the development of atherosclerotic plaques and, as increased glucose transport is an early response common to all mitogens, it is reasonable to presume that increased proliferation of VSMCs in atherosclerotic plaques is accompanied by an increase in glucose transport in these cells. To date, however, very little is known about the regulation of glucose transport in VSMCs. The work presented in this thesis examines the regulation of glucose transport in VSMCs.

Firstly the glucose transporters expressed in VSMCs were studied. It was determined that in VSMC freshly isolated from aorta GLUT-4 was present, however, as the cells were passaged in culture GLUT-4 was lost and GLUT-3 levels increased. GLUT-1 was present in both freshly isolated VSMCs and in cells that had been passaged in cell culture. The effects of PDGF, a growth factor believed to play an important role in mediating increased VSMC proliferation in atherosclerotic plaque development, on glucose transport was examined. PDGF could stimulate a 2- to 5-fold increase in glucose transport in cultured VSMCs, and this was dependent on both MAP kinase (p38 and p42/44) and PI3' kinase activity, as determined by the use of specific inhibitors of these kinases.

Both cAMP and cGMP are known to be important regulators of VSMC function and as such the ability of cyclic nucleotides to regulate glucose transport was studied. Analogues of cAMP were capable of stimulating a 2-fold increase in glucose transport, and like PDGF-stimulated transport it was dependent on PI3' kinase and p38 MAP kinase activity, however there was no role for p42/44 MAP kinase. Agonists that stimulated adenylyl cyclase activity in VSMCs were unable to stimulate an increase in glucose transport, but inhibitors of PDE 3 activity did stimulate a two-fold increase in glucose transport in

VSMCs. The cGMP analogue (8-Br cGMP) had no effect on basal glucose transport rates, but was inhibitory with regard to PDGF-stimulated glucose transport.

Finally, the mechanisms by which glucose transport is increased in response to mitogens were studied. To determine if translocation of GLUT-1 may be responsible for increased glucose transport, chimeras of GLUT-1 and green fluorescent protein were made to allow the movement of GLUT-1 within the cell to be followed. As well as translocation of GLUTs it is possible that altered GLUT activity, perhaps mediated by phosphorylation of the transporters, may be responsible for increased glucose transport. To address this possibility the phosphorylation state of both GLUT-1 and GLUT-3 from VSMCs was investigated under different conditions. The results from this work indicated that phosphorylation of the GLUTs is unlikely to be responsible for increased glucose transport in VSMCs.

## **Acknowledgements**

I would like to thank the Medical Research Council for funding my research along with the Division of Biochemistry and Molecular Biology for providing me with the facilities to complete my project.

I would also like to thank my supervisors, Professors Gwyn Gould and Graeme Milligan, and all of the members of my lab C36.

Finally, special thanks go to all my friends and family for their continuing support and encouragement.

## TABLE OF CONTENTS

<b>CHAPTER 1</b>	<b>INTRODUCTION</b>	<b>1</b>
<b>1.1</b>	<b>GENERAL INTRODUCTION</b>	<b>2</b>
1.1.1	PATHOPHYSIOLOGY OF ATHEROSCLEROSIS	2
1.1.2	REGULATION OF VASCULAR SMOOTH MUSCLE CELLS IN PLAQUE FORMATION	4
<b>1.2</b>	<b>REGULATION OF GLUCOSE UPTAKE</b>	<b>6</b>
1.2.1	THE FACILITATIVE GLUCOSE TRANSPORTER FAMILY (GLUTS)	6
1.2.2	STRUCTURE AND MEMBRANE TOPOLOGY OF THE GLUTs	8
1.2.3	SIGNALLING PATHWAYS MEDIATING GLUCOSE TRANSPORT	9
1.2.3.1	Growth factor-mediated glucose transport	9
1.2.3.2	Insulin-stimulated glucose transport	15
1.2.3.3	Cyclic nucleotide regulation of glucose transport	17
1.2.4	GLUCOSE TRANSPORT IN VASCULAR SMOOTH MUSCLE CELLS	18
<b>1.3</b>	<b>CYCLIC 3'5'-ADENOSINE MONOPHOSPHATE</b>	<b>19</b>
1.3.1	GENERATION OF cAMP	20
1.3.2	DEGRADATION OF cAMP	21
1.3.3	cAMP SIGNALLING	22
<b>1.4</b>	<b>CYCLIC GUANOSINE 3'5'-MONOPHOSPHATE</b>	<b>24</b>
1.4.1	GUANYL CYCLASE	24
1.4.2	DEGRADATION OF cGMP	26
1.4.3	SIGNALLING VIA cGMP	26
<b>1.5</b>	<b>CYCLIC NUCLEOTIDE SIGNALLING IN VSMC</b>	<b>28</b>
<b>1.6</b>	<b>AIMS OF THE STUDY</b>	<b>29</b>



<b>CHAPTER 2</b>	<b>MATERIALS AND METHODS</b>	<b>38</b>
<b>2.1</b>	<b>MATERIALS</b>	<b>39</b>
2.1.1	GENERAL REAGENTS	39
2.1.2	ANTIBODIES	41
2.1.3	CELLS	41
2.1.4	CELL CULTURE MEDIA AND REAGENTS	41
2.1.5	CELL CULTURE PLASTICS	42
2.1.6	RADIOACTIVE REAGENTS	42
2.1.7	AGONISTS AND INHIBITORS	43
2.1.8	MOLECULAR BIOLOGY REAGENTS	44
2.1.9	PROTEIN A	45
2.1.10	TRANSFERRIN TEXAS RED	45
<b>2.2</b>	<b>BUFFERS AND MEDIA</b>	<b>45</b>
2.2.1	CELL CULTURE MEDIA	45
2.2.2	GENERAL BUFFERS	46
2.2.3	SDS-PAGE BUFFERS	46
2.2.4	WESTERN BLOT BUFFERS	47
2.2.5	MOLECULAR BIOLOGY BUFFERS	47
<b>2.3</b>	<b>RAT AORTIC VASCULAR SMOOTH MUSCLE CELL CULTURE</b>	<b>48</b>
2.3.1	PREPARATION AND GROWTH OF VASCULAR SMOOTH MUSCLE CELLS FROM RAT AORTA	48
2.3.2	TRYPSINATION OF VSMC	49
2.3.3	STORAGE OF RAT AORTIC VSMC IN LIQUID NITROGEN	50
2.3.4	RESURRECTION OF FROZEN CELL STOCKS FROM LIQUID NITROGEN	50
<b>2.4</b>	<b>3T3-L1 FIBROBLAST CULTURE</b>	<b>50</b>
2.4.1	GROWTH OF 3T3-L1 FIBROBLASTS	50
2.4.2	TRYPSINATION OF 3T3-L1 FIBROBLASTS	50
2.4.3	STORAGE OF 3T3-L1 FIBROBLASTS IN LIQUID NITROGEN	51
2.4.4	RESURRECTION OF FROZEN CELL STOCKS FROM LIQUID NITROGEN	51
<b>2.5</b>	<b>2-DEOXY-D-GLUCOSE UPTAKE IN RAT AORTIC VSMC</b>	<b>51</b>

<b>2.6</b>	<b>3-<i>O</i>-METHYL GLUCOSE TRANSPORT IN VSMC</b>	<b>52</b>
<b>2.7</b>	<b>SDS/POLYACRYLAMIDE GEL ELECTROPHORESIS</b>	<b>52</b>
<b>2.8</b>	<b>WESTERN BLOTTING OF PROTEINS</b>	<b>53</b>
2.8.1	DETECTION OF PROTEINS ON NITROCELLULOSE WITH PONCEAU S	53
2.8.2	IMMUNODETECTION OF PROTEINS ON NITROCELLULOSE MEMBRANES	54
<b>2.9</b>	<b>PREPARATION OF WHOLE CELL LYSATES</b>	<b>54</b>
<b>2.10</b>	<b>PREPARATION OF TOTAL CELL MEMBRANES</b>	<b>55</b>
<b>2.11</b>	<b>THYMIDINE INCORPORATION</b>	<b>55</b>
<b>2.12</b>	<b>IMMUNOPRECIPITATION OF GLUTs FROM VSMC</b>	<b>56</b>
<b>2.12</b>	<b>IN VITRO PHOSPHORYLATION OF GLUTs WITH PKA</b>	<b>56</b>
<b>2.14</b>	<b>IN VIVO PHOSPHORYLATION OF GLUTs</b>	<b>57</b>
<b>2.15</b>	<b><math>\beta</math>2 BINDING ASSAYS</b>	<b>58</b>
<b>2.16</b>	<b>ADENYL CYCLASE ASSAY IN VSMC</b>	<b>58</b>
<b>2.17</b>	<b>MOLECULAR BIOLOGY METHODS</b>	<b>59</b>
2.17.1	PCR REACTIONS	59
2.17.2	AGAROSE GEL ELECTROPHORESIS OF DNA	60
2.17.3	PREPARATION OF COMPETENT BACTERIA	60
2.17.4	TRANSFORMATION OF COMPETENT BACTERIA	60
2.17.5	PREPARATION OF DNA	60
2.17.6	GEL EXTRACTION OF DNA	61
2.17.7	RESTRICTION OF DNA	61
2.17.8	LIGATION OF DNA	62
2.17.9	PHENOL/CHLOROFORM EXTRACTION OF DNA	62
2.17.10	ETHANOL PRECIPITATION OF DNA	62
2.17.11	SEQUENCING OF DNA	62

2.17.12 RT-PCR	63
2.18 CONFOCAL MICROSCOPY	64
CHAPTER 3 CHARACTERISATION OF GLUCOSE TRANSPORT IN RAT AORTIC VASCULAR SMOOTH MUSCLE CELLS IN RESPONSE TO PLATELET-DERIVED GROWTH FACTOR	65
3.1 AIMS	66
3.2 INTRODUCTION	67
3.3 RESULTS	69
3.3.1 ANALYSIS OF GLUCOSE TRANSPORTER EXPRESSION IN RAT AORTIC VASCULAR SMOOTH MUSCLE CELLS	69
3.3.2 CHARACTERISATION OF PDGF-BB-STIMULATED GLUCOSE TRANSPORT IN RAT AORTIC VASCULAR SMOOTH MUSCLE CELLS	70
3.3.3 CELL SIGNALLING PATHWAYS INVOLVED IN MEDIATING PDGF-BB-STIMULATED GLUCOSE TRANSPORT IN RAT AORTIC VASCULAR SMOOTH MUSCLE CELLS.	72
3.4 DISCUSSION	75
3.4.1 GLUCOSE TRANSPORTER CONTENT OF RAT AORTIC VASCULAR SMOOTH MUSCLE CELLS	75
3.4.2 PDGF-BB-STIMULATED GLUCOSE TRANSPORT IN	77
3.4.3 CHARACTERISATION OF SIGNALLING MECHANISMS INVOLVED IN MEDIATING PDGF-BB-STIMULATED GLUCOSE TRANSPORT IN VSMC	79
3.5 SUMMARY	81
CHAPTER 4 THE ROLE OF CYCLIC NUCLEOTIDES IN REGULATING GLUCOSE TRANSPORT IN RAT AORTIC VASCULAR SMOOTH MUSCLE CELLS	95
4.1 AIMS	96
4.2 INTRODUCTION	97

<b>4.3</b>	<b>RESULTS</b>	<b>100</b>
4.3.1	EFFECTS OF CAMP ANALOGUES ON BASAL AND PDGF-STIMULATED GLUCOSE TRANSPORT	100
4.3.2	CELL SIGNALLING MECHANISMS REGULATING CAMP-STIMULATED GLUCOSE TRANSPORT IN VSMCs	101
4.3.3	ENDOGENOUS MECHANISMS OF INCREASING [CAMP] AND RATES OF GLUCOSE TRANSPORT IN VSMC	104
4.3.4	EFFECTS OF cGMP ON BASAL AND PDGF-STIMULATED GLUCOSE TRANSPORT IN VSMCs	105
<b>4.4</b>	<b>DISCUSSION</b>	<b>107</b>
4.4.1	EFFECTS OF CAMP ON BASAL AND PDGF-STIMULATED GLUCOSE TRANSPORT	107
4.4.2	CELL SIGNALLING MECHANISMS INVOLVED IN MEDIATING CAMP- STIMULATED GLUCOSE TRANSPORT	109
4.4.3	ENDOGENOUS MECHANISMS FOR GENERATING CAMP AND STIMULATING GLUCOSE TRANSPORT	111
4.4.4	EFFECT OF cGMP ON BASAL AND PDGF-STIMULATED GLUCOSE TRANSPORT IN VSMCs	112
<b>4.5</b>	<b>SUMMARY</b>	<b>114</b>
<b>CHAPTER 5</b>	<b>INVESTIGATION OF THE MECHANISMS LEADING TO INCREASED GLUCOSE TRANSPORT IN RAT AORTIC VASCULAR SMOOTH MUSCLE CELLS</b>	<b>136</b>
<b>5.1</b>	<b>AIMS</b>	<b>137</b>
<b>5.2</b>	<b>INTRODUCTION</b>	<b>138</b>
<b>5.3</b>	<b>RESULTS</b>	<b>140</b>
5.3.1	GENERATION OF GLUT-1/GFP CHIMERAS	140
5.3.2	STIMULATION OF MOVEMENT OF GLUT-1/GFP WITH PDGF IN 3T3-L1 FIBROBLASTS	141

5.3.3	ANALYSIS OF PHOSPHORYLATION STATE OF GLUT-1 AND GLUT-3 IN VSMCs	142
5.4	DISCUSSION	144
5.4.1	GENERATION OF GLUT-1/GFP CHIMERAS	144
5.4.2	STIMULATION OF MOVEMENT OF GLUT-1/GFP WITH PDGF IN 3T3-L1 FIBROBLASTS	145
5.4.3	ANALYSIS OF PHOSPHORYLATION STATE OF GLUT-1 AND GLUT-3 IN VSMCs	146
5.5	SUMMARY	148
CHAPTER 6	DISCUSSION	158
REFERENCES		163

## **TABLE OF FIGURES**

### **CHAPTER 1 INTRODUCTION**

1.1	AN OVERVIEW OF ATHEROSCLEROTIC PLAQUE DEVELOPMENT	34
1.2	THE TWELVE MEMBRANE SPANNING DOMAIN MODEL OF THE GLUTs	35
1.3	A PROPOSED SCHEME OF CELLULAR SIGNALLING PATHWAYS INVOLVED IN GROWTH FACTOR CONTROL OF GLUCOSE TRANSPORT	36
1.4	THE SIGNAL TRANSDUCTION MECHANISMS ACTIVATED BY TYROSINE KINASE RECEPTORS AND G-PROTEIN-COUPLED GROWTH FACTOR RECEPTORS	37

### **CHAPTER 3 CHARACTERISATION OF GLUCOSE TRANSPORT IN RAT AORTIC VASCULAR SMOOTH MUSCLE CELLS**

3.1	ANALYSIS OF GLUCOSE TRANSPORTERS IN CULTURED VSMCs	83
3.2	ANALYSIS OF GLUCOSE TRANSPORTERS IN FRESH AORTIC VSMCs	84
3.3	TIME-COURSE OF 2-DEOXYGLUCOSE TRANSPORT IN VSMCs IN RESPONSE TO PDGF-BB	85
3.4	2-DEOXYGLUCOSE TRANSPORT IN VSMCs IN RESPONSE TO PDGF-BB IN THE PRESENCE OR ABSENCE OF CYCLOHEXIMIDE	86
3.5	DOSE-RESPONSE CURVE OF 2-DEOXYGLUCOSE TRANSPORT IN VSMCs IN RESPONSE TO PDGF-BB	87
3.6	3-O-METHYL GLUCOSE TRANSPORT IN VSMCs IN RESPONSE TO PDGF-BB	88
3.7	[ <sup>3</sup> H] THYMIDINE INCORPORATION IN VSMCs IN RESPONSE TO PDGF-BB	89
3.8	ANALYSIS OF PI3 <sup>γ</sup> KINASE ISOFORMS IN VSMCs	90
3.9	EFFECTS OF PI3 <sup>γ</sup> KINASE INHIBITORS ON PDGF-STIMULATED 2-DEOXYGLUCOSE TRANSPORT	91
3.10	EFFECTS OF PDGF-BB ON THE PHOSPHORYLATION/ACTIVATION OF MAP KINASES	92
3.11	EFFECTS OF INHIBITORS OF MAP KINASES, p38 AND p42/44, ON PDGF-STIMULATED 2-DEOXYGLUCOSE TRANSPORT	93
3.12	ANALYSIS OF THE SPECIFICITY OF THE MAP KINASE INHIBITORS SB 203580 AND PD 98059	94

# **CHAPTER 4 THE ROLE OF CYCLIC NUCLEOTIDES IN REGULATING GLUCOSE TRANSPORT IN RAT AORTIC VASCULAR SMOOTH MUSCLE CELLS**

4.1	2-DEOXYGLUCOSE TRANSPORT IN VSMCs IN RESPONSE TO 8-Br cAMP WITH OR WITHOUT PDGF-BB	117
4.2	EFFECT OF cAMP ANALOGUES ON 2-DEOXYGLUCOSE TRANSPORT IN VSMCs	118
4.3	TIME-COURSE OF 2-DEOXYGLUCOSE TRANSPORT IN VSMCs IN RESPONSE TO 8-Br cAMP	119
4.4	3-O-METHYL GLUCOSE TRANSPORT IN VSMCs IN RESPONSE TO 8-Br cAMP	120
4.5	[ <sup>3</sup> H] THYMIDINE INCORPORATION IN VSMCs IN RESPONSE TO 8-Br cAMP	121
4.6	EFFECT OF PKA INHIBITOR, H89, ON 8-Br cAMP-STIMULATED 2- DEOXYGLUCOSE TRANSPORT	122
4.7	RT-PCR ANALYSIS OF ADENYLYL CYCLASE ISOFORMS EXPRESSED IN VSMCs	123
4.8	EFFECT OF H89 ON BASAL AND PDGF-BB-STIMULATED 2-DEOXYGLUCOSE TRANSPORT	124
4.9	EFFECT OF WORTMANNIN ON 8-Br cAMP-STIMULATED 2-DEOXYGLUCOSE TRANSPORT	125
4.10	EFFECTS OF 8-Br cAMP ON THE ACTIVATION/PHOSPHORYLATION OF MAP KINASES	126
4.11	EFFECTS OF SB 203580 ON BASAL AND 8-Br cAMP STIMULATED 2- DEOXYGLUCOSE TRANSPORT	127
4.12	EFFECT OF H89 ON 8-Br cAMP-STIMULATED p38 PHOSPHORYLATION/ACTIVATION	128
4.13	ISOPRENALINE-STIMULATED cAMP GENERATION AND 2-DEOXYGLUCOSE TRANSPORT IN VSMCs	129
4.14	ILOPROST-STIMULATED cAMP GENERATION AND 2-DEOXYGLUCOSE TRANSPORT IN VSMCs	130
4.15	EFFECT OF PDE 3 INHIBITOR MILRINONE, ON 2-DEOXYGLUCOSE TRANSPORT IN VSMCs	131
4.16	EFFECTS OF THE PDE INHIBITORS, ZAPRINAST AND Ro-20-1724, ON 2- DEOXYGLUCOSE TRANSPORT IN VSMCs	132
4.17	EFFECTS OF 8-Br cGMP ON BASAL AND PDGF-BB-STIMULATED 2- DEOXYGLUCOSE TRANSPORT	133

4.18	EFFECTS OF ANF AND SNP ON PDGF-BB-STIMULATED 2-DEOXYGLUCOSE TRANSPORT IN VSMCS	134
4.19	EFFECT OF ANF ON PDGF-STIMULATED MAP KINASE, p38, p42/44, PHOSPHORYLATION/ACTIVATION	135

## CHAPTER 5 INVESTIGATION OF THE MECHANISMS LEADING TO INCREASED GLUCOSE TRANSPORT IN RAT AORTIC VASCULAR SMOOTH MUSCLE CELLS

5.1	PCR BASED METHOD USED TO SYNTHESIZE GLUT-/GFP CHIMERAS	149
5.2	OPTIMISING TRANSIENT TRANSFECTION METHOD FOR EXPRESSION OF GLUT-1/GFP CHIMERAS	150
5.3	COMPARISON OF DISTRIBUTION OF N- AND C-TERMINAL TAGGED GLUT-1/GFP CHIMERAS	151
5.4	COLOCALISATION OF C-TERMINAL GLUT-1/GFP WITH TRANSFERRIN TEXAS RED	152
5.5	TRANSLOCATION OF N-TERMINAL GLUT-1/GFP IN RESPONSE TO PDGF-BB	153
5.6	IMMUNOPRECIPITATION OF GLUTs 1 AND 3 FROM VSMCS	154
5.7	IN VITRO PHOSPHORYLATION OF GLUTs 1 AND 3 WITH PKA	155
5.8	IN VITRO PHOSPHORYLATION OF GLUTs 1 AND 3 WITH PKA AFTER DEPHOSPHORYLATION WITH PP2A	156
5.9	IN VIVO PHOSPHORYLATION OF GLUTs 1 AND 3 IN VSMCS IN RESPONSE TO PDGF AND 8-Br CAMP	157

## TABLES

TABLE 1.1	MAJOR SITES OF EXPRESSION OF THE DIFFERENT GLUCOSE TRANSPORTERS IN HUMAN AND RODENT TISSUES	31
TABLE 1.2	REGULATION OF ADENYLYL CYCLASE ISOFORMS	32
TABLE 1.3	PROPERTIES OF PDE FAMILIES	33
TABLE 4.1	PRODUCTS AND PRIMERS FOR RT-PCR ANALYSIS OF ADENYLYL CYCLASE ISOFORMS	116



## ABBREVIATIONS

AC	Adenylyl cyclase
AKAP	A protein (PKA) anchoring protein
ANF	Atrial natriuretic peptide
ATP	Adenosine triphosphate
bFGF	Basic fibroblast growth factor
BSA	Bovine serum albumin
c-AKT	see PKB
cAMP	Cyclic 3'5'-adenosine monophosphate
8-Br cAMP	8-Bromo cyclic 3'5'-adenosine monophosphate
cDNA	Complimentary deoxyribonucleic acid
cGMP	Cyclic 3'5'-guanosine monophosphate
8-Br cGMP	8-Bromo cyclic 3'5'-guanosine monophosphate
DAG	sn 1,2-diacyl glycerol
DHA	1-[propyl-2,3- <sup>3</sup> H]dihydroalprenolol
DMEM	Dulbecco's modified Eagle's medium
EGF	epidermal growth factor
FCS	Foetal calf serum
FGF	Fibroblast growth factor
GC	Guanylyl cyclase
GEFs	Guanine nucleotide exchange factors
GFP	Green fluorescent protein
GLUTs	Glucose transporters
G-protein	Guanine nucleotide binding protein
Grb 2	Growth factor residue binding protein 2
GTP	Guanosine triphosphate
HRP	Horseradish peroxidase
IBMX	3 isobutyl-1-methylxanthine

IGF-1	Insulin-like growth factor-1
IL-1	Interleukin-1
IP <sub>3</sub>	Inositol triphosphate
IRS	Insulin receptor substrates
JNK	c Jun NH-2 terminal kinase
KRP	Kreb's Ringer phosphate buffer
MAP kinase	Mitogen activated protein kinase
MAPKAP	MAP kinase activated protein kinase
mRNA	messenger ribonucleic acid
NCS	Newborn calf serum
NO	Nitric oxide
PBS	Phosphate buffered saline
PCR	Polymerase chain reaction
PDE	Cyclic nucleotide phosphodiesterase
PDGF	Platelet-derived growth factor
PGE <sub>1</sub>	Prostaglandin E <sub>1</sub>
PGI	Prostaglandin I
PH	pleckstrin homology domain
PI3' kinase	Phosphatidyl inositol 3' kinase
PI(4,5)P <sub>2</sub>	Phosphatidyl inositol (4,5) bisphosphate
PI(1,4,5)P <sub>3</sub>	Phosphatidyl inositol (1,4,5) trisphosphate
PKA	cAMP activated protein kinase
PKB	protein kinase B
PKG	cGMP activated protein kinase
PLC	Phospholipase C
PP2A	Protein phosphatase 2A
Ras GAP	Ras GTPase activating protien
RT-PCR	Reverse transcription polymerase chain reaction
SH2	<i>src</i> homology domain 2
SNP	Sodium nitroprusside

SOS	Son of sevenless
TBS-T	Tris buffered saline-tween
TE	Tris EDTA buffer
TEMED	N,N,N',N'-tetramethylethylenediamine
TGF $\beta$	Transforming growth factor $\beta$
TNF $\alpha$	Tumour necrosis factor $\alpha$
VSMC	Rat aortic vascular smooth muscle cells

## **CHAPTER 1**

### **INTRODUCTION**

## **1.1 GENERAL INTRODUCTION**

Cardiovascular disease is the principal cause of death in the USA, Europe and much of Asia. Atherosclerosis is an inflammatory disease of the vasculature and is a major contributor to the progression of cardiovascular disease (Ross, 1999, Ross, 1993). It can lead to myocardial and cerebral infarction, which can result in heart attack, stroke, gangrene and loss of function of the extremities. The process of atherosclerosis is, in normal circumstances, a protective response to the insults that the endothelium and smooth muscle cells of the artery are exposed to. Several factors can be important in atherosclerotic plaque development, including increased serum cholesterol, which is considered to be the most important factor in the development of atherosclerotic lesions. Hypertension appears to accelerate plaque formation, and patients with diabetes mellitus are more likely to develop severe lesions (Ross, 1999). Vascular smooth muscle cell (VSMC) proliferation and migration is fundamental to the development of atherosclerotic plaques. Since growing cells have an increased energy requirement, one of the early events which follows re-entry into the cell cycle is the stimulation of glucose uptake, an effect which is common to all mitogens. In the work described below, the mechanisms involved in regulating glucose uptake in vascular smooth muscle cells were investigated.

### **1.1.1 PATHOPHYSIOLOGY OF ATHEROSCLEROSIS**

The lesions of atherosclerosis occur principally in the large and medium-sized elastic and muscular arteries. Atherosclerotic plaques are likely to be present throughout a person's lifetime, and the earliest form of lesion, the so-called fatty streak, is common in infants and young children (Napoli *et al.*, 1997). The fatty streak is a pure inflammatory lesion and consists of an aggregation of lipid-rich macrophages and VSMCs, known as foam cells, and T lymphocytes within the inner-most layer of the artery wall, the intima (Stary *et al.*, 1994). In people with hypercholesterolaemia, the influx of these cells into the intima is preceded by the extracellular deposition of amorphous and membranous lipids. The development of the fatty streak precedes the formation of intermediate lesions which are composed of layers of macrophages and

smooth muscle cells, which in turn develop into the more advanced, complex, occlusive lesions called fibrous plaques. The fibrous plaques increase in size, and by projecting into the lumen of the artery may impede blood flow. Lesions consist of a fibrous cap of connective tissue, beneath which there is a cell-rich layer consisting of lipid loaded smooth muscle cells, macrophages and activated T-cells. The cell-rich region usually overlays a core of lipid and necrotic debris, containing cholesterol crystals and insoluble calcium salt. Most sudden deaths from myocardial infarcts are due to the rupturing or fissures in the plaque resulting in haemorrhage, thrombosis and occlusion of the artery (Ross, 1993, Ross, 1999).

A number of observations gave rise to the “response to injury” hypothesis for the formation of plaques, which initially proposed the denudation of the endothelium as the first step in atherosclerosis (Ross & Glomset 1973, Ross & Glomset 1976). The most recent version of this hypothesis is that endothelial dysfunction rather than denudation is the initiating factor for progression of atherosclerosis (Ross, 1993, Ross, 1999). The endothelial dysfunction that occurs in response to the injury leads to compensatory responses that alter the normal homeostatic properties of the endothelium. The formation of fibrous lesions in response to injury is in itself not remarkable; wound healing, for example follows such a course. But the response to arterial injury differs from that of injury to most other organs in that the sources of injury (hypercholesterolaemia, hypertension, cigarette smoking, diabetes, obesity etc.) are likely to be chronic, so that progression of fatty streak to fibrous plaque is unlikely to be interrupted.

An overview of plaque development is shown in Figure 1.1. The injury to the endothelium increases its adhesiveness with regard to leukocytes or platelets, as well as its permeability. The injury also induces the endothelium to have procoagulant instead of anticoagulant properties and to produce and secrete vasoactive molecules, cytokines and growth factors (Rocsnick *et al.*, 1993, Lin *et al.*, 1997, Nakashima *et al.*, 1998). If the inflammatory response does not immediately remove or neutralise the offending agent then the response can continue indefinitely. The monocytes and T-lymphocytes migrate between the endothelial cells under the influence of growth factors and chemoattractants released by the altered endothelium, activated platelets

and adherent leukocytes. The major chemoattractant is lipoprotein that has been oxidised by the endothelium, smooth muscle cells or early-arriving monocytes or macrophages (Quinn *et al.*, 1987). Migrating cells reach further beneath the arterial surface, where the monocytes become macrophages, accumulate lipids and become foam cells and, together with the accompanying lymphocytes, form a fatty streak. If the inflammatory response continues there is stimulation of proliferation and migration of vascular smooth muscle to form an intermediate lesion. If these responses continue unabated, they can thicken the artery wall, resulting in a compensatory dilation of the blood vessel to maintain a constant lumen volume. Continued inflammation results in increased numbers of macrophages and lymphocytes, which both migrate from the blood stream and multiply within the lesion. Activation of these cells leads to the release of hydrolytic enzymes, cytokines, chemokines and growth factors, which can induce further damage and eventually lead to focal necrosis. Thus, cycles of accumulation of mononuclear cells, migration and proliferation of smooth muscle cells, and formation of fibrous tissue lead to further enlargement and restructuring of the lesion, so that it becomes covered by a fibrous cap that overlies a necrotic core. At some point the artery can no longer compensate by dilation and the lesion may alter blood flow (see Ross 1993, Ross 1999 for reviews).

### **1.1.2 REGULATION OF VASCULAR SMOOTH MUSCLE CELLS IN PLAQUE FORMATION**

Any concept of atherogenesis must account for the stimulation of vascular smooth muscle cell proliferation, which is fundamental to the development of the plaque. Vascular smooth muscle cells are subject to regulation by a huge number of growth factors, cytokines and small molecules (such as nitric oxide, NO) in normal blood vessels as well as in atherosclerotic lesions. It is the alteration in equilibrium between factors secreted from the endothelium and smooth muscle cells that is probably crucial to migration and hyperproliferation of VSMCs. Some of the most important growth factors and cytokines, in terms of VSMC proliferation are platelet derived growth factor (PDGF), basic fibroblast growth factor (bFGF), insulin-like growth factor 1 (IGF-1), interleukin-1 (IL-1), tumour necrosis factor  $\alpha$  (TNF $\alpha$ ) and transforming

growth factor  $\beta$  (TGF $\beta$ ) (Bobik & Campbell, 1993). All of these can induce VSMC proliferation and are up regulated in the lesions of atherosclerosis. Many of the growth factors that contribute to these often dramatic changes in artery vessel wall structure are vessel wall derived. Activated platelets adhering to the endothelium will release their granules and the growth factors contained within. The adherent macrophages and T-lymphocytes will secrete growth factors and cytokines such as IL-1, TNF $\alpha$  and TGF $\beta$ . The dysfunctional endothelial cells in lesions secrete growth factors and small signalling molecules such as NO. Other important growth factors are produced from the VSMC themselves and act in an autocrine manner (see Ross, 1993 and Bobik & Campbell, 1993 for reviews).

It is unlikely that any of these growth factors work alone in the process of atherogenesis. Through a network of cellular interactions, the release of one factor will stimulate the expression of a second factor in a target cell that can then stimulate cells in a paracrine or autocrine manner. One example of this is the secretion of cytokines and growth factors by macrophages. Activated macrophages in the lesions will secrete PDGF, which can act directly on the VSMC. As well as PDGF secretion, they release IL-1, TNF $\alpha$  and TGF $\beta$ . These cytokines can act on both endothelial cells and VSMC to induce production of PDGF, which can further stimulate the proliferation of VSMCs. Interestingly, when there are high levels of IL-1, TNF $\alpha$  and TGF $\beta$  an inhibition of the proliferative effect of the secreted PDGF occurs, by downregulating the PDGF receptor (Battegay *et al.*, 1990).

There may be great diversity in the smooth muscle cells in the lesions of atherosclerosis, as smooth muscle cells are derived from individual organ parenchyma during embryogenesis, whereas the endothelium appears to be derived from the embryonic vasculature that invades the organ (Schwartz *et al.*, 1990). Therefore the smooth muscle cells in different arteries have different origins. As well as differences in VSMC in different arteries there also appears to be heterogeneity of VSMCs within a single area of the vessel (Benzakour *et al.*, 1996). Different sub-populations of VSMCs may give rise to smooth muscle cells that can respond very differently to the same stimuli.



VSMCs are also able to display at least two phenotypes, contractile and synthetic (Mosse *et al.*, 1985, Campbell and Campbell 1985). These phenotypes can be differentiated based on the distribution of myosin filaments and the amounts of secretory protein apparatus, such as rough endoplasmic reticulum and Golgi (Chamley-Campbell *et al.*, 1979, Gonzales-Crussi 1971). It is likely that these phenotypes are the extremes of a spectrum of phenotypes that may coexist in the vessel wall. When the cells are in the contractile phenotype they respond to agents that induce either vasoconstriction or vasodilation. In contrast, in the synthetic state the cells are capable of expressing genes for a number of growth regulatory molecules and cytokines (Libby *et al.*, 1988, Slöjund *et al.*, 1988). Several observations have suggested that smooth muscle cells in lesions are of the synthetic phenotype and are therefore more susceptible to proliferative stimuli than contractile VSMCs.

## **1.2 REGULATION OF GLUCOSE UPTAKE**

Increased glucose transport is an early response to growth factors in all cells (Thomson & Gould, 1997). Despite the importance of smooth muscle cell proliferation in the development of atherosclerotic plaques, little is known about the mechanism and regulation of glucose transport in VSMCs.

### **1.2.1 THE FACILITATIVE GLUCOSE TRANSPORTER FAMILY (GLUTS)**

A summary of the tissue distribution of the facilitative glucose transporters is shown in Table 1.1.

The transport of glucose across the plasma membrane and into the cytosol is arguably the most important function a cell performs, as D-glucose is required for cellular growth, homeostasis, and metabolism. The existence of a protein moiety responsible for glucose transport was first demonstrated by Jung, 1971, who showed that the transport capacity of erythrocytes was retained by erythrocyte ghosts but not by erythrocyte lipids alone. In 1982 Lienhard and his colleagues purified and partially sequenced the first member of the family, now known as the facilitative glucose

transporters or GLUTs (Baldwin *et al.*, 1982). These transporters allow the movement of glucose across the plasma membrane down its concentration gradient, either into or out of the cell. Furthermore, this family of proteins are specific for the D-enantiomer of glucose and are not coupled to any energy-requiring components, such as ATP hydrolysis or a  $H^+$  gradient. GLUT-1 was purified from erythrocytes and antibodies were raised against the polypeptide. Using the partial sequence obtained from the purified protein a cDNA clone was isolated in 1985 (Meukler *et al.*, 1985) and subsequently the isolation of the gene coding for GLUT-1 (Fukomoto *et al.*, 1988). GLUT-1 protein and mRNA is present in many tissues and cells. In humans GLUT-1 is expressed at highest levels in brain and erythrocytes, but is also enriched in tissues of the blood-tissue barriers, such as the blood-brain barrier and the placenta (Gould & Holman, 1993). GLUT-1 is located on the plasma membrane and in the recycling endosomes. It is widely regarded as the "house-keeping" glucose transporter (Flier *et al.*, 1987).

Subsequent to the isolation of the GLUT-1 cDNA, more members of the glucose transporter family were isolated by screening of cDNA libraries of several tissues with the GLUT-1 cDNA under low stringency conditions. Using this method, a cDNA encoding GLUT-2 was isolated from hepatocytes (Fukomoto *et al.*, 1988; Thorens *et al.*, 1988). Analysis of the properties of this transporter revealed that it is a high-capacity, high  $K_m$  transporter for glucose. These properties are ideally suited to allow the liver to function as one of the key tissues involved in glucose homeostasis; the high  $K_m$  and transport capacity endows GLUT-2 with properties enabling the rapid influx of glucose into the liver after eating, and rapid efflux of glucose from the liver following gluconeogenesis and glycogenolysis.

GLUT-3 was identified by Nagamatsu *et al.*, 1992, and was found to be the prominent isoform expressed in brain and neural tissue. GLUT-3 is expressed in human foetal muscle, but Northern blot analysis of the adult skeletal muscle revealed no trace of GLUT-3 mRNA. High levels of GLUT-3 mRNA are present in a range of other adult tissues such as the placenta, liver, heart and kidney. The mRNA for GLUT-3 has been found at high levels in these tissues, but the sites of protein expression are more

restricted, indicating that perhaps GLUT-3 may undergo negative post-translational regulation (Gould & Holman, 1993).

The GLUT-4 isoform is the insulin-responsive glucose transporter. Adipose and skeletal muscle are unique with respect to glucose transport, in that they exhibit acute insulin-stimulated increases in transport, up to 30-fold (fat) and 10-fold (muscle) (Gould, 1997). These tissues have a large pool of the GLUT-4 glucose transporter sequestered inside the cells which is not normally available for glucose transport. Upon exposure of the cells to insulin the GLUT-4 is rapidly translocated to the cell surface (Cushman *et al.*, 1980; Suzuki & Kono, 1980). This means that the cells have a low resting rate of glucose transport, but are able to achieve a rapid and large increase in glucose transport in response to insulin.

cDNA library screening also identified GLUT-5, the major facilitative glucose transporter of the small intestine (Kayano *et al.*, 1988). GLUT-5 is localised to the apical brush border on the luminal side of the absorptive epithelial cells (Davidson *et al.*, 1992). This transporter has a high affinity for fructose and a low affinity for glucose, therefore it seems reasonable to assume that it plays a major role in the uptake of dietary fructose (Burant *et al.*, 1992). GLUT-5 is also found in several other human tissues, including muscle, brain, adipose tissue, kidney and testis (Shepherd *et al.*, 1992).

In 1990 Kayano *et al.* identified a further transporter-like transcript by homology screening. This transcript has a ubiquitous tissue distribution and is 79.6% identical to GLUT-3. However, sequence analysis of the cDNA revealed that it contained several stop codons and frame shifts, and is therefore unlikely to encode a functional glucose transporter and most likely a pseudogene.

### **1.2.2 STRUCTURE AND MEMBRANE TOPOLOGY OF THE GLUTs**

After cloning of the GLUTs analysis of the predicted amino acid sequences revealed a high degree of homology between the mammalian glucose transporters and those of other species including bacteria, yeast, algae and protozoa (Walmsley *et al.*, 1998,

Barrett *et al.*, 1999). This degree of similarity probably relates to a common mechanism of transport catalysis, a common type of substrate and is suggestive of a common evolution from a single gene. The common features revealed by sequence alignment and analysis of the transporters include 12 predicted amphipathic helices arranged so that both the N- and C-termini are at the cytoplasmic surface (Gould, 1997). Also predicted are large loops between helices 1 and 2 and between helices 6 and 7 (Figure 1.2). The loop between helices 6 and 7 divides the structure into two halves, usually referred to as the N-terminal domain and the C-terminal domain. The loops between the remainder of the helices are very short and the length of these loops is a conserved feature of the entire family. The short loops place severe constraints on the possible tertiary structure of the protein, and suggest very close packing of the helices at the inner surface of the membrane, in each half of the protein. The length and sequence identity of the loops at the extracellular surface of these proteins is very varied but is generally longer than the loops on the cytoplasmic surface. This may potentially result in a less compact helical packing at the external surface. The general features of this model including the membrane-spanning topology have been confirmed by extensive experimental analysis using a range of approaches (Barrett *et al.*, 1999).

### **1.2.3 SIGNALLING PATHWAYS MEDIATING GLUCOSE TRANSPORT**

#### **1.2.3.1 Growth factor-mediated glucose transport**

Exposure of quiescent cells to mitogens results in the stimulation of numerous intracellular signalling cascades, culminating in cell growth and division several hours later. Due to the increased energy requirements of growing cells, one of the early responses of cells common to all mitogens is an increase in the rate of glucose uptake. GLUT-1 is thought to be the glucose transporter responsible for growth factor-stimulated increases in glucose transport (Thomson & Gould, 1997).

Time-courses of growth-factor induced glucose transport reveal a biphasic pattern, consisting of an acute phase response occurring within minutes and a chronic phase after about 4-12 hours. The acute phase of transport is thought to occur by a

movement of GLUT-1 from the recycling endosomal system to the plasma membrane, therefore increasing the number of functional transporters at the plasma-membrane, and also possibly via an increase in the intrinsic activity of the transporters (Gould & Holman, 1993, Czech *et al.*, 1992). However the molecular mechanisms underlying these effects are poorly understood.

The chronic effect of mitogens on glucose transport is inhibited by cycloheximide, suggesting that it is dependent on new protein synthesis. Several studies have shown that GLUT-1 mRNA is increased during the late phase of growth-factor stimulated uptake (Kitagawa *et al.*, 1989, Rollins *et al.*, 1988, Hiraki *et al.*, 1988).

Different classes of growth factors exist which work at structurally distinct receptors and mediate intracellular signals via distinct mechanisms. There are two classes of mitogen receptor, the protein tyrosine kinase receptors, which transduce their signals via intrinsic tyrosine kinase activities in their cytoplasmic domain, and the seven-transmembrane domain receptor family, which transduce their signals by coupling with heterotrimeric G-proteins. Despite their distinct receptors and the differences in the initial signal transduction mechanisms, activation of both receptor types leads to a similar biphasic profile of glucose transport, suggesting that the signal transduction pathways activated by these distinct classes of receptor converge (Thomson & Gould, 1997).

#### *Receptor tyrosine kinase signalling*

Receptor tyrosine kinase signalling is probably the best understood mechanism of growth factor signal transduction. Following growth-factor binding to receptor, the receptors undergo a conformational change, which activates the intrinsic tyrosine kinase activity of the receptor, resulting in autophosphorylation of the specific tyrosine residues within the cytoplasmic domain of the receptor and receptor dimerisation (Fantl *et al.*, 1993). These specific phosphotyrosine residues can act as “docking sites” for intracellular signalling proteins. The phosphotyrosine residues are contained within specific amino acid sequences, which result in highly selective binding sites for SH2 domains (Pawson & Gish, 1995). Many proteins contain such

SH2 domains and are able to bind the phosphotyrosines on active receptors, including PI3-K, PLC  $\gamma$ , Ras GTPase activating protein (Ras GAP), growth factor residue binding protein-2 (Grb-2), SHPTP-2 (the phosphotyrosine phosphatase) and the *Src* family of non-receptor tyrosine kinases. Upon binding to the receptors these signalling proteins are thought to undergo tyrosine phosphorylation, and those with a catalytic domain are subsequently activated, thus propagating the signal. Not all proteins that bind to the receptors have catalytic activity, but instead act as adaptor proteins which couple the activated receptor to intracellular signalling molecules i.e. Grb 2 (Egan *et al.*, 1993). It should be noted that the insulin receptor and IGF-1 receptor, both tyrosine kinases receptors, transduce their signals via a distinct mechanism, utilising the adaptor proteins, insulin receptor substrate (IRS-1, 2, 3), described below.

#### *G-protein coupled receptor signalling*

G-protein coupled receptors transduce their signals by activating heterotrimeric G-proteins. Heterotrimeric G-proteins consist of  $\alpha$ ,  $\beta$  and  $\gamma$  subunits. When an agonist binds to receptor it results in the exchange of GTP for GDP on the  $\alpha$  subunit of the G-protein. This causes the  $\alpha$  subunit to separate from the  $\beta\gamma$  subunits. Both the GTP-bound  $\alpha$  subunit and the  $\beta\gamma$  dimer are important activators for a number of signalling molecules (for review see Milligan, 1993, Sternweis, 1994). It is clear that G-protein coupled receptors can stimulate many of the same intracellular signalling molecules that the protein tyrosine kinase receptors activate. It is probable, therefore, that stimulation of glucose transport by protein tyrosine kinase receptors and G-protein coupled receptors utilise common signal transduction pathways (see Figure 1.3 for overview).

#### *Phospholipid hydrolysis and PKC*

Both receptor tyrosine kinases and G-protein  $\beta\gamma$  subunits can stimulate phospholipase C (PLC) activity (Rönstrand *et al.*, 1992, Milligan, 1993, Sternweis, 1994). This results in the hydrolysis of PI(4,5)P<sub>2</sub> to Ins(1,4,5)P<sub>3</sub> and diacylglycerol (DAG). Ins(1,4,5)P<sub>3</sub> can mobilise Ca<sup>2+</sup> from intracellular pools and DAG can stimulate the

protein kinase C (PKC) family of serine/threonine kinases. Both  $\text{Ca}^{2+}$  and PKC have been implicated in a number of physiological functions and as such a role for these in glucose transport has been sought.

It has been shown that purified PKC can phosphorylate GLUT-1 *in vitro* (Witters *et al.*, 1985), but as yet there has been no demonstration of a functional consequence of this event. Pharmacological activators of PKC, such as phorbol esters, have been shown to stimulate glucose uptake in Swiss 3T3 fibroblasts (Farese *et al.*, 1986, Kitagawa *et al.*, 1986), further implying a role for PKC in glucose transport. However, although PLC, DAG and PKC can all stimulate glucose transport, subsequent studies have all but ruled out a role for PKC in glucose transport in response to many mitogens. For example down-regulation of PKC by prolonged incubation with phorbol esters has no effect on PDGF or IGF-1 stimulated glucose transport in fibroblasts (Merrall *et al.*, 1993). In addition, IGF-1 and PDGF do not stimulate PKC activity in fibroblasts, but can stimulate glucose transport (Merrall *et al.*, 1993).

Recently it has been shown that  $[\text{Ca}^{2+}]$  may be important with regard to glucose transport. Quinn *et al.*, 1998, have shown that angiotensin II stimulated glucose transport in rat aortic VSMC is dependant on the levels of extracellular  $[\text{Ca}^{2+}]$ . When the cells were incubated in growth media without calcium, angiotensin failed to stimulate glucose transport, as compared to cells grown in media with normal calcium levels. It was also shown that the inhibitors of calmodulin, W-7 and calmidazolium could inhibit angiotensin II stimulation of glucose transport in these cells. These results point to a role for calcium in regulating glucose transport.

#### *Mitogen Activated Protein Kinase*

A wide variety of growth factors stimulate the mitogen activated protein kinase (MAPK) family, an event that is believed to play a major role in the transduction of mitogenic signals into intracellular responses. Both tyrosine kinase receptors and GPCR stimulate the activation of p42/44 MAP kinase via a similar mechanism, by the activation of a sequential phosphorylation cascade (see Figure 1.3). The MAP kinase family consists of the p42/44 MAPK, p38 MAPK and JNK (reviews Canos *et al.*,

1995, Davis, 1994). This family of proteins are stimulated by distinct but parallel phosphorylation cascades in response to mitogens, stress and cytokines respectively (Canos *et al.*, 1995).

There is now good evidence supporting a role for MAPK involvement in mitogen-stimulated glucose transport. By using specific inhibitors of p42/44 MAPK (PD 98059) it is possible to inhibit IGF-1 stimulated glucose uptake in KB cells (Gould *et al.*, 1995). Therefore it seems likely that p42/44 is involved in the growth factor-stimulated signal transduction transport from protein tyrosine kinase receptors leading to glucose uptake. In contrast, the p42/44 inhibitor had no effect on IL-1 stimulated transport in these cells, instead this uptake was completely inhibited by the p38 specific inhibitor, SB 203580, indicating that p38 MAPK is involved in mediating cytokine stimulated glucose transport.

The mechanism by which MAPKs regulate glucose uptake is poorly understood. Two known downstream targets of MAPK, MAPKAP and insulin-sensitive protein kinase, were without effect on glucose transport when injected into oocytes (Merrall *et al.*, 1993), suggesting that the effect of MAPK on glucose transport is direct, or via some as yet unidentified downstream target. Previous work has shown, however, that direct phosphorylation of the glucose transporter does not occur in response to PDGF, EGF and insulin in 3T3-L1 fibroblasts (GWG unpublished data). Furthermore the GLUT1 transporter is not phosphorylated *in vitro* by either MAPK or MAPKK, so it would seem unlikely that MAPK stimulates glucose transport by modulating phosphorylation of the GLUT-1 protein itself (FJT & GWG unpublished results).

#### *Phosphatidyl 3' Kinase (PI3' kinase)*

The widespread activation of PI3' kinase by growth factors points to a common fundamental role for this enzyme in growth factor signalling, and thus PI3' kinase has been investigated as a possible mediator of glucose uptake. PI3' kinase catalyses the phosphorylation of phosphoinositides at the 3 position of the inositol ring, to generate PI(3)P, PI(3,4)P<sub>2</sub> and PI(3,4,5)P<sub>3</sub> (Leevers *et al.*, 1999).



There are three classes of PI3' kinase; class I PI3' kinases are stimulated by both receptor tyrosine kinases and G-protein-coupled receptors and can generate all 3 phosphoinositide forms. Class II PI3' kinases generate PI(3)P and PI(3,4)P<sub>2</sub> and class III PI3' kinases generate PI(3)P only (Leevers *et al.*, 1999). These phosphoinositide products of PI3' kinase act as second messengers for signal transduction by interacting with proteins containing specific phosphoinositide binding domains. Examples of such domains include: FYVE domains, which are cysteine-rich zinc-finger-like motif (Stenmark *et al.*, 1996), which bind PI(3)P specifically (Patki *et al.*, 1998) and pleckstrin homology domains (PH domains) which are modules of ~100 amino acids which bind PI(3,4,5)P<sub>3</sub> and PI(3,4,5)P<sub>2</sub> (Lemmon *et al.*, 1997).

Many groups have studied the role of PI3' kinase in glucose transport. It has been shown that growth factor stimulated glucose transport can be inhibited by using PI3' kinase inhibitors, such as wortmannin and LY 294002, in a variety of cell types (Gould *et al.*, 1994, Clarke *et al.*, 1994, Barros *et al.*, 1995).

The exact role of PI3' kinase in growth factor stimulated glucose transport remains to be elucidated. PI3' kinase activation of c-AKT in insulin-stimulated glucose transport is known to be vital (see section 1.2.3.2) and perhaps PI3' kinase plays a similar important second messenger role in mitogen-stimulated glucose transport. It has been difficult to elucidate a signalling role for PI3' kinase in mitogen-stimulated glucose transport, as the downstream effectors of PI3' kinase are as yet poorly defined. PI3' kinase activation is also involved in regulating a variety of vesicular trafficking events (Corvera & Czech, 1998, Wusmer *et al.*, 1999) and may therefore be important in recruiting GLUT-1 to the plasma membrane. However demonstrating a role for PI3' kinase in regulating specifically signalling events or specifically trafficking events involved in glucose transport would be technically very difficult. It may be that PI3' kinase is important in mediating mitogen-stimulated glucose transport via its both its roles as a signalling protein and in trafficking, however as yet this is speculation.

### 1.2.3.2 Insulin-stimulated glucose transport

Insulin can activate a number of cellular intracellular signalling pathways, however its primary function is to regulate metabolism of sugars, amino acids and fats in its peripheral target tissues, adipocytes, heart and skeletal muscle as well as in the liver. Insulin acts at the insulin receptor, which is a receptor tyrosine kinase. Insulin-stimulated increases in glucose transport results from a redistribution of GLUT4 from an intracellular pool to the cell surface, thus increasing the total number of transporters at the cell surface available for transport (Cushman *et al.*, 1980, Suzuki & Kono, 1980).

#### *IRS-1 and -2*

Insulin receptor substrate 1 and 2 (IRS-1 & 2) have been identified as major substrates of the insulin receptor (Sun *et al.*, 1991, Sun *et al.*, 1995). IRS-1 and 2 will bind to the insulin receptor upon receptor stimulation, via an SH2 domain (see above for description of receptor tyrosine kinase activation). Upon binding to the insulin receptor these proteins become phosphorylated on specific tyrosine residues and can then act as an adaptor for proteins containing SH2 domains. IRS-1 and 2 bind many of the same proteins that will be bound by classical tyrosine kinase receptors such as Grb-2, SHPTP2 and PI3'K (Skolnik *et al.*, 1993, Kuhne *et al.*, 1993, Myers *et al.*, 1992, Backer *et al.*, 1993). These proteins can then mediate insulin's myriad of actions in the cell.

#### *PI3' K*

Insulin, as well as many other growth factors (see above) rapidly stimulates the activation of PI3' kinase. PI3' kinase stimulates the accumulation of 3' phosphoinositides. These molecules can then act as second messengers by interacting with proteins containing specific phosphoinositide binding domains (see above). Phosphorylation of IRS-1 and 2 by the insulin receptor results in binding sites for the p85 subunit of PI-3' K, and upon binding to IRS-1 or 2 the enzyme is activated (Myers *et al.*, 1992, Carpenter *et al.*, 1993).

Insulin stimulated hexose transport and GLUT-4 translocation in 3T3-L1 adipocytes and *Xenopus* oocytes can be inhibited by the use of specific inhibitors of PI3'K, wortmannin and LY 294002 (Clarke *et al.*, 1994, Evans *et al.*, 1995, Gould *et al.*, 1994). Therefore it is clear that PI3'K activity is very important in mediating insulin-stimulated glucose transport. However, the ability of PI3'K alone to stimulate glucose transport is controversial. Both insulin and PDGF stimulate PI3'K activity to the same extent in 3T3-L1 adipocytes, but only insulin significantly stimulates glucose transport in these cells (Wiese *et al.*, 1995).

#### *c-AKT/PKB*

Since discovering that PI3'K is involved in mediating insulin-stimulated glucose transport, efforts have been made to identify possible down-stream effectors. Recently a serine/threonine kinase, protein kinase B (PKB), has been shown to be down-stream of PI3'K (Bos, 1995, Coffey *et al.*, 1998). PKB is also known as c-AKT, and as yet the nomenclature for this kinase has not been resolved. Currently three isoforms of PKB are known,  $\alpha$ ,  $\beta$  and  $\gamma$ . PKB is able to act as a down-stream target for PI3'K by virtue of its pleckstrin homology domain, which mediates binding to PI(3,4)P<sub>2</sub> and PI(3,4,5)P<sub>3</sub>. Upon binding to phosphoinositides PKB is itself phosphorylated and activated (Coffey *et al.*, 1998).

A role for PKB in insulin-stimulated glucose transport has been sought. Work has shown that if a constitutively active form of PKB is transfected in to 3T3-L1 preadipocytes spontaneous differentiation of these cells into mature adipocytes occurs (Magun *et al.*, 1996). Expression of the constitutively active PKB stimulated glucose uptake and GLUT-4 translocation levels similar to those seen upon insulin treatment in 3T3-L1 adipocytes (Kohn *et al.*, 1996). It is interesting to note here that PDGF can stimulate PI3'K activity in these cells but is unable to stimulate phosphorylation of PKB (Nave *et al.*, 1996). This demonstrates a parallel between an agonist's ability to stimulate GLUT-4 translocation and PKB activation. These results suggest an important role for PKB in insulin-mediated glucose transport. The mechanism by which PKB mediates insulin-stimulated glucose transport is as yet unclear.

### *MAP Kinase Cascade*

The insulin receptor can stimulate the MAP kinase cascade via activation of the small molecular weight G-protein p21<sup>ras</sup>. Insulin activates p21<sup>ras</sup> via two different mechanisms, one requiring IRS-1 and the other independent of IRS-1 (Myers *et al.*, 1994). The activation of ras requires the exchange of GDP for GTP. This exchange is catalysed by the guanine-nucleotide exchange factor SOS (Sakaue *et al.*, 1995). Upon binding of insulin to its receptor, Grb2/SOS is recruited to the membrane via interaction with IRS-1 or Shc, an insulin receptor adapter protein (Skolnik *et al.*, 1993, Myers *et al.*, 1994). Once at the membrane the Grb/SOS complex can catalyse the nucleotide exchange on ras, and ultimately the activation of the MAP kinase cascade (see Figure 1.4).

However, the use of an inhibitor of p42/44 MAP kinase activation, PD98059, fails to inhibit insulin stimulated glucose transport in 3T3-L1 adipocytes (Lazar *et al.*, 1995). These results indicate that the MAP kinase pathway is not responsible for mediating insulin-stimulated glucose transport.

#### **1.2.3.3 Cyclic nucleotide regulation of glucose transport**

To date very little is known about the role of cyclic nucleotides in regulating glucose transport. Depending on the tissue studied cAMP can be either stimulatory, inhibitory or without effect on glucose transport. In 3T3-L1 preadipocytes the cAMP analogue, 8-Br cAMP, was found to be stimulatory with regard to glucose transport (Cornelius *et al.*, 1991). In fat cells cAMP is without effect on basal glucose transport rates but is inhibitory with regard to insulin-stimulated transport in these cells (Lönnroth *et al.*, 1987). In cultured rat thyroid cells glucose transport is increased by thyroid-stimulating hormone in a cAMP-dependent manner (Hosaka *et al.*, 1992). In these cells it was seen that cAMP analogues stimulated an increase in GLUT-1 mRNA levels but caused a decrease in GLUT-4 mRNA levels. This, along with the effect of cAMP in fat cells and preadipocytes, seems to suggest that cAMP may be stimulatory with regard to GLUT-1 mediated glucose transport, but inhibitory with regard to GLUT-4 mediated transport. In pancreatic  $\beta$  cells phosphorylation of the glucose

transporter GLUT-2 by protein kinase A (PKA) results in a decrease in glucose transport (Thorens *et al.*, 1996). In cardiomyocytes agents altering intracellular levels of cAMP had no effect on glucose transport (Fischer *et al.*, 1996).

Less is known about the ability of cGMP to regulate glucose transport. In cardiomyocytes, there are early reports of cGMP being able to stimulate glucose transport in these cells (Shanahan & Edwards, 1989), but later publications report that cGMP is without effect on glucose transport in cardiomyocytes (Fischer *et al.*, 1996).

#### **1.2.4 GLUCOSE TRANSPORT IN VASCULAR SMOOTH MUSCLE CELLS**

As stated earlier, VSMC proliferation is an important factor in the development of atherosclerotic plaques. Glucose transport is an early response common to all mitogens, however very little is known about the regulation of glucose transport in VSMC.

Most studies of glucose transport in vascular smooth muscle cells have concentrated on the effects of insulin and IGF-1. In these studies it has been shown that both insulin and IGF-1 are capable of eliciting a two- to three-fold increase in glucose transport in these cells (Sowers, 1996, Fujiwara & Nakai, 1996). In both studies it was shown that IGF-1 is a more potent stimulator of glucose transport than insulin in VSMCs. It has been suggested that the effects of insulin on VSMC are mediated via the IGF-1 receptor. Both insulin and IGF-1 stimulated glucose transport are inhibited by the PI3'K inhibitor, wortmannin (Fujiwara & Nakai, 1996), therefore insulin and IGF-1 both mediate glucose transport via a PI3'kinase-dependent mechanism.

Angiotensin II, an endogenous vasoconstrictor that acts at a G-protein-coupled receptor, has also been shown to be able to increase glucose transport in VSMCs (Quinn & McCumbee, 1998). This agonist also elicits an approximately two-fold increase in glucose transport. Inhibition of PKC did not affect the ability of angiotensin II to stimulate glucose transport in VSMC. However it was shown that extracellular calcium and calmodulin are important in mediating angiotensin II-stimulated glucose uptake. Reducing the extracellular calcium concentration or

inhibiting calmodulin, with W-7 or calmidazolium, reduces angiotensin II-stimulated uptake by approximately 50%, but had no effect on basal rates of transport.

As well as various agonists being able to modulate glucose transport in VSMCs, it has been shown that the concentration of glucose that the cells are exposed to is also very important. In cells grown in media with high concentrations of glucose (25 mM) both basal and stimulated rates of uptake are lower than in cells grown in 0, 2.5 or 5 mM glucose. This is true in response to both insulin and angiotensin II (Fujiwara *et al.*, 1996, Quinn & McCumbee, 1998). The fold stimulation of glucose transport is much greater in cells grown in high glucose concentrations, due to the very low basal levels of uptake, than in cells grown in low glucose concentrations. The mechanisms underlying the regulation of transport by the concentration of glucose in the growth medium are poorly understood.

There is some controversy as to which glucose transporter(s) are responsible for increased glucose uptake in VSMC. Sowers' work indicates that the insulin responsive glucose transporter GLUT-4 is present in the cells and may be involved in mediating the insulin/IGF-1 increase in uptake (Sowers, 1996). However other groups investigating glucose transport in VSMC found GLUT-1 mRNA but failed to find mRNA for GLUT-4 in these cells (Kihara *et al.*, 1998), implying that it is GLUT-1, and not GLUT-4, which is responsible for mediating the increases in glucose transport. This point is returned to later in this thesis.

### **1.3 CYCLIC 3'5'-ADENOSINE MONOPHOSPHATE**

Cyclic 3'5'-adenosine monophosphate (cAMP) is an important second messenger involved in mediating a wide range of cellular functions. cAMP can regulate many cellular processes including cell growth and differentiation (Kronemann *et al.*, 1999, Yarwood 1995, Schmidt *et al.*, 1990), relaxation of smooth muscle (Murray, 1990, Murthy & Makhlouf, 1995), glucose transport (Piper *et al.*, 1993, Cornelius *et al.*, 1991), secretory processes (Katsura *et al.*, 1997, Muñiz *et al.*, 1996) and ion channel conductance (Brüggermann *et al.*, 1993, Jurevičius *et al.*, 1996) and many others.

The intracellular concentration of cAMP is determined by both its rate of synthesis, by a family of adenylyl cyclases (Tesmer & Sprang, 1998), and its rate of degradation, by the multi-enzyme family of phosphodiesterases (PDEs) (Manganiello *et al.*, 1995, Houslay & Milligan, 1997).

### 1.3.1 Generation of cAMP

cAMP is synthesised by adenylyl cyclase which catalyses the conversion of ATP to cAMP. Mammalian cells express up to nine adenylyl cyclase isoforms. Adenylyl cyclases are integral membrane glycoproteins with twelve transmembrane spanning helices (Tesmer & Sprang, 1998). Both the N- and C- terminal are intracellular, and the active site of the enzyme is formed by the intracellular loop between helices 6 and 7 (C<sub>1</sub> domain) and the C-terminal tail (C<sub>2</sub> domain) (Tesmer & Sprang, 1998), which forms a wreath-like structure (Tesmer & Sprang, 1998). The activity of the enzyme requires the presence of the divalent cation Mg<sup>2+</sup> (Smit & Iyengar, 1998) and can be regulated by a number of mechanisms within the cell depending on the isoform (Iyengar, 1993, Smit & Iyengar 1998). An overview of the adenylyl cyclase isoforms and how they are regulated is shown in Table 1.2.

The best understood means of regulating adenylyl cyclase activity is by the action of heterotrimeric G-proteins. Heterotrimeric G-proteins consist of an  $\alpha$ ,  $\beta$  and  $\gamma$  subunit. Stimulation of a G-protein coupled receptor leads to the exchange of GDP for GTP on the  $\alpha$  subunit of the receptor-associated G-protein. This results in the activation of the G-protein and dissociation of the  $\alpha$  subunit from the  $\beta\gamma$  subunits. Both the  $\alpha$  subunit and the  $\beta\gamma$  subunits are capable of transducing signals. There are a number of  $\alpha$  subunits in cells and these can be stimulatory, inhibitory or without effect on adenylyl cyclase activity (for review see Milligan, 1993). The G<sub>s</sub>  $\alpha$  subunits are stimulatory with regard to all nine adenylyl cyclase isoforms, whereas the G<sub>i</sub>  $\alpha$  subunits inhibit adenylyl cyclase I, V, VI and VIII (Houslay & Milligan, 1997, Smit & Iyengar, 1998). The  $\beta\gamma$  subunits can also regulate the activity of adenylyl cyclase (Sternweis, 1994, Smit & Iyengar, 1998). The effects of the  $\beta\gamma$  subunits can be either stimulatory or

inhibitory, depending on the isoform of adenylyl cyclase. G $\beta\gamma$  inhibits type I and VIII adenylyl cyclase, whereas it is stimulatory with regard to types II, IV and VII. The effects of the G $\beta\gamma$  are most efficacious in the presence of an activating agent (such as Gs  $\alpha$ ). Thus G $\beta\gamma$  acts primarily to enhance or dampen the activity of the stimulated enzyme.

As well as regulation by the heterotrimeric G-proteins adenylyl cyclase activity can be modulated by several other mechanisms, including protein kinase C and intracellular calcium (Smit and Iyengar, 1998, Iyengar, 1993), see table 1.2. Many growth factors and hormones signal via receptor tyrosine kinases. This can result in the stimulation of protein kinase C and an increase in the levels of intracellular calcium (see figure 1.3). The ability of certain adenylyl cyclase isoforms to be regulated by Ca<sup>2+</sup> and PKC allows a mechanism for crosstalk between signals from receptor tyrosine kinases and those from G-protein coupled receptors.

Protein kinase A can phosphorylate and inhibit the activity of type V and VI adenylyl cyclases. This is thought to provide means of desensitisation of cAMP signalling. As cAMP accumulates, the activity of PKA increases. PKA, as well as mediating intracellular signals, phosphorylates and inhibits adenylyl cyclase activity, therefore inhibiting further production of cAMP and further stimulation of PKA (Smit & Iyengar, 1998).

### 1.3.2 Degradation of cAMP

As stated above the intracellular levels of cAMP is determined both by its rate of synthesis and its rate of degradation. The breakdown of cAMP is catalysed by a large multi-gene family of phosphodiesterases (Bolger, 1994, Manganiello, 1995). Currently ten families of PDE have been identified which are differentiated between based on their biochemical and pharmacological characteristics (see table 1.3 for an overview of the properties of PDEs). Some PDE isoforms degrade cGMP specifically, such as PDE VI and IX, some degrade cAMP specifically, such as III, IV, VII and VIII whereas PDEs I, II and X are promiscuous and catalyse the degradation of both cAMP and cGMP (Manganiello *et al.*, 1995, Soderling *et al.*, 1998, Fisher *et al.*, 1998,



Soderling *et al.*, 1998, Soderling *et al.*, 1999). Seven families of PDE are known to hydrolyse cAMP: I, II, III, IV, VII, VIII and X (Manganiello *et al.*, 1995).

The PDE isoforms all have a central core region of about 330 amino acids, which contains the active site. Outside this core region the PDE isoforms are distinct. Alternative mRNA splicing leads to a huge number of isoforms within each PDE family, and this gives rise to a sophisticated system for generating PDE isoforms targeted to distinct intracellular structures. This is exemplified in the PDE IV family (Bolger, 1994). Four genes encode the mammalian types IV PDEs. Analysis of cDNAs from human PDE4A, 4B and 4D revealed that each locus produces clones with regions of variant sequence consistent with alternative mRNA splicing (reviewed Bolger, 1994). This takes the form of 5'-domain swapping, leading to a family of over 16 different active isoforms being produced, each of which has a distinct amino-terminal region. Analyses of the PDE 4A isoforms has shown that amino-terminal truncation produces a highly active core region, which is localised entirely in the cytosol. This is in contrast to the full-length isoforms, which show diminished catalytic activity and are found associated at specific subcellular sites (Bolger *et al.*, 1996, McPhcc *et al.*, 1995, O'Connell *et al.*, 1996).

Due to the large number of PDE families and the ability of the cells to produce many splice variants within each PDE family, the cell has a wide range of ways to terminate cAMP signalling. The specific subcellular localisation and activity of PDEs may play a very important role in the compartmentalisation of cAMP signalling (Houslay & Milligan, 1997). It is believed that the compartmentalisation of cAMP signals could be vital in leading to the specific downstream effects of this very ubiquitous second messenger.

### **1.3.3 cAMP signalling**

As has been discussed above there are a large number of receptors, G-proteins, adenylyl cyclases and PDEs responsible for generating and terminating cAMP signals.

Protein kinase A (PKA) is the most common and best understood mechanism for cAMP to mediate its signal. The PKA holoenzyme is a heterotetramer composed of a regulatory subunit dimer ( $R_2$ ), which maintains two catalytic subunits (C) in a dormant state (Rubin, 1994 for review). When intracellular levels of cAMP rise each regulatory subunit binds to two cAMP molecules and the inactive holoenzyme dissociates into an  $R_2$ -cAMP<sub>4</sub> complex and active C monomers. To date there are three C subunits ( $\alpha$ ,  $\beta$  and  $\gamma$ ) and four R subunits ( $RI\alpha$ ,  $RI\beta$ ,  $RII\alpha$  and  $RII\beta$ ) known in mammals (Gamm *et al.*, 1996, Beebe *et al.*, 1990, Taylor *et al.*, 1990). Dissociated C subunits catalyse the phosphorylation of substrate molecules on serine/threonine residues presented in the sequences RRXS/T or RXS/T or KRXXS/T (reviewed by Kemp & Pearson, 1990) thereby regulating their functional and/or structural properties.

As PKA phosphorylation sequences are abundant in the cell there are various regulatory mechanisms in place to ensure that indiscriminate phosphorylation does not occur. Firstly, the levels of cAMP present in the cell are tightly regulated by its rate of synthesis and degradation by adenylyl cyclases and PDEs, and the subcellular localisation of PDEs leads to further localised reduction of cAMP (discussed above). Access to cAMP is the primary requirement for PKA activation, but there are additional factors responsible for returning the enzyme to its inactive state. The R subunit is expressed in excess over the C subunit, favouring reformation of the holoenzyme when cAMP levels return to the basal state. The subcellular localisation of the PKA isoforms is also believed to play a regulatory role. The type I PKA holoenzymes, containing  $RI\alpha$  or  $\beta$ , are predominantly cytoplasmic whereas the type II holoenzymes are targeted to certain intracellular locations (reviewed Rubin, 1994). RII isoforms are by means of A Protein Anchoring Proteins, or AKAPs (reviewed in Colledge & Scott, 1999, Faux & Scott, 1996). This targeting of type II PKA to subcellular compartment may allow a mechanism for the cell to selectively activate PKA II depending on the availability of cAMP at this subcellular site (reviewed in Dell'Acqua & Scott, 1997).

PKA is known to be involved in regulating a large number of cellular activities including natriuretic peptide-dependent cGMP accumulation (Ledoux *et al.*, 1997),

stimulation and inhibition of MAPKs by altering Raf activity (Yarwood *et al.*, 1996, Yao *et al.*, 1998), exocytosis (Muñiz *et al.*, 1996, Katsura *et al.*, 1997) and relaxation of smooth muscle cells (Murthy & Makhlouf, 1995).

As well as signalling via PKA, cAMP is also capable of mediating some of its effects directly. cAMP can directly activate cardiac pacemaker channels and a voltage-gated  $K^+$  and  $Ca^{2+}$  channel, independent of any phosphorylation of the channel (DiFrancesco & Tortora, 1991, Brüggemann *et al.*, 1993). This is thought to occur by direct cAMP binding to the channel. As well as direct activation of ion channels, cAMP can bind and activate specific guanine nucleotide exchange factors, GEFs (de Rooij *et al.*, 1998). It also appears that cAMP can inhibit glucose transport by a mechanism that is not dependent on PKA phosphorylation (Piper *et al.*, 1993).

These mechanisms of signal transduction via cAMP allow a whole array of possible downstream effectors and countless opportunities for crosstalk with many different signalling pathways.

## **1.4 CYCLIC GUANOSINE 3'5'-MONOPHOSPHATE**

Like cAMP, intracellular levels of cGMP are controlled both by its rate of synthesis by guanylyl cyclases and its rate of degradation by PDEs. cGMP has been implicated in regulating many cellular processes including inhibition of the MAPK pathway (Suhassini *et al.*, 1998), regulation of proliferation in VSMC (Ciche *et al.*, 1998, Kronemann *et al.*, 1999), inhibition of protein kinase C activation in VSMC (Kumar *et al.*, 1997), smooth muscle relaxation and vasodilation (Landgraf *et al.*, 1992, Murthy & Makhlouf, 1995) and stimulation of glucose transport (Shanahan & Edwards, 1989).

### **1.4.1 Guanylyl Cyclase**

cGMP is generated by conversion of GTP to cGMP by guanylyl cyclases, by a mechanism that is stereochemically analogous to that of adenylyl cyclases (Hurley, 1998 for review). Guanylyl cyclases occur in both transmembrane and soluble forms.

Both soluble and transmembrane guanylyl cyclases function as dimers, with the soluble guanylyl cyclases forming  $\alpha\beta$  heterodimers and transmembrane guanylyl cyclases forming homodimers. Both the soluble and transmembrane guanylyl cyclase require  $Mg^{2+}$  for activity (Hurley, 1998). The catalytic domains of both the soluble and transmembrane guanylyl cyclases are homologous to the  $C_1$  and  $C_2$  domains of mammalian adenylyl cyclases (Tesmer & Sprang, 1998). These C domains form the wreath-like active site analogous to that of adenylyl cyclase when dimerised (Tesmer & Sprang, 1998).

To date four members of the transmembrane guanylyl cyclase receptors have been identified: GC-A, GC-B, GC-C and RetGC (the retinal isoform) (Garbers & Lowe, 1994). The transmembrane forms consist of a single transmembrane domain and a single intracellular catalytic domain and an intracellular protein kinase homology domain. The transmembrane isoforms appear to function as homodimers, but it is possible that heterodimers may also exist based on work carried out on cells overexpressing GC-A and -B (Chinkers & Wilson, 1992). The extracellular domain of transmembrane guanylyl cyclases acts as a ligand-binding site. The known peptide ligands for these guanylyl cyclases fall into two families: the natriuretic peptides (ANP, BNP, and CNP) or the heat stable enterotoxins/guanylylins (Garbers & Lowe, 1994). Upon binding of the appropriate ligand the enzyme activity is stimulated, and GTP is converted to cGMP. As well as being regulated by ligand binding, the activity of transmembrane guanylyl cyclases can be regulated by PKC and  $Ca^{2+}$  (Garbers & Lowe, 1994). This allows a mechanism for cross talk between cGMP signalling pathways and those which utilise PKC and  $Ca^{2+}$ , such as PDGF (see section 1.2.3).

Soluble guanylylate cyclase (sGC) is a haem-containing protein found in the cytosolic fraction of virtually all mammalian cells. The haem group in soluble guanylylate cyclase confers the NO-sensitivity of the protein. Upon NO binding to the haem group the guanylyl cyclase activity is stimulated (Garbers & Lowe, 1994). To date three  $\alpha$  and three  $\beta$  subunits of soluble guanylylate cyclase are known, and these function as heterodimers of  $\alpha$  and  $\beta$  subunits (Hobbs, 1997). The  $\alpha_1$  and  $\beta_1$  subunits are found ubiquitously expressed in mammalian tissues and the  $\alpha_2$  subunit is found in kidney,

vascular tissue, chemosensory cells and dorsal root ganglion. The expression of the  $\beta_2$ ,  $\alpha_3$  and  $\beta_3$  subunits is much more restricted with the  $\beta_2$  isoform being expressed only in liver and the  $\alpha_3$  and  $\beta_3$  isoforms only expressed in vascular smooth muscle and endothelial cells (Hobbs, 1997). Soluble guanylyl cyclases can be divided, arbitrarily, into three domains: haem-binding domain, a catalytic domain and a domain that mediates the dimerisation of monomers (Hobbs, 1997). As yet it is unclear how the activity of soluble guanylyl cyclase is regulated beyond the role of NO. It is believed that sGC activity may be regulated at the transcriptional level. It has been shown that agents which cause an increase in the intracellular levels of cAMP can decrease  $\beta_1$  mRNA, resulting in a diminished ability of the cell to generate cGMP in response to NO (Hobbs, 1997). sGC activity could also be regulated by the actions of an endogenous inhibitor which has been partially purified from bovine lung (Hobbs, 1997).

#### **1.4.2 Degradation of cGMP**

Like cAMP, the large multi-gene family of phosphodiesterases degrades cGMP. Of these PDEs, types I, II, III, V and VI will degrade cGMP. Types I, II and III can degrade both cAMP and cGMP, whereas types V and VI are cGMP specific. These PDEs are regulated by a number of different mechanisms. PDEs are discussed in more detail in section 1.3.2, and a table of properties of PDEs is shown in table 1.3.

#### **1.4.3 Signalling via cGMP**

Many of cGMP's downstream effects are mediated by the cGMP regulated protein kinase PKG. PKG is a serine/threonine kinase and currently there are two types of PKG known, types I and II.

Two isoforms of type I PKG exist, cGK I $\alpha$  and cGK I $\beta$  (Wolfe *et al.*, 1989). These isoforms differ only in their amino termini and both function as homodimers. It is thought that the isoforms dimerise by means of a conserved, amino-terminal leucine zipper motif (Francis *et al.*, 1994, Jarchau *et al.*, 1994). Each subunit contains a

catalytic and a regulatory, cyclic nucleotide binding domain (reviewed in Walter, 1989, Edelmann *et al.*, 1987) and can bind two molecules of cGMP. The  $K_m$  for PKG activation is ~20-100 nM cGMP (Heil *et al.*, 1987).

The type II PKG isoform was first identified from microvilli as a monomer associated with the membrane fractions (de Jonge, 1981). Type II PKG from mouse brain shows 66% homology with the cGMP binding domain and the catalytic domain of cGK I. Initially type II PKG was thought to function as a monomer, but it also contains an amino-terminal leucine zipper (like type I PKGs), and recent work has revealed that the type II PKG does, in fact, function as a homodimer (Gamm *et al.*, 1995).

PKG is involved in regulating a large number of cellular processes including inhibition of the Ras/MAPK pathway (Suhasini *et al.*, 1998), VSMC proliferation (Chiche *et al.*, 1998), inhibition of PKC (Kumar *et al.*, 1997), relaxation of smooth muscle (Murthy & Makhlouf, 1995) and many more.

As well as signalling via PKG, cGMP is capable of eliciting some of its responses by direct interaction with effector proteins. Like cAMP, cGMP is capable of regulating cyclic nucleotide-gated channels. The best characterised of these is probably the cyclic nucleotide-gated channels in the olfactory and phototransduction systems (Nakamura & Gold, 1987, Molokanova *et al.*, 1999). The activity of PDEs can also be altered by direct interaction with cGMP (see table 1.3 for details). Depending on the isoform, interaction of PDEs with cGMP can be stimulatory, inhibitory or without effect on PDE activity (Manganiello *et al.*, 1995). This allows a mechanism for cross talk between the cAMP and the cGMP signalling cascades.

By using a large number of mechanisms to generate, terminate and mediate cGMP signals the cell is capable of tailoring very specific signals via an ubiquitous second messenger.

## 1.5 CYCLIC NUCLEOTIDE SIGNALLING IN VSMC

cAMP and cGMP signalling are responsible for a wide range of cellular effects in many cell types (as discussed above). One of the most important role for these nucleotides in VSMCs is controlling relaxation of these cells (Landgraf *et al.*, 1992, Murthy & Makhlouf, 1995, Toyoshima *et al.*, 1998). The contraction of smooth muscle occurs when intracellular levels of  $\text{Ca}^{2+}$  rise and  $\text{Ca}^{2+}$ -calmodulin activates myosin light chain kinase. Myosin light chain kinase then phosphorylates and activates myosin light chain and the cell contracts (reviewed in Horowitz *et al.*, 1996). The relaxation of smooth muscle is associated with a decrease in cytosolic calcium and an increase in cAMP or cGMP concentration. In VSMC stimulation of  $\text{PLC}\beta$  results in the production of  $\text{IP}_3$  and  $\text{DAG}$ ,  $\text{IP}_3$  will then bind  $\text{IP}_3$  receptors on the sarcoplasmic reticulum, which results in the release of  $\text{Ca}^{2+}$  from this store thereby increasing intracellular  $[\text{Ca}^{2+}]$  (see section 1.2.3). cAMP and cGMP have been shown to be able to reduce intracellular  $[\text{Ca}^{2+}]$  and therefore cause relaxation of smooth muscle cells. PKG and PKA can phosphorylate  $\text{PLC}\beta$  and inhibit its activity, thereby inhibiting  $\text{IP}_3$  production and release of  $\text{Ca}^{2+}$  from the sarcoplasmic reticulum (Murthy *et al.*, 1993). PKA and PKG can also phosphorylate the  $\text{IP}_3$  receptor itself, although the functional consequences of this phosphorylation are as yet not clear (Komalavilas & Lincoln, 1994, Komalavilas & Lincoln, 1996). It is clear that PKG and PKA can act alone or in concert to regulate the relaxation of smooth muscle (Murthy & Makhlouf, 1995).

As well as being able to regulate relaxation of vascular smooth muscle cells, cGMP and cAMP appear to be able to inhibit proliferation of these cells (Kronemann *et al.*, 1999, Chiche *et al.*, 1998). It appears that the growth inhibitory effects of these cyclic nucleotides are mediated by an inhibition of the expression of certain cyclins necessary for cell cycle progression (Kronemann *et al.*, 1999). cAMP appears to be more potent in inhibiting proliferation in VSMC, but this may in part be due to the decreased levels of expression of PKG in VSMC which have been passaged in culture. In studies where PKG expression and activity has been augmented by

transfection of PKG into VSMC, the cells show enhanced sensitivity to the antiproliferative effects of NO/cGMP (Chiche *et al.*, 1998).

It is interesting to note here that two of the principle effects of cyclic nucleotides in VSMC are relaxation and inhibition of proliferation of these cells. It is therefore tempting to speculate here that perhaps aberrant cyclic nucleotide signalling is involved, at some level, in the progression of plaque formation and ultimately atherosclerosis (see section 1.1.1 and 1.1.2).

## **1.6 AIMS OF THE STUDY**

An increase in VSMC proliferation is a major contributor to the development of atherosclerotic plaques. As glucose transport is an early response to all mitogens it is of interest, therefore, to better characterise mitogen-stimulated glucose transport in rat aortic vascular smooth muscle cells. The stimulation of glucose transport in response to the mitogen PDGF will be characterised and the signalling mechanisms mediating this investigated.

Currently there is controversy as to which glucose transporters mediate transport in these cells, some studies report the presence of GLUT-4 whereas others find only GLUT-1. The GLUT content of rat aortic vascular smooth muscle cells used will be studied.

As cyclic nucleotide signalling is very important in causing relaxation and inhibiting proliferation of VSMC, it is tempting to speculate that aberrant cyclic nucleotide signalling may be involved in the development of atherosclerosis. The role of the cyclic nucleotides, cAMP and cGMP, in regulating glucose transport will, therefore, be assessed in these cells. The signalling mechanisms mediating cyclic nucleotide regulation of glucose transport will also be studied.

Finally, it is currently unclear whether increases in glucose transport mediated by GLUT-1 result from an increase of transporter activity, an increase in the number of



functional GLUT-1 transporters at the plasma membrane, or a combination of both. To address this question, GLUT-1 - green fluorescent protein (GFP) chimeras will be utilised to try to visualise movement of GLUT-1 within the cell. The phosphorylation of the GLUTs in the cell will also be studied.

**TABLE 1.1****MAJOR SITES OF EXPRESSION OF THE DIFFERENT GLUCOSE  
TRANSPORTERS IN HUMAN AND RODENT TISSUES.**

<b>ISOFORM</b>	<b>TISSUE</b>
GLUT-1	Placenta; brain; blood-tissue barrier; adipose and muscle tissue (low levels); tissue culture cells; transformed cells.
GLUT-2	Liver; pancreatic $\beta$ -cell; kidney proximal tubules and small intestine (basolateral membranes).
GLUT-3	Brain and nerve cells in rodents. Brain, nerve; low levels in placenta, liver and heart (humans).
GLUT-4	Muscle; heart; adipose.
GLUT-5	Small intestine (apical membranes); kidney, testis, brain, muscle and adipose at low levels (humans). Small intestine (apical membranes); kidney (rat).

**TABLE 1.2 REGULATION OF ADENYLYL CYCLASE ISOFORMS**

ISOFORM	REGULATORS				
	Ca <sup>2+</sup>	Gβγ	G <sub>i</sub> -α	PKC	PKA
AC-I	↑	↓	↓	↑	?
AC-II	nc	↑ (+G <sub>s</sub> -α)	nc	↑	?
AC-III	↑ (+G <sub>s</sub> -α)	nc	?	↑	?
AC-IV	nc	↑ (-G <sub>s</sub> -α)	nc	nc/↓	?
AC-V	↓	nc	↓	nc/↑	↓
AC-VI	↓	nc	↓	nc/↑	↓
AC-VII	nc	(↑)	?	(↑)?	?
AC-VIII	↑	(↓)	(↓)	?	?
AC-IX	↑	nc	?	?	?

Shown are various regulators of adenylyl cyclase isoforms. ↑ indicates an increase in adenylyl cyclase activity, ↓ represents a decrease in adenylyl cyclase activity and nc indicates that the agent elicits no change in adenylyl cyclase activity. ? indicates that the effect of the agent on adenylyl cyclase activity is unknown.

TABLE 1.3

PROPERTIES OF PDE FAMILIES

GENE FAMILY	FAMILY NAME	K <sub>M</sub>	REGULATION	
			MOLECULAR	INTACT CELLS
1 (A,B,C)	Ca <sup>2+</sup> /calmodulin sensitive	cGMP ≤ cAMP	Ca <sup>2+</sup> , calmodulin Phosphorylation by PKA or CaM-K	Cholinergic muscarinic agents Opiates
2(A)	cGMP-stimulated positive cooperativity	cGMP < cAMP	cGMP	ANF, NO
3 (A,B)	cGMP-inhibited	cAMP ≅ cGMP	cGMP Phosphorylation by PKA	Insulin, NO, dexamethasone
4 (A,B,C,D)	cAMP-specific	cAMP « cGMP	cAMP (gene expression) Phosphorylation by PKA	TSH FSH
5 (A)	cGMP-specific	cGMP « cAMP	Phosphorylation by PKG	ANF
6 (A,B,C)	Photoreceptor	cGMP « cAMP	Transducin, PKC, prenylation.	Light
7 (A)	cAMP-specific	cAMP « cGMP		
8 (A)	cAMP-specific	cAMP « cGMP	) ) Isolated in 1998/99	Soderling <i>et al.</i> , 1998
9 (A)	cGMP-specific	cGMP « cAMP	) Little known about ) regulation	Soderling <i>et al.</i> , 1998 Fisher <i>et al.</i> , 1998
10 (A)	c-AMP/cGMP	cAMP < cGMP	)	Soderling <i>et al.</i> , 1999

## **Figure 1.1 An overview of atherosclerotic plaque development**

The initial trigger for plaque development is poorly understood. It is believed that some form of endothelial cell dysfunction or injury can result in an inflammatory response. Leukocytes and platelets then adhere to the “injured” area, and induce the endothelium to produce and secrete vasoactive molecules, cytokines and growth factors. Monocytes and T lymphocytes then migrate between the endothelial cells where the monocytes become macrophages. These macrophages, along with VSMCs, accumulate lipids and become foam cells forming a fatty streak. If the inflammatory response continues there is stimulation of migration and proliferation of VSMCs to form an intermediate lesion. Continued inflammation results in increased numbers of macrophages and lymphocytes in the plaque, and activation of these leads to the release of hydrolytic enzymes, cytokines, chemokines and growth factors, which can induce further damage and eventually lead to focal necrosis.

Cells are represented as defined below:

Blue VSMCs

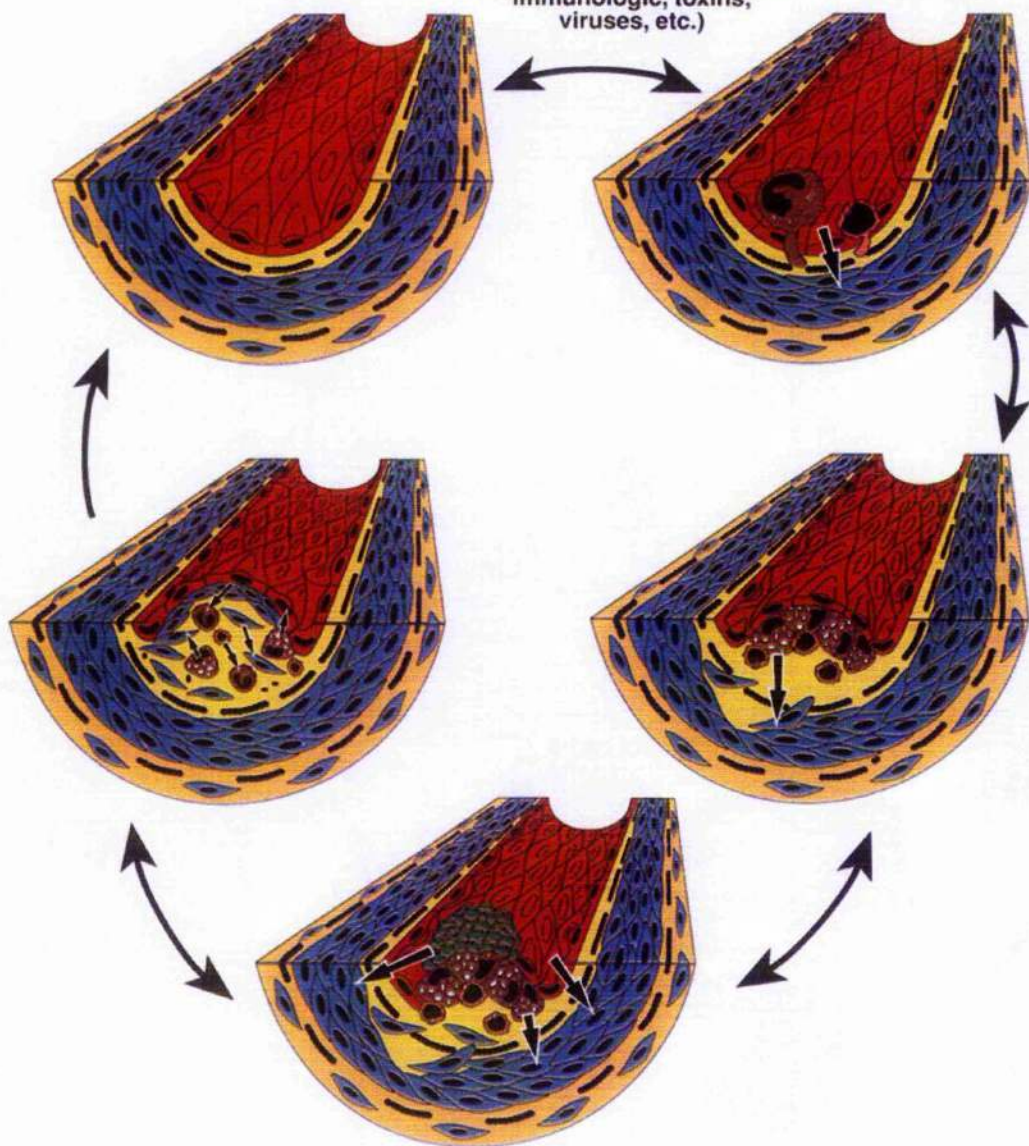
Red Endothelial cells

Purple Macrophages

Pink T lymphocytes

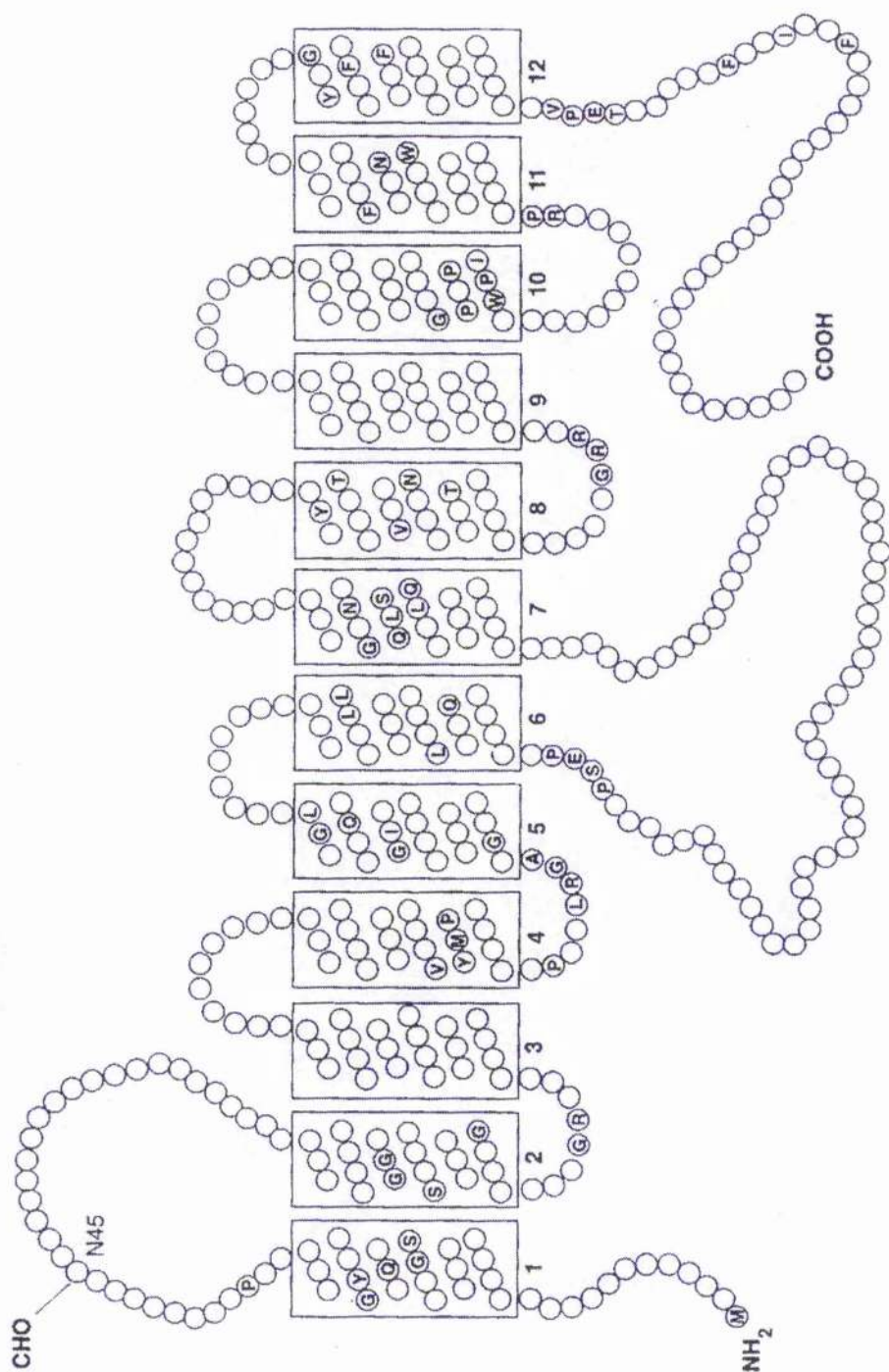
Green Platelets

**"INJURY"**  
Ox LDL,  
(mechanical, homocysteine,  
immunologic, toxins,  
viruses, etc.)



## **Figure 1.2 The twelve membrane spanning helix model of the GLUTs.**

Shown is a schematic representation of the twelve-membrane spanning domain structure of the GLUT family members. Residues indicated by single letter codes are conserved between GLUTs 1 to 5. The site for N-linked glycosylation in the large extracellular loop is also indicated.



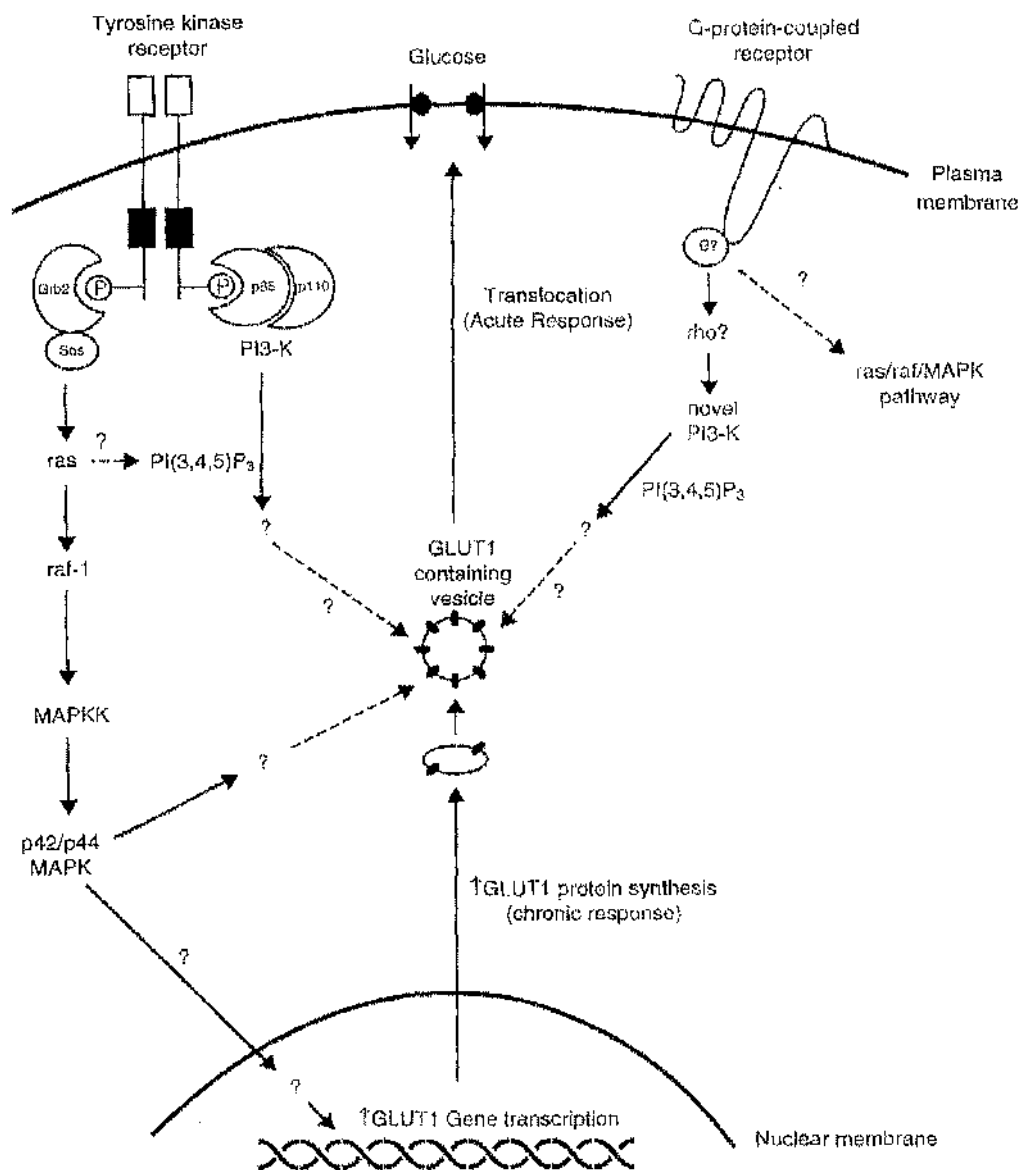


### **Figure 1.3 A proposed scheme of cellular signalling pathways involved in growth factor control of glucose transport**

The pathways that are activated by tyrosine kinase and G-protein-coupled receptors, leading to changes in glucose transport, are illustrated schematically. Both tyrosine kinase receptor and G-protein-coupled receptor mediated glucose transport are dependant on PI3' kinase.

Both receptor tyrosine kinases and G-protein-coupled receptors also stimulate the ras/raf/MAPK pathways, which can also be involved in regulating glucose transport.

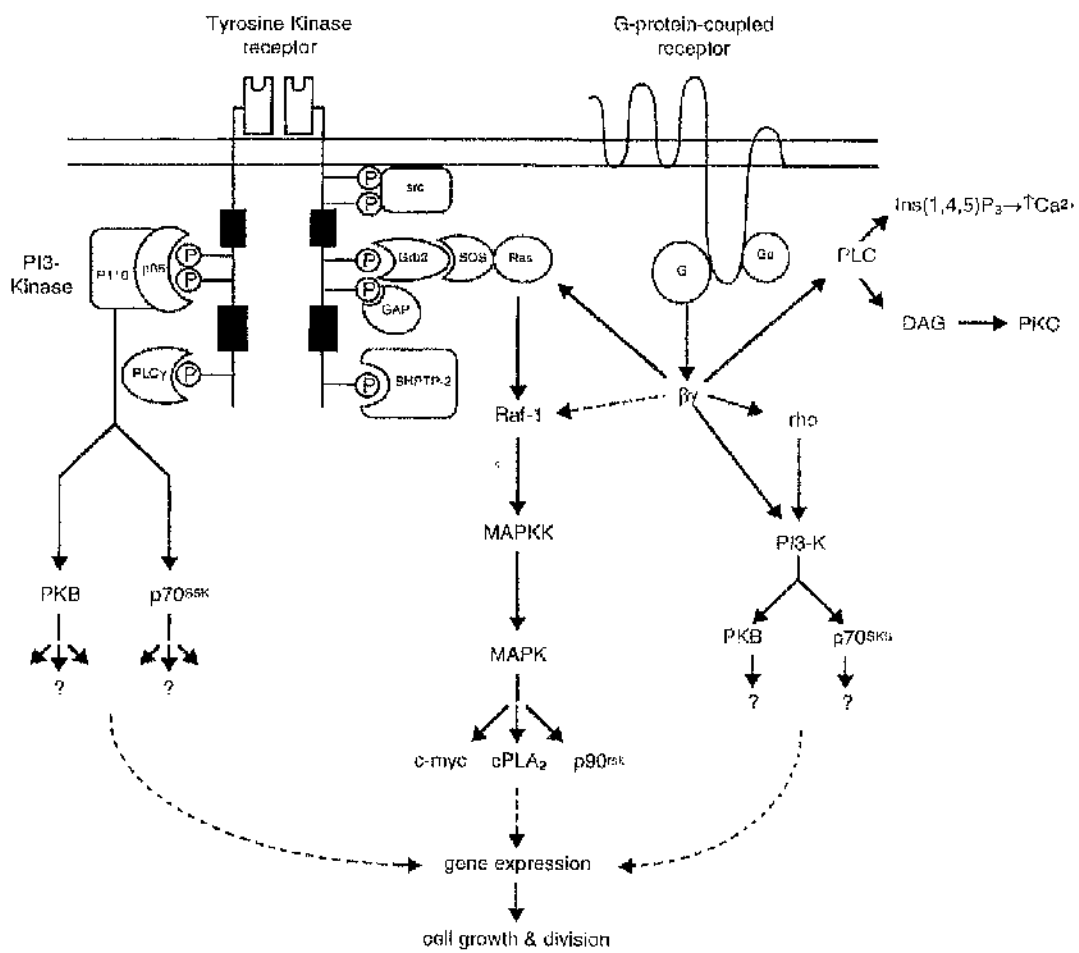
The acute phase of mitogen-stimulated glucose transport is accounted for by translocation of GLUT-1 containing vesicles to the cell surface, and also possibly by an increase in the intrinsic activity of the transporter. The chronic phase of glucose transport is mediated by an increase in GLUT-1 gene transcription and ultimately an increase in the number of glucose transporters in the cell.



# **Figure 1.4 The signal transduction mechanisms activated by tyrosine kinase receptors and G-protein-coupled growth factor receptors**

This schematic diagram illustrates a summary of the major signal transduction pathways that are activated following growth factor stimulation of the two distinct classes of receptor.

Many of the same pathways are regulated by the two distinct receptor classes i.e. phospholipase C (PLC), PI3' kinase, *ras/raf*/MAPK.



## **CHAPTER 2**

### **MATERIALS AND METHODS**

## **2.1 MATERIALS**

All reagents used in the course of the project were of a high quality and were obtained from the following suppliers:

### **2.1.1 General reagents**

All general chemicals were purchased from Fisher Scientific, Loughborough, UK or BDH, Merck Ltd, Lutterworth, Leicestershire, UK, unless otherwise stated.

#### ***Anachem, Luton, Beds, UK***

Acrylamide/ bis acrylamide mix

#### ***Boehringer Mannheim, Lewes, UK***

Tris base

Complete protease inhibitor cocktail™

#### ***Kodak Ltd, Hemel Hempstead, Hertfordshire, UK***

RP X-Omat liquid fixer/replenisher

RP X-Omat Liquid developer/replenisher

X-Omat AR film

X-Omat S film

#### ***Fisons Chemicals, Loughborough, UK***

Optiflow Safe 1 liquid scintillation cocktail

#### ***Pierce, Rockford, Illinois, USA***

BCA protein estimation kit

#### ***Premier Brands UK, Knighton Adbaston, Staffordshire, UK***

Marvel powdered milk

***Schleicher and Schuell, Dassel, Germany***

Nitrocellulose membrane (0.45µm)

***Sigma Chemical Company Ltd, Poole, Dorset, UK***

Adenosine triphosphate

Alumina

Ampicillin

Bromophenol blue

BSA Fraction V

Collagenase

Cyclic adenosine monophosphate

Cytochalasin B

2-deoxy-D-glucose

DL-dithiothreitol (DTT)

Dowex

Elastase

Ethidium bromide

3-isobutyl-1-methylxanthine (IBMX)

3-O-methyl glucose

N,N,N',N'-tetramethylethylenediamine (TEMED)

Okadaic acid

Ponceau S

Protein Kinase A, catalytic subunit

Soybean trypsin inhibitor

Triton X-100

Xylene cyanol

***Whatman International Ltd, Maidstone, UK***

Whatman 3mm filter paper

Brandell filters, FPD-200 Whatman GF/C

### **2.1.2 Antibodies**

#### ***Chemicon International, Harrow, UK***

Rabbit anti-GLUT-1

#### ***New England Biolabs, Hitchin, Herts, UK***

Rabbit anti-phospho p42/44 antibody

Rabbit anti-p42/44 antibody

Rabbit anti-phospho p38 antibody

Rabbit anti-phospho JNK antibody

#### ***Sigma, Poole, Dorset, UK***

Horseradish peroxidase (HRP)-conjugated donkey anti-rabbit IgG antibody

Antibodies to GLUT-3 and -4 were prepared in house as described in Gould *et al.*, 1992 and Brant *et al.*, 1992 respectively.

### **2.1.3 Cells**

#### ***American Type Culture Collection, Rockville, USA***

3T3-L1 Fibroblasts

Rat aortic vascular smooth muscle cells (VSMC) were prepared from Wistar-Kyoto rat aorta as described in methods section 2.3.1

### **2.1.4 Cell culture media and reagents**

#### ***Gibco BRL, Paisley, Lanarkshire, UK***

Dulbecco's modified Eagle's media (without sodium pyruvate, with 4500 mg/l glucose) (DMEM)

10000 U/ml penicillin,

10000 U/ml streptomycin,



L-glutamine 200 mM (100x)

Foetal calf serum

New born calf serum

***Sigma, Poole, Dorset, UK***

1 X Trypsin

### **2.1.5 Cell culture plastics**

***Bibby Sterilin Ltd, Stone, Staffordshire, UK***

Sterile Pipettes

13.5 ml centrifuge tubes

***Costar, Corning Incorporated, Corning, NY, USA***

75 cm<sup>2</sup> culture flasks

6-well cell culture plates

12-well cell culture plates

***AS Nunc, DK Rokslide, Denmark***

50 ml centrifuge tubes

### **2.1.6 Radioactive reagents**

***Amersham Life Science, Bucks, UK***

[<sup>32</sup>P<sub>γ</sub>] -ATP

1-[propyl-2,3-<sup>3</sup>H] Dihydroalprenolol, Code TRK 551 (DHA)

2,8-[<sup>3</sup>H] adenine

[<sup>3</sup>H] Thymidine

***NEN Dupont (UK) Ltd, Stevenage, Hertfordshire, UK***

2-deoxy-D-[2,6-<sup>3</sup>H] glucose

[<sup>3</sup>H] methyl 3-O-methyl glucose

[<sup>32</sup>P] inorganic phosphate

### **2.1.7 Agonists and inhibitors**

*Alexis, Bingham, Nottingham, UK*

8-Bromo cAMP

8-Bromo cGMP

*Calbiochem, Boston, Nottingham, UK*

Dibutyl cAMP

Dipyridamole

Milrinone

Rat recombinant PDGF-BB

Rat IGF-1

SB203580

Zaprinast

*New England Biolabs, Hitchin, Herts, UK*

PD98059

*Novo Nordisk, Copenhagen, Denmark*

Insulin

*Schering Health Care, Burgess Hill, West Sussex, UK*

Iloprost

*Sigma, Poole, Dorset, UK*

IBMX

Isoprenaline

Dihydroalprenolol

PGE<sub>1</sub>

Ro 20-1724

### **2.1.8 Molecular biology reagents**

#### ***Boehringer Mannheim, Lewes, East Sussex, UK***

T4 DNA ligase

#### ***Genosys Biotechnologies Ltd, Pampisford, Cambs, UK***

Oligonucleotide primers, as described in the results chapters

#### ***Gibco Life Technologies, Paisley, UK***

DNA size markers, 1 kilobase ladder

#### ***Invitrogen, Leek, The Netherlands***

pcDNA3 vector

#### ***New England Biolabs, Hitcham, Herts, UK***

Vent Polymerase,

#### ***Oxoid, Basingstoke, Hamps, UK***

Bacto tryptone

Yeast extract

Agar

#### ***Promega***

Restriction enzymes, Bgl II, Bam HI, Eco RI, Kpn I, Xho I

Wizard™ mini-prep kits

#### ***Qiagen, Crawley, West Sussex, UK***

Qia spin prep kits

Qiagen maxi prep kits

Qiagen Superfect transfection kit

*Stratagene, La Jolla, California, USA*

*Escherichia coli* XL1-Blue

Pfu I DNA polymerase

## **2.1.9 Protein A**

*Sigma, Poole, Dorset, UK*

Protein A sepharose

HRP-linked protein A

## **2.1.10 Transferrin texas red**

*Molecular probes, Leiden, The Netherlands*

## **2.2 BUFFERS AND MEDIA**

### **2.2.1 Cell culture media**

*Serum-free DMEM*

100 U/ml penicillin, 100 U/ml streptomycin, 2 mM glutamine in DMEM

*10% NCS/DMEM*

100 U/ml penicillin, 100 U/ml streptomycin, 2 mM glutamine, 10% (v/v) NCS in DMEM

*10% FCS/DMEM*

100 U/ml penicillin, 100 U/ml streptomycin, 2 mM glutamine, 10% (v/v) FCS in DMEM

*VSMC digestion media*

800 µg/ml collagenase, 250 µg/ml elastase, 500 µg/ml soybean trypsin inhibitor in serum-free DMEM (see above)

### ***HEPES buffered DMEM***

Serum free DMEM (see above) with 20 mM HEPES

### **2.2.2 General Buffers**

#### ***Phosphate buffered saline (PBS)***

150 mM NaCl, 10 mM NaH<sub>2</sub>PO<sub>4</sub>·2H<sub>2</sub>O, (pH 7.4)

#### ***Krebs Ringer Phosphate Buffer (KRP)***

64 mM Na Cl, 2.5 mM KCl, 2.5 mM NaH<sub>2</sub>PO<sub>4</sub>·2H<sub>2</sub>O, 0.6 mM MgSO<sub>4</sub>·7H<sub>2</sub>O, 0.6 mM CaCl<sub>2</sub>, (pH 7.4)

#### ***Lysis Buffer***

0.05% SDS (w/v), 20 mM Hepes (pH7.4), 1 mM EDTA, Complete protease inhibitor cocktail™, 1 μM NaVO<sub>4</sub>, 1 μM NaF, 1% Triton X-100 (v/v)

#### ***Tris EDTA (TE)***

10 mM Tris, 1mM EDTA (pH7.4)

#### ***PKA in vitro phosphorylation buffer***

50 mM Tris HCl (pH 7.5), 6 mM MgCl<sub>2</sub>, 1 mM DTT, 50 μM EGTA, 150 μM ATP

#### ***Adenyl cyclase assay stop solution***

5% TCA, 1 mM cAMP, 1 mM ATP

### **2.2.3 SDS-PAGE Buffers**

#### ***Running Buffer***

25 mM Tris-base, 192 mM glycine, 0.1% (w/v) SDS

### ***Sample buffer***

93 mM Tris hydrochloride pH6.8, 20 mM dithiothreitol, 1 mM sodium EDTA, 10% glycerol (w/v), 2% SDS (w/v), 0.002% bromophenol blue (w/v).

The dithiothreitol was added immediately before use.

### ***Urea sample buffer***

As normal sample buffer with the addition of 40 mM urea

## **2.2.4 Western Blot Buffers**

### ***Transfer Buffer***

25 mM  $\text{NaH}_2\text{PO}_4 \cdot 2\text{H}_2\text{O}$ , (pH 6.5)

### ***TBS-T***

150 mM NaCl, 150 mM Tris, 0.02% Tween 20 (v/v), (pH 7.4)

### ***Stripping Buffer***

100 mM  $\beta$ -Mercaptoethanol, 2% SDS (w/v), 62.5 mM Tris (pH 6.7)

## **2.2.5 Molecular Biology Buffers**

### ***DNA Loading Buffer***

0.25% Bromophenol blue (w/v), 0.25% xylene cyanol FF (w/v), 30% glycerol in  $\text{H}_2\text{O}$  (v/v)

### ***Ethidium bromide***

Stock of 10 mg/ml in  $\text{H}_2\text{O}$  made, use at final concentration of 0.5  $\mu\text{g/ml}$

### ***L-Agar***

As L-Broth plus 1.5% agar (w/v)

### ***L-Broth***

1% Bacto tryptone (w/v), 0.5% yeast extract (w/v), 1% NaCl (w/v)

### ***TAE***

40 mM Tris-acetate, 10 mM EDTA

### ***Competent bacteria buffer 1***

30 mM potassium acetate, 100 mM RbCl, 10 mM CaCl<sub>2</sub>, 50 mM MnCl<sub>2</sub>, 15% glycerol (v/v)

### ***Competent bacteria buffer 2***

10 mM MOPS (pH6.5), 75 mM CaCl<sub>2</sub>, 100 mM RbCl, 15% glycerol (v/v)

## **2.3 RAT AORTIC VASCULAR SMOOTH MUSCLE CELL CULTURE**

### **2.3.1 Preparation and growth of vascular smooth muscle cells from rat aorta**

Rat aortic vascular smooth muscle cells were kindly prepared and supplied by Alison Devlin from Anna Dominczak's group, Department of Medicine and Therapeutics, University of Glasgow, Western Infirmary, Glasgow. Vascular smooth muscle cells were isolated from the thoracic aorta of Wistar-Kyoto (WKY) rats by enzymic digestion (as described Stanley *et al.*, 1993). All utensils and media used were sterile. Thoracic aorta were dissected from the rat and placed into a sterile universal containing 20 ml of serum free DMEM (2.2.1) on ice. Fatty tissue was removed by blunt dissection and the aorta was washed clean of blood. The intercostal branches and arch were removed from the aorta. The aorta was transferred into a small sterile cell culture dish and 2.5 ml of digestion media was added (section 2.2.1) and incubated at 37 °C in a humidified atmosphere of 5% CO<sub>2</sub> for 30 minutes. The adventitia was then stripped from the aorta, which comes off like a "sleeve". The aorta was cut longitudinally with small scissors and placed in a further 2.5 ml of fresh digestion media to digest endothelium and was incubated for 15 minutes at 37 °C in a humidified atmosphere of 5% CO<sub>2</sub>. Subsequently the aorta was chopped very finely

with small scissors and then transferred to a clean dish where 2.5 ml of a 1:8 (v/v) dilution of the digestion media added and incubated overnight at 37 °C in a humidified atmosphere of 5% CO<sub>2</sub>. The following morning 1.05 ml of 2.5 mg/ml collagenase in serum free DMEM (section 2.2.1) was added to the aorta digestion (final concentration of 1.5mg/ml collagenase, ~ 3 mg per aorta) and was incubated at 37°C in a humidified atmosphere of 5% CO<sub>2</sub> for 30-60 minutes. The cells were triturated with a fine-bore pasteur pipette to disaggregate the tissue into a single cell suspension. The cells were removed to a sterile universal on ice. 10 ml of 20% FCS/DMEM (section 2.2.1) was added to the cells and centrifuged at 1000 x g for 10 minutes at 4 °C. The supernatent was aspirated from the cells and the cell pellet was resuspended in 20% FCS/DMEM.

Cells prepared as described above were positively identified as vascular smooth muscle cells by immunofluorescent staining for smooth muscle-specific  $\alpha$ -actin and skeletal muscle/smooth muscle myosin (as described in Stanley *et al.*, 1993).

Cells, once positively identified as VSMC, were maintained in 10% FCS/DMEM (section 2.2.1), and grown in a humidified incubator at 37 °C in an atmosphere of 5% CO<sub>2</sub>. The media was replaced every two days.

### **2.3.2 Trypsination of VSMC**

When the cells were approaching 100% confluent they were removed from flasks using trypsin. The media was aspirated from the flasks and the cells rinsed in 5ml of sterile PBS. The PBS was aspirated and replaced with 5 ml of a 1:5 dilution of trypsin in PBS. The flask was then placed in the incubator for 5 minutes, allowing the cells to float before stopping trypsination by addition of an appropriate volume of 10% FCS/DMEM (section 2.2.1). The diluted cells were subsequently seeded on to new cell culture dishes. VSMC were not diluted more than 1:7.



### **2.3.3 Storage of rat aortic VSMC in liquid nitrogen**

Cells were grown to confluency on 75 cm<sup>2</sup> flasks and trypsinised as described 2.3.2. The cells were resuspended in 5 ml of 10% FCS/DMEM (section 2.2.1). The cell suspension was centrifuged at 1000 x g at room temperature for 2 minutes, the supernatant was aspirated and the cells resuspended in 1 ml of 10% FCS/DMEM with 10% DMSO (v/v) previously equilibrated in 5% CO<sub>2</sub> for 1 hour at 37 °C. The cell suspension was aliquoted into cryotubes, packed in cotton wool and frozen overnight at -80 °C. The tubes were then transferred to liquid nitrogen for long-term storage.

### **2.3.4 Resurrection of frozen cell stocks from liquid nitrogen**

Cell aliquots were removed from liquid nitrogen and placed in a 37 °C water bath. The tube was transferred to the cell culture sterile flow hood where the cells were triturated gently with a sterile pipette to disperse any large aggregates of cells. The cells were then seeded onto 25 cm<sup>2</sup> flasks containing 10% FCS/DMEM and maintained in an incubator at 37 °C in a humidified atmosphere of 5% CO<sub>2</sub>.

## **2.4 3T3-L1 FIBROBLAST CULTURE**

### **2.4.1 Growth of 3T3-L1 fibroblasts**

3T3-L1 fibroblasts were grown on cell culture flasks and plates in 10% NCS/DMEM (section 2.2.1). The medium was replaced every 2 days, the cells being kept in an incubator at 37 °C in a humidified atmosphere at 10% CO<sub>2</sub>.

### **2.4.2 Trypsination of 3T3-L1 fibroblasts**

When the cells were 70-80% confluent they were removed from flasks using trypsin. The media was aspirated from the flasks and the cells rinsed in 5 ml of sterile PBS. The PBS was aspirated and replaced with 2 ml of trypsin. The flask was then placed in the incubator for 5 minutes, allowing the cells to float before stopping trypsination by

addition of an appropriate volume of 10% NCS/DMEM. The diluted cells were subsequently seeded on to new cell culture dishes. 3T3-L1 cells were not diluted more than 1:10.

#### **2.4.3 Storage of 3T3-L1 fibroblasts in liquid nitrogen**

Cells were grown to confluency on 75 cm<sup>2</sup> flasks and trypsinised as described 2.4.2. The cells were resuspended in 5 ml of 10% (v/v) NCS/DMEM. The cell suspension was centrifuged at 1000 x g at room temperature for 2 minutes. The supernatant was aspirated and the cells resuspended in 1 ml of 10% NCS/DMEM with 10% DMSO (v/v) equilibrated in 10% CO<sub>2</sub> for 1 hour. The cell suspension was aliquoted into cryotubes, packed in cotton wool and frozen overnight at -80 °C. The tubes were then transferred to liquid nitrogen for long-term storage.

#### **2.4.4 Resurrection of frozen cell stocks from liquid nitrogen**

Cell aliquots were removed from liquid nitrogen and placed in a 37 °C water bath. The tube was transferred to the cell culture sterile flow hood where the cells were triturated gently with a sterile pipette to disperse any large aggregates of cells. The cells were then seeded onto 25 cm<sup>2</sup> flasks containing 10% NCS/DMEM and maintained in an incubator at 37 °C in an atmosphere of 10% CO<sub>2</sub>.

### **2.5 2-DEOXY-D-GLUCOSE UPTAKE IN RAT AORTIC VSMC**

Uptake of 2-deoxy-D-glucose was measured using the method of Gibbs *et al.* (1988) and Frost and Lane (1985).

In all experiments cells were used at passages 5-16. For transport assays cells were grown to confluency on 6-well plates. Prior to use cells were quiesced in serum-free DMEM for 36-48 hours. The cell monolayer was washed in 2 ml KRP (section 2.2.2) at 37 °C, then incubated in 950 µl of KRP, 0.25% BSA. Drugs/agonists were added at the appropriate concentration and cells were incubated for the appropriate period of time in humidified 37 °C incubator, as noted in the figure legends/text.

5 minutes prior to the end of incubation time the cells were transferred on to a hot plate at 37 °C. The uptake of sugar was initiated by the addition of 50 µl of [<sup>3</sup>H] 2-deoxy-D-glucose to a final concentration of 50 µM and 0.5 µCi/ml. The reaction was terminated 5mins after addition of deoxy glucose by rapidly decanting the KRP buffer (containing [<sup>3</sup>H] 2-deoxy-D-glucose) and immediately immersing the 6-well plate in a large volume of ice-cold PBS. After air-drying the plates 1 ml of 1% Triton X-100 (v/v) in water was added to each well and plates shaken for 1 hour. The cell-associated radioactivity was measured by scintillation counting. To determine the non-specific glucose uptake of 2-deoxy-D-glucose, the inhibitor cytochalasin B, was added to three of the 6 well of each plate, at a final concentration of 10 µM, just before the addition of the radioactive deoxy glucose. The radioactivity in the wells treated with cytochalasin B is a measure of non-specific deoxy-glucose associated with the monolayer. This value was subtracted from the counts obtained in the absence of cytochalasin B to provide specific transport rates.

## **2.6 3-*O*-METHYL GLUCOSE TRANSPORT IN VSMC**

The uptake of 3-*O*-methyl glucose transport is measured exactly as described for 2-deoxy-D-glucose (section 2.5) except that cold 3-*O*-methyl glucose and [<sup>3</sup>H] 3-*O*-methyl glucose replace labelled and unlabelled for 2-deoxy-D-glucose at the same concentrations, and the times of incubation with cells was adjusted as shown in the figure legends.

## **2.7 SDS/POLYACRYLAMIDE GEL ELECTROPHORESIS**

SDS/PAGE was carried out using Bio-Rad mini-PROTEAN II or Hoefer large gel apparatus.

The Bio-Rad Mini-PROTEAN gels had a stacking gel of 2 cm and the Hoefer stacking gel was 5 cm. The stacking gel was composed of 5% acrylamide (w/v),

0.136% bisacrylamide (w/v) in 125 mM Tris-HCl (pH 6.8), 0.1% SDS (w/v), polymerised with 0.1% ammonium persulphate (w/v) and 0.05% N, N, N', N'-tetramethylethylenediamine (TEMED) (v/v).

The separating gel consisted of an appropriate percentage of acrylamide in 0.383 mM Tris-HCl (pH 8.8), 0.1% SDS (w/v), and polymerised with 0.1% ammonium persulphate (w/v) and 0.019% N, N, N', N'-tetramethylethylenediamine (TEMED) (v/v).

The protein samples were solubilised in sample buffer (see 2.2.3) and loaded into the wells of the stacking gel. The gel was then immersed in running buffer (section 2.2.3) and electrophoresed until the tracking dye had run to the bottom of the gel.

## **2.8 WESTERN BLOTTING OF PROTEINS**

After separation of proteins by SDS/PAGE, as described 2.5, gels were removed from the apparatus. Each gel was then placed on a nitrocellulose sheet (pore size 0.45  $\mu\text{m}$ ) pre-soaked in transfer buffer. This was then sandwiched between two layers of Whatman 3MM filter paper, also presoaked in transfer buffer. The sandwich was placed in a cassette and transfer of the proteins onto the nitrocellulose was performed using either a Bio-Rad trans-blot tank for large gels or Bio-Rad mini trans-blot tank for the mini-gels. Transfer was achieved at a constant current of 250 mA for 2 hours at room temperature. The nitrocellulose membranes were then removed and the efficiency of transfer was determined by staining the nitrocellulose with Ponceau S solution prior to blocking (section 2.8.1).

### **2.8.1 Detection of proteins on nitrocellulose with Ponceau S**

To detect proteins transferred onto nitrocellulose sheets, the nitrocellulose was soaked in a 1:5 dilution (in distilled water) of ponceau S solution for 1-2 minutes. When bands could be seen the excess ponceau S solution was rinsed from the nitrocellulose

in distilled water. The nitrocellulose was then used for immunodetection of proteins (section 2.8.2).

### **2.8.2 Immunodetection of proteins on nitrocellulose membranes**

To block non-specific binding sites on the nitrocellulose, the membrane was incubated in 5% milk powder (w/v) in TBS-T (section 2.2.4) overnight at 4°C. The membrane was then incubated in 1% milk powder in TBS-T containing the appropriate antibody at the concentration specified, for 1 hour at room temperature on a shaking platform. After incubation with primary antibody the membrane was washed in TBS-T (two rinses, two 5 minute washes and two 15 minute washes, wash with large volume). The membrane was then incubated with appropriate HRP-linked secondary antibody or HRP-linked protein A (HRP-linked donkey anti-rabbit at 1:2000 dilution or HRP-linked protein A at 1:500 dilution) in 1% milk powder in TBS-T for 1 hour at room temperature on a platform shaker. Membranes were washed as described above. The blot was developed using ECL reagent from Amersham, according to the manufacturers directions. ECL generates light when horseradish peroxidase (linked to the secondary antibody or protein A) along with H<sub>2</sub>O<sub>2</sub> (in the ECL reagent mix) catalyse the oxidation of luminol (also in the ECL mix). Immediately after oxidation the luminol is in an excited state which then decays to the ground state via a light-emitting pathway. The membrane was therefore exposed to Kodak X-Omat S film and developed in an X-Omat processor.

## **2.9 PREPARATION OF WHOLE CELL LYSATES**

Cells were grown to confluency in 75 cm<sup>2</sup> flasks. Media was aspirated from the cells and the cells washed in 2 x 5 ml of ice-cold PBS per flask. The cells were scraped into 5 ml of ice-cold PBS per flask and the cells from 4-5 flasks pooled. Cells were pelleted by centrifuging the cells at 1000 x g at 4 °C for 10 minutes, the supernatant was aspirated and the cell pellet was resuspended in 1ml of lysis buffer (section 2.2.2). The cells were then incubated on ice for 30 minutes. The cells were passed through a gauge 25 needle several times to ensure thorough lysis of cells. The lysate was then

measured for protein content using BCA protein estimation kit (section 2.1.1), from Pierce, according to manufacturer's instructions.

For 6-well plates, each well was rinsed twice in 1 ml ice-cold PBS before the addition of 200  $\mu$ l of SDS-PAGE loading buffer (section 2.2.3). Cells were left at room temperature with the SDS-PAGE loading buffer for 30 minutes and then scraped into eppendorfs. To ensure that the cells were properly lysed they were passed through a gauge 25 needle several times.

## **2.10 PREPARATION OF TOTAL CELL MEMBRANES**

Cells were grown to confluency in 75 cm<sup>2</sup> flasks. The media was aspirated from the cells and the cells were washed in 2 x 5 ml of ice-cold PBS per flask. The cells were scraped into 5 ml of ice-cold PBS per flask and the cells from 4-5 flasks pooled. Cells were pelleted by centrifugation at 1000 x g at 4 °C for 10 minutes and the cell pellet resuspended in 1ml TE (section 2.2.1). Cells were passed through a gauge 25 needle five times and then dounce homogenised with ~30 twisting strokes. The homogenate was centrifuged for 7 minutes at ~500 x g, 4 °C in a microfuge to pellet the nuclei. The supernatant was centrifuged at 40 000 x g at 4 °C for 30 minutes and the pellets were resuspended in 200-500  $\mu$ l TE depending on pellet size. The membrane preparations were measured for protein content using BCA protein estimation kit, from Pierce, according to manufacturers instructions (2.11).

## **2.11 THYMIDINE INCORPORATION**

VSMC were grown to ~ 40% confluency on 6-well plates. The media was aspirated from the cells and 1 ml of serum free DMEM (section 2.2.1) added per well. The appropriate drugs were added to the wells and the cells were incubated for at 37 °C in a humidified atmosphere of 5% CO<sub>2</sub> for 24 hours. For the last 6 hours of the 24 hour stimulation 0.5  $\mu$ Ci of [<sup>3</sup>H] thymidine was added to each well. The reactions were

terminated by washing each well twice with 2 ml ice-cold PBS. Proteins were precipitated by washing each well three times with 2 ml of ice-cold 5% TCA (w/v) and twice with 2 ml ice-cold ethanol. The plates were left to air dry for 15 minutes, and the precipitate was dissolved in 1 ml of 0.3M NaOH. The plates were shaken overnight to ensure the precipitate was thoroughly dissolved. The radioactivity associated with each well was determined by scintillation counting.

## **2.12 IMMUNOPRECIPITATION OF GLUTs FROM VSMC**

30  $\mu$ l of protein A sepharose was washed three times with 1 ml lysis buffer (section 2.2.2). 6  $\mu$ l of the appropriate antibody was added to the protein A sepharose and ~15  $\mu$ l of lysis buffer (2.2.2) to give a final volume of ~ 50  $\mu$ l. The mixture was then shaken on vibramax at setting 18 for 4 hours at 4 °C. 500  $\mu$ g - 1 mg of VSMC whole cell lysate (see section 2.9) was added to the antibody, protein A sepharose mix and incubated with end over end rotation overnight at 4 °C. Samples were centrifuged at 1500 x g in microfuge to pellet the protein A sepharose beads along with any immunoprecipitated protein. The beads were washed in twice with 1 ml lysis buffer and then once with 1 ml lysis buffer containing 0.1% Triton X-100. The beads with protein bound were then used in assays or resuspended in urea sample buffer (section 2.2.3) for western blotting.

## **2.13 *IN VITRO* PHOSPHORYLATION OF GLUTs WITH PROTEIN KINASE**

### **A**

The reactions were set up as follows:

20 units of PKA catalytic subunit was mixed with substrate prepared by immunoprecipitation (section 2.12) and made to a total volume of 47  $\mu$ l with assay buffer (section 2.2.2). To start the phosphorylation 3  $\mu$ l of [ $\gamma^{32}$ P] ATP, 1  $\mu$ Ci/ $\mu$ l, was added to each reaction and incubated at 30 °C for 30 minutes. Adding an appropriate volume of SDS-PAGE urea buffer stopped reactions. Samples were then run on SDS-

PAGE (section 2.7) and the gels were fixed in 14% acetic acid, 7% methanol, dried and exposed to X-ray film to identify proteins that had been phosphorylated.

Immunoprecipitates could also be dephosphorylated prior to *in vitro* phosphorylation as described below:

To each immunoprecipitate 250 U of protein phosphatase 2A (gift from Professor H. Nimmo, Bower Building, I.B.I.S, University of Glasgow) was added and buffer (50 mM Tris pH 7.5, 1 mM DTT, 50  $\mu$ M EGTA) added to a final volume of 50  $\mu$ l. This mix was incubated for 30 minutes at 30 °C on a vibramax shaker. The phosphatase was inactivated by the addition of okadaic acid (200 nM) and phosphorylation carried out as described above.

## **2.14 *IN VIVO* PHOSPHORYLATION OF GLUTs**

VSMCs were grown to confluency on 6-well plates and quiesced in serum-free DMEM (section 2.2.1) for 36-48 hours. The cells were washed twice with 2 ml of phosphate-free DMEM per well and 0.75 ml of phosphate-free DMEM with 0.2 mCi/ml [ $^{32}$ P] orthophosphoric acid added per well, and the cells incubated for 90 minutes at 37°C in a humidified atmosphere of 5% CO<sub>2</sub>. This allows the intracellular pool of ATP to become  $^{32}$ P labelled. After the 90-minute labelling, appropriate agonists/drugs were added to the cells (as indicated in the text) and cells incubated at 37°C in a humidified atmosphere of 5% CO<sub>2</sub>. To stop the reactions the cells were placed on ice, the media was aspirated off and the cells were washed twice with 3 ml ice-cold PBS (section 2.2.2). The cells were scraped into 500  $\mu$ l of lysis bufer per well (section 2.2.2), transferred into eppendorfs, then incubated on ice for 30 minutes to lyse cells. The lysates were then used for immunoprecipitation, as described in section 2.12. After immunoprecipitation the samples were resuspended in ~40  $\mu$ l of urca sample buffer (section 2.2.3) and run on a 10% SDS-PAGE (section 2.7). Gels were then dried and exposed to X-ray film to identify proteins that had been phosphorylated.



## 2.15 $\beta$ 2 BINDING ASSAYS

Assays were carried out as described in MacEwan *et al.* (1996)

Briefly, total cell membranes were prepared as described in section 2.10. Reactions were assembled as follows:

To determine total DHA binding, an appropriate amount of membrane protein (~10  $\mu$ g) and 2 nM [ $^3$ H] DHA were mixed in a total volume of 250 $\mu$ l TE (section 2.2.2). To determine non-specific binding reactions were set up as for total binding but in the presence of 1mM unlabelled DHA to compete for specific binding sites. The reactions were incubated at 30°C for 30 minutes. Reactions were terminated by rapid filtration through Brandell apparatus with a Whatman GF/C filter fitted and washed three times in ~5 ml of ice-cold TE buffer. The [ $^3$ H] DHA associated with each filter was determined by scintillation counting.

To determine the amount of specific binding sites in each sample, the dpm obtained for non-specific binding is subtracted from that of total binding to get specific dpm. Using the specific activity of the [ $^3$ H] DHA the amount of DHA binding sites can be determined using the calculation below.

$$\frac{\text{Specific dpm}}{\text{Specific activity}} \times \frac{1000}{\mu\text{g protein}} = \text{fmol/mg}$$

## 2.16 ADENYL CYCLASE ASSAY IN VSMC

Determination of adenylyl cyclase catalytic activity was carried out as described by Wong *et al* (1994) Cells were grown on 12-well plates to confluency and then quiesced by incubation in serum free DMEM for 36-48 hours. 24 hours prior to assay the cells were labelled with [ $^3$ H] adenine at 1  $\mu$ Ci/ml. Cells were washed in 2 ml of HEPES buffered DMEM (section 2.2.1) and then 0.5 ml of HEPES buffered DMEM with 1mM IBMX was added to each well with the appropriate drugs or agonists. Cells

were then incubated on a hot plate at 37°C for 30 minutes. To terminate the reactions, the media was aspirated from cells and 1 ml of ice-cold stop solution (section 2.2.2) was added to each well and incubated on ice for 30 minutes to lyse cells. Separation of radiolabelled cAMP from ATP was achieved using the double-column method described by Wong *et al* (1994).

## **2.17 MOLECULAR BIOLOGY METHODS**

### **2.17.1 PCR reactions**

PCR reactions were carried out with the following basic components

20 ng template DNA  
40 pmol primer 1  
40 pmol primer 2  
200 µM dNTPs (200µM of each A, C, G, T)  
2.5 units Pfu I polymerase  
10 µl Pfu I polymerase buffer (10x)  
X µl sterile H<sub>2</sub>O to final volume of 100µl

All components were mixed except for Pfu I. The reactions were incubated for 10 minutes at 95°C then Pfu I was added ("hot start" PCR). After addition of Pfu I the cycles were as follows:

3 cycles of     95°C 1 minute  
                  40°C 5 minutes  
                  72°C 5 minutes

Followed by

27 cycles of    95°C 1 minute  
                  75°C 2minutes  
                  72°C 5 minutes

PCR products were then analysed by agarose gel electrophoresis.

### **2.17.2 Agarose gel electrophoresis of DNA**

DNA was analysed by agarose gel electrophoresis. All gels used were 0.7% agarose in 1 x TAE, containing 0.5 µg/ml ethidium bromide. DNA was visualised under UV light. The size of DNA fragments was determined with the use of DNA 1 kB ladder.

### **2.17.3 Preparation of competent bacteria**

*E.coli* (strain XL1-Blue) were grown in L-broth (section 2.2.4) to an optical density of 0.4 at. The cells were chilled on ice, and then centrifuged at 1000 x g for 10 minutes at 4°C. The L-broth was aspirated from cells and the cells were resuspended in 40ml buffer 1 (section 2.2.5). The cells were chilled on ice for 5 minutes and then centrifuged at 1000 x g. The cell pellet was resuspended in 4 ml buffer 2 (section 2.2.5) and aliquoted in 220 µl aliquots and stored at -80°C prior to use.

### **2.17.4 Transformation of competent bacteria**

An aliquot of competent bacteria (prepared as described 2.17.1) was thawed and 50µl of the cells were added to a sterile tube. Add an appropriate amount of DNA was added to the cells (about 1-50ng) and incubated on ice for 15 minutes. The cells were heat shocked by incubation at 42°C for 90 seconds, then returned to ice for 2 minutes. 450µl of L-broth was added and the cells incubated at 37°C for 45 minutes with shaking. 100µl of each transformation reaction was plated on to L-agar plates with the appropriate antibiotic mix. The plates were incubated overnight at 37°C to allow growth of colonies.

### **2.17.5 Preparation of DNA**

Both large and small scale DNA preparations were made using QIAGEN DNA prep kits according to manufacturers instructions. Small scale preps were made using the

QIA spin prep kit, and large scale preps were made using the QIAGEN maxi prep kit. Both kits follow a basic alkaline lysis method. Cells were lysed under alkaline conditions in the presence of RNase A and the lysate subsequently neutralised and adjusted to high salt binding conditions. The lysate was passed over the QIAGEN silica-gel membrane, which ensures only DNA is absorbed but all other components are not retained on the membrane. DNA was washed on the membrane and eluted in the appropriate buffer.

#### **2.17.6 Gel Extraction of DNA**

Gel extractions were carried out using Promega Wizard™ prep kits according to manufacturers instructions. Briefly, to purify DNA from agarose gel the band of interest was excised from the gel and 1 ml of resin (from kit) was added. The gel slice was melted in the resin at 65°C for 10-15 minutes. The melted gel slice is passed over a Wizard™ mini prep column, to bind DNA and resin. DNA was washed on column and eluted in TE.

#### **2.17.7 Restriction of DNA**

Restriction of double stranded DNA was carried out using restriction enzymes from Promega according to manufacturers instructions. In general reactions were as follows:

1-5 µg DNA

5 µl restriction enzyme(s)

5 µl Buffer

X µl H<sub>2</sub>O to 50 µl final volume

Reactions were incubated for 1-2 hours at 37°C. Products of restriction were visualised by agarose gel electrophoresis.

### **2.17.8 Ligation of DNA**

DNA was restricted with the appropriate enzymes as described 2.16.7 ready for ligation. Ligations were carried using T4 DNA ligase from Boehringer Mannheim according to manufacturers directions. Generally twice as much insert DNA as vector DNA was used in each ligation, as quantified by gel electrophoresis. Reaction were typically carried out in a final volume of 10-15  $\mu$ l.

### **2.17.9 Phenol/Chloroform extraction of DNA**

To stop enzyme reactions and extract DNA from these reactions a phenol/chloroform extraction was carried out. This involved washing the reaction in an equal volume of phenol twice, then washing in an equal volume of chloroform once. DNA was then concentrated by ethanol precipitation (section 2.17.10).

### **2.17.10 Ethanol precipitation of DNA**

To concentrate DNA samples ethanol precipitation was carried out. Samples were mixed with 2 x volume of ethanol and 0.1 x volume of 5 M Na Acetate. The mixture was incubated for 1 hour at  $-20^{\circ}\text{C}$  then centrifuged at 15 000 x g for 10 minutes to pellet precipitated DNA. The pellet was then washed in 1 ml of 70% ethanol, and centrifuged at 10 000 x g to re-pellet DNA. The 70% ethanol was aspirated from the pellet, the pellet air-dried and resuspended in a small volume of TE. DNA was quantified by agarose gel electrophoresis.

### **2.17.11 Sequencing of DNA**

Samples sequenced by the University of Glasgow Molecular Biology Support Unit (MBSU) using the Big Dyes kit from Perkin Elmer and analysed using the ABI Prism 377 sequencer.

### 2.17.12 RT-PCR

mRNA was made using the Rneasy kit from QIAGEN. Two 75 cm<sup>2</sup> flasks of VSMCs were grown to confluency and cells scraped from flasks into 2 ml of ice-cold sterile PBS, and RNA prepared according to manufacturers instructions. Reverse transcription and PCR carried out using Wizard RT-PCR kit from Promega. Reverse transcription reactions were as follows:

3 µg VSMC RNA

3 µl dT primer (use 0.5 µg primer/ µg of RNA)

X µl RNase free H<sub>2</sub>O to a final volume of 10 µl

Reactions incubated at 70 °C for five minutes to allow primer/RNA annealing. Then to each reaction the following reagents are added:

5 µl MgCl<sub>2</sub> (25 mM)

5 µl 5 x AMV/tfl buffer

2.5 µl dNTPs (200µM of each A, C, G, T)

0.5 µl RNasin

2 µl AMV

X µl RNase free H<sub>2</sub>O to final volume of 25 µl

The reaction is then incubated at 42 °C for 60 minutes to allow extension.

PCR reactions were then set up as below:

5 µl Reverse transcription

5 µl Taq Mg free buffer

5 µl MgCl<sub>2</sub> (25 mM)

1 µl dNTPs (to a final of 200 µM)

25 pmol primer 1      ) Primers are defined in main text

25 pmol primer 2      )

1 µl Taq

X µl Sterile H<sub>2</sub>O to a final volume of 50 µl

PCR cycles were as follows:

1 x     95°C   5 minutes

5 x     95°C   45 seconds  
         55°C   1 minute  
         72°C   1.5 minutes

25 x    95°C   45 seconds  
         55°C   1 minute  
         72°C   1.5 minutes

1 x     72°C   10 minutes

PCR products were analysed by agarose gel electrophoresis (section 2.17.2).

## **2.14 CONFOCAL MICROSCOPY**

Cells were visualised using a Zeiss 4 laser scanning confocal microscope using either 40X, 63X or 100X Plan-APOCHROMAT 1.4 NA oil-immersion objectives, with samples on a heated stage to provide a bathing medium 37°C. Images were collected using either (or both) a 488 nm or a 543 nm laser with the appropriate filter sets for collection of the GFP signal (band-pass 505-520 nm) or red signals (long-pass 590 nm). Data files were saved in .TIF format and analysed using Metamorph software (Universal Imaging, CA).

## **CHAPTER 3**

### **CHARACTERISATION OF GLUCOSE TRANSPORT IN RAT AORTIC VASCULAR SMOOTH MUSCLE CELLS IN RESPONSE TO PLATELET-DERIVED GROWTH FACTOR**



### 3.1 AIMS

The aims of this chapter are:

1. To determine which glucose transporters are expressed in the aortic vascular smooth muscle cells (VSMC).
2. To determine the effect of platelet-derived growth factor (PDGF-BB) on the rate of glucose transport in VSMC.
3. To determine which signalling pathways are involved in mediating the effects of PDGF-BB on glucose transport in VSMC.

### 3.2 INTRODUCTION

An increase in vascular smooth muscle cell proliferation is fundamental to the progression of atherosclerotic plaques (Ross, 1993). Many growth factors are secreted from the cells involved in plaque formation, which can stimulate VSMC proliferation (Bobik & Campbell, 1993). Platelet derived growth factor (PDGF) is considered to be a principle regulator of VSMC proliferation in plaque development, and is secreted from the endothelial cells, platelets, activated macrophages and the smooth muscle cells themselves during plaque development (see section 1.1.2) (Ross, 1993, Bobik & Campbell, 1993).

A common early response of cells to all growth factors is an increase in the rate of glucose transport, to provide the cells with the extra energy required for cell growth and differentiation (Thomson & Gould, 1997). As an increase in proliferation of VSMC is an important step in atherosclerotic plaque development, it is reasonable to hypothesize that this is accompanied by an increase in glucose transport in these cells. However, very little is known about the regulation of glucose transport in these cells. Most studies on glucose transport in VSMC, to date, have concentrated on the effects of insulin and IGF-1. Both insulin and IGF-1 have been reported to induce a 1.2 to 3-fold stimulation of glucose transport in VSMCs (Sowers, 1996, Fujiwara & Nakai, 1996). In both of these studies, IGF-1 stimulates a greater increase in glucose transport than insulin. This suggests that the effect of insulin in these cells may be mediated by its interaction with the IGF-1 receptor, rather than via the insulin receptor itself. To date, no published studies have described the effect of PDGF on the rates of glucose transport in these cells.

Currently there is controversy as to which glucose transporters are expressed in VSMC. Sower's group have reported that the insulin-responsive glucose transporter GLUT-4 is present in VSMC (Sowers, 1996), whereas others have been unable to detect GLUT-4 mRNA and demonstrated the presence of GLUT-1 mRNA only (e.g. Kihara *et al.*, 1998). As insulin stimulates a relatively low fold increase in glucose transport in these cells, it is unlikely that this is mediated by GLUT-4.

Very little is known about the signalling mechanisms mediating glucose transport in response to growth factors (discussed fully in Chapter 1). To date, it is clear that there is a role for PI3' kinase (Gould, *et al.*, 1994, Clarke *et al.*, 1994, Barros *et al.*, 1995), and MAP kinase (Gould *et al.*, 1995) in mediating growth factor-stimulated glucose transport. Apart from the involvement of these two signalling pathways, the mechanisms by which growth factors increase glucose transport are largely unclear.

In VSMC, PI3' kinase has been shown to be involved in mediating insulin and IGF-1 stimulated transport (Fujiwara & Nakai, 1996). Both wortmannin and LY294002 inhibited insulin- and IGF-1-stimulated glucose transport. As well as the involvement of PI3' kinase, studies have shown a role for  $Ca^{2+}$  in regulating glucose transport in VSMC. Angiotensin II stimulated transport was inhibited by growing VSMC in media with low levels of  $Ca^{2+}$  (Quinn *et al.*, 1998). Apart from the role of PI3' kinase and calcium, very little is known about the regulation of glucose transport in VSMC.

Here, the level of the glucose transporters GLUT-1, GLUT-3 and GLUT-4 in the rat aortic vascular smooth muscle cell line was determined by immunoblotting. The levels of different GLUT isoforms in cultured VSMCs and VSMCs freshly isolated from aorta was determined. The ability of platelet-derived growth factor to regulate glucose transport in these cells was also determined. PDGF-BB was found to be stimulatory with regard to glucose transport in VSMC, and the role of the signalling molecules PI3' kinase and the MAP kinases, p38, p42/44 and JNK, in regulating PDGF-BB-stimulated glucose transport was determined.

### 3.3 RESULTS

#### 3.3.1 Analysis of glucose transporter expression in rat aortic vascular smooth muscle cells

The presence of glucose transporters in VSMCs was examined. GLUT-1 and GLUT-4 have been reported in VSMC, and GLUT-3, the brain-type glucose transporter, is expressed in various non-neuronal tissues, so I sought to determine whether these isoforms were expressed in VSMCs.

To analyse which of the glucose transporters were present in VSMCs, samples of whole cell lysates from cultured VSMCs (passage 12) were subjected to immunoblotting. Both GLUT-1 and GLUT-3 were expressed in VSMC as determined by the detection of a band of ~49 kDa with antibodies to the C-terminal regions of GLUT-1 and GLUT-3 respectively (Figure 3.1). However there was no detectable GLUT-4, as determined by immunoblotting, in the VSMC lysates (Figure 3.1). This contradicts some previous publications which had demonstrated the expression of GLUT-4 (Sowers, 1996) in freshly isolated aortic VSMCs. Our inability to detect GLUT-4 could be because *GLUT-4* expression was decreased during passage. We therefore sought to determine if GLUT-4 was present in freshly isolated cells. VSMCs were isolated from fresh aorta and whole cell lysates were prepared and subjected to immunoblotting. A band of ~49 kDa, corresponding to GLUT-4 was indeed detected by immunoblotting, as was GLUT-1 (Figure 3.2). There was, however, no detectable GLUT-3 protein in fresh vascular smooth muscle cells (Figure 3.2). To determine at what stage of cell culture the changes in the levels of the glucose transporters occurs, samples of cells from passages 2, 6 and 16 were analysed. By immunoblotting it was determined that GLUT-4 protein was not present at detectable levels as early as passage 2, whereas GLUT-1 and GLUT-3 proteins were detected in all passages analysed (data not shown).

Therefore, freshly isolated aortic vascular smooth muscle cells do express GLUT-1 and GLUT-4. However, as these cells are passaged in culture GLUT-4 expression is

lost immediately and expression of GLUT-3, the brain-type glucose transporter, is increased. Glucose transport in cultured rat aortic VSMC is therefore mediated by GLUT-1 and also possibly GLUT-3.

### **3.3.2 Characterisation of PDGF-BB-stimulated glucose transport in rat aortic vascular smooth muscle cells**

We next set out to characterize the effects of PDGF-BB on glucose transport in VSMC. Firstly we wished to determine if PDGF-BB-stimulated glucose transport in these cells followed the biphasic pattern typically seen in response to mitogens (see section 1.2.3.1). Cells were treated with PDGF-BB (10 ng/ml) for different lengths of time prior to assay of 2-deoxyglucose uptake (section 2.5). The results are shown in figure 3.3. There was an initial increase in glucose transport, peaking after about 1 hour (Figure 3.3), with an  $5.57 \pm 0.52$ -fold stimulation over basal rates of transport ( $n=3$  experiments). This acute phase of transport plateaued after 1 hour, but after 2 hours a chronic increase in glucose transport became apparent (Figure 3.3). The chronic increase in glucose transport plateaued after about 6 hours and the maximum rate of transport was  $10.13 \pm 0.27$ -fold over basal rates ( $n=3$  experiments). This biphasic pattern is consistent with previous studies on mitogen-stimulated glucose transport in a range of cells (Thomson & Gould, 1997).

To determine if the increase in transport was dependent on new protein synthesis, cells were treated with 10 ng/ml PDGF-BB in the presence or absence of cycloheximide (50  $\mu$ M), an inhibitor of protein synthesis. 2-deoxyglucose transport was then measured, as above. In cells that were treated with PDGF-BB for 2 hours the addition of cycloheximide had no effect on rates of glucose transport (Figure 3.4). However after 3 hour and 4 hour treatments of cells with PDGF-BB, cycloheximide inhibited glucose transport as compared to cells treated with PDGF-BB alone. This indicates that the acute phase of PDGF-BB-stimulated glucose transport in VSMC is not dependant on new protein synthesis (up to 2 hours), however the chronic phase of glucose transport observed (greater than 3 hours) is dependent upon synthesis of new proteins. This is

consistent with previous work on mitogen-stimulated glucose transport. All further work in this thesis studies the acute phase of glucose transport in VSMC.

Next, the  $EC_{50}$  of the acute phase of PDGF-BB-stimulated 2-deoxy glucose transport in VSMC was determined. Cells were treated with PDGF-BB (0-500 ng/ml) for one hour and then subjected to 2-deoxyglucose transport assay (Figure 3.5). The  $EC_{50}$  for the acute phase of PDGF-BB-stimulated glucose transport in VSMC was ~10 ng/ml. The rate of 2-deoxyglucose transport in VSMC in response to a 1 hour treatment of 10 ng/ml PDGF-BB was  $381 \pm 34$  pmol/min/mg protein, representing a ~7 fold increase over basal ( $n=3$  experiments). This figure is high, as compared with that seen using other mitogens, this will be returned to in the discussion.

Glucose can be transported across the plasma membrane in both directions (Walmsley *et al.*, 1998). To prevent this happening glucose is immediately phosphorylated once it enters the cell. Glucose-6-phosphate is not a substrate for glucose transporters, so cannot be transported back across the plasma membrane. To ensure that the increase in the rate of 2-deoxyglucose transport in response to PDGF-BB is not limited by the rate of its phosphorylation, analogues of glucose that cannot be phosphorylated can be used. 3-*O*-methyl glucose is an analogue of glucose that cannot be phosphorylated, therefore by using 3-*O*-methyl glucose the rate of glucose flux can be measured. The ability of PDGF-BB to stimulate 3-*O*-methyl glucose transport was measured. Cells were treated with or without 10 ng/ml PDGF-BB for 1 hour, and 3-*O*-methyl glucose transport was measured over different times (as outlined in section 2.6). Cells treated with PDGF-BB showed a higher rate of 3-*O*-methyl glucose transport at all time points measured (Figure 3.6). The rates of transport were converted to give a straight line using the equation:

$$-\ln [(C_m - C_t)/C_m]$$

where  $C_m$  is the maximum cpm/well, and  $C_t$  is the cpm/well at the time point,  $t$  (Figure 3.6). The gradient of each line represents the rate constant,  $k$ , for glucose transport in

these cells. The  $k$  of basal and PDGF-BB-stimulated 3-*O*-methyl glucose transport were  $0.36 \text{ min}^{-1}$  and  $0.54 \text{ min}^{-1}$  respectively. Therefore the rate of PDGF-BB-stimulated 3-*O*-methyl glucose transport in VSMCs is ~1.5-fold that of basal. This is not a 7-fold increase in transport, as is seen when measuring 2-deoxyglucose transport (see above). When 2-deoxyglucose is transported onto the cell it is immediately phosphorylated by hexokinase and is no longer a substrate for glucose transporters. 3-*O*-methyl glucose, on the other hand, does not undergo phosphorylation when it enters the cell and so is still a substrate for glucose transport. Therefore, rates of 3-*O*-methyl glucose transport will be lower than rates of 2-deoxyglucose transport, measured under the same conditions as there will be a degree a back flux of 3-*O*-methyl glucose out of the cell.

The ability of PDGF-BB to stimulate growth of VSMCs was then assessed by measuring [ $^3\text{H}$ ] thymidine incorporation into the cells. Cells were treated with varying doses of PDGF-BB (0-40 ng/ml) for 24 hours and [ $^3\text{H}$ ] thymidine incorporated was measured. PDGF-BB elicited a  $2.81 \pm 0.15$  fold increase in [ $^3\text{H}$ ] thymidine incorporation in VSMC at doses of 10 ng/ml ( $n=3$  experiments) (Figure 3.7). The levels of thymidine incorporation increased in a dose dependent manner with a  $4.65 \pm 0.2$  fold increase seen at the maximum dose used, 40 ng/ml ( $n=3$  experiments) (Figure 3.7).

Therefore, PDGF-BB can stimulate a biphasic increase in 2-deoxyglucose transport. A 7-fold increase in 2-deoxyglucose at doses of 10 ng/ml PDGF-BB occurs within 1 hour, with a rate of ~380 pmol/min/mg protein, and this is not dependent on the synthesis of new protein. After ~2 hours a chronic increase in 2-deoxyglucose transport becomes apparent, with a ~10-fold increase in transport after 6 hours. The chronic phase of transport is dependent on new protein synthesis. The 2-deoxyglucose transport is not dependent on the rate of phosphorylation of 2-deoxyglucose as 3-*O*-methyl glucose transport, an analogue of glucose that is not a substrate for phosphorylation, is also stimulated by 10 ng/ml PDGF-BB. 10 ng/ml PDGF-BB stimulates an approximately two-fold increase VSMC growth, as determined by thymidine incorporation.

### **3.3.3 Cell signalling pathways involved in mediating PDGF-BB-stimulated glucose transport in rat aortic vascular smooth muscle cells.**

As described in the introduction (see section 1.2.3.1), the only cell signalling mechanisms known to be involved in mediating growth-factor stimulated glucose transport, to date, are PI3' kinase, MAP kinases and  $Ca^{2+}$ . The role of these signalling molecules in mediating PDGF-BB-stimulated glucose transport in VSMC was examined.

#### *PI3' kinase*

Firstly, to determine which regulatory subunits of PI3' kinase are present, p85 and/or p55, in VSMCs, immunoblotting was carried out on whole cell lysates. p85 PI3' kinase was present in VSMC as determined by the presence of a band of ~85 kDa, however there was no detectable p55 in VSMCs (Figure 3.8). The role of PI3' kinase in mediating PDGF-BB-stimulated glucose transport was assessed by using specific inhibitors of PI3' kinase, wortmannin and LY 294002. Cells were treated with inhibitors for 30 minutes followed by a 1 hour treatment with PDGF-BB (10 ng/ml) prior to 2-deoxyglucose transport assay. Both LY 294002 and wortmannin inhibited PDGF-BB-stimulated glucose transport (Figure 3.9). Wortmannin inhibited PDGF-BB-stimulated transport with an  $IC_{50}$  of ~10-20 nM, with 100% inhibition at ~100 nM. LY 294002 also inhibited PDGF-BB-stimulated glucose uptake, although higher concentrations of LY 294002 were required, with the  $IC_{50}$  being ~1.3  $\mu$ M. These figures for inhibition of glucose transport by inhibitors of PI3' kinase are consistent with those previously reported for a specific inhibition of PI3' kinase (Thomson *et al.*, 1996). This data suggests that PI3' kinase does indeed play a role in mediating PDGF-BB-stimulated glucose transport in VSMCs.

#### *MAP kinase*



As described in the introduction (see section 1.2.3.1), there are three families of MAP kinase, p42/44, p38 and JNK. To determine which, if any of these MAP kinases might be involved in PDGF-BB-stimulated glucose transport, we assessed which of these undergo phosphorylation, and therefore activation (Canos *et al.*, 1995), in response to PDGF-BB in VSMC. The phosphorylation and activation of each MAP kinase can be determined by immunoblotting using phospho-specific antibodies to each protein. 10 ng/ml PDGF-BB was capable of stimulating p42/44 phosphorylation, as determined by the presence of immunoreactive bands at 42 and 44 kDa, within 5 minutes (Figure 3.10). This intensity of this band, therefore the phosphorylation and activation of p42/44, began to decline after 15 minutes stimulation with PDGF-BB, and by 60 minutes the phosphorylation had returned to basal levels. Phosphorylation of p38 was also stimulated by PDGF-BB (10 ng/ml), as determined by the presence of an immunoreactive band of ~38 kDa (Figure 3.10). As with p42/44, phosphorylation and activation of p38 was highest after a 5 minute stimulation with PDGF-BB and was declining after 15 minutes. After 60 minutes the phosphorylation of p38 had returned to basal levels. JNK did not appear to be phosphorylated and activated in response to PDGF-BB (Figure 3.10), however the cross-reactivity of the antibody with phospho-p42/44 did not allow accurate analysis of this.

As both p38 and p42/44 are phosphorylated and activated by PDGF-BB in VSMC, the role of these in mediating PDGF-BB-stimulated glucose transport was assessed by using the specific inhibitors of p38, SB 203580, and of p42/44 activation, PD 98059 (Gould *et al.*, 1995). Cells were pretreated for one hour with the appropriate inhibitor then treated for a further one hour with 10 ng/ml PDGF-BB prior to 2-deoxyglucose transport assay (section 2.5). Both SB 203580 and PD 98059 were capable of inhibiting PDGF-BB-stimulated glucose transport in VSMC (Figure 3.11). SB 203580 inhibited PDGF-BB-stimulated glucose transport with an  $IC_{50}$  of ~10  $\mu$ M, whereas PD 98059 inhibited transport with an  $IC_{50}$  of ~50  $\mu$ M. These  $IC_{50}$  values were consistent with those previously reported to inhibit glucose transport in other cells (Gould *et al.*, 1995). To ensure specificity of the MAP kinase inhibitors, immunoblotting of cell lysates, treated as above, was carried out to determine the relative levels of phosphorylation,

and therefore activation of the MAP kinases in the presence of SB 203580 and PD 98059. Figure 3.12 shows that PD 98059 only inhibited p42/44 phosphorylation and had little effect on p38 levels of phosphorylation and that SB 203580 had little effect on the phosphorylation of p42/44.

These results show that PDGF-BB is capable of stimulating both p38 and p42/44 in VSMC, however it has no apparent effect on JNK. The activation of both p38 and p42/44 is necessary for PDGF-BB-stimulated 2-deoxyglucose transport in VSMCs as determined by the use of the specific inhibitors SB 203580 and PD 98059.

### **3.4 DISCUSSION**

Increased glucose transport is an early response of all cells to mitogens (Thomson & Gould, 1997). Increased vascular smooth muscle cell proliferation, and presumably therefore glucose transport, is fundamental to atherosclerotic plaque development (Ross, 1993, Ross, 1999). However very little is known about glucose transport in vascular smooth muscle cells. It is as yet unclear which glucose transporters are present in VSMC, with some groups reporting the presence of the insulin-responsive glucose transporter, GLUT-4, and GLUT-1 in VSMCs, whereas others have failed to find GLUT-4 mRNA (Sowers, 1996, Kihara et al., 1998). It is therefore important to establish which glucose transporters are expressed in the cultured VSMC used in this study. As well as little being known about which glucose transporters are expressed, very little is known about what regulates glucose transport in these cells. Most studies to date have concentrated on the effects of insulin and IGF-1 to regulate glucose transport (Sowers, 1996, Fujiwara & Nakai, 1996), but there has been no work on the growth factors suspected of being major regulators of VSMC proliferation in plaque development. PDGF is thought to be the principle regulator of VSMC proliferation in atherosclerotic plaques (Bobik & Campbell, 1993), and as such it is of interest to study the effects of PDGF on glucose transport in cultured rat aortic vascular smooth muscle cells. The cell signalling mechanisms involved in mediating mitogen-stimulated glucose transport in any cell system are poorly defined. To date only PI3' kinase and MAP kinases are known to be involved (Thomson & Gould 1997), and hence we wished to determine what role, if any, these play in mediating PDGF-BB-stimulated glucose transport.

#### **3.4.1 Glucose transporter content of rat aortic vascular smooth muscle cells**

We found that GLUT-1 and GLUT-3 were present in the cultured VSMC used, but there was no detectable GLUT-4 (Figure 3.1). As the reports of GLUT-4 expression were from freshly isolated VSMC, and not cultured VSMCs, the levels of GLUT-1, -3 and -4 were investigated in fresh VSMC. In fresh vascular smooth muscle cells GLUT-

4 was indeed present (Figure 3.2). GLUT-1 was also present in fresh aortic smooth muscle cells, however there was no detectable GLUT-3 (Figure 3.2). When the levels of GLUTs in cells from a number of different passages was studied, GLUT-4 expression was only observed in vascular smooth muscle cells freshly extracted from aorta, and GLUT-3 protein was only detected when the cells were cultured (data not shown). The level of GLUT-1 was similar in freshly isolated vascular smooth muscle cells and in all passages of cultured smooth muscle cells looked at.

Therefore, fresh rat aortic smooth muscle cells express GLUT-4 and GLUT-1, however the expression of GLUT-4 is lost immediately after the cells are isolated for culture, and the cells start to express GLUT-3. This loss of expression of a protein with the culturing of cells is not unusual. In vascular smooth muscle cells, for example, it is known that expression of protein kinase G is lost with increasing passage (Cornwell *et al.*, 1994). It is possible that as GLUT-4 is lost that the cell compensates for this by increasing the levels of GLUT-3. However GLUT-3 and GLUT-4 have quite different properties. Both GLUT-3 and GLUT-4 have a relatively low  $K_m$  for glucose transport (Gould, 1997), but GLUT-4 is localised predominantly in specialized intracellular vesicles in the absence of insulin. Upon exposure to insulin GLUT-4 is mobilised to the plasma membrane (Cushman *et al.*, 1980, Suzuki & Kono, 1980), this is believed to be the case for GLUT-3. There are, however, reports of GLUT-3 being recruited to the plasma membrane in response to appropriate signals. When platelets are activated they have a vastly increased demand for energy in the form of glucose. It has been reported that in platelets activated by thrombin, the amount of GLUT-3 at the plasma membrane can be increased by 2.7-fold with a  $T_{1/2}$  of 1-2 minutes (Sorbara *et al.*, 1997). So, perhaps the cultured VSMCs are compensating for the lack of GLUT-4 expression by increasing levels of GLUT-3. Unfortunately, it is difficult to perform sub-cellular fractionation on VSMCs. This means that the subcellular localisation of GLUT-3 could not be readily determined. It is therefore unclear if GLUT-3 is stored in an intracellular compartment and is capable of being mobilised in response to an appropriate signal, and therefore capable of replacing the role of GLUT-4 in these cells.

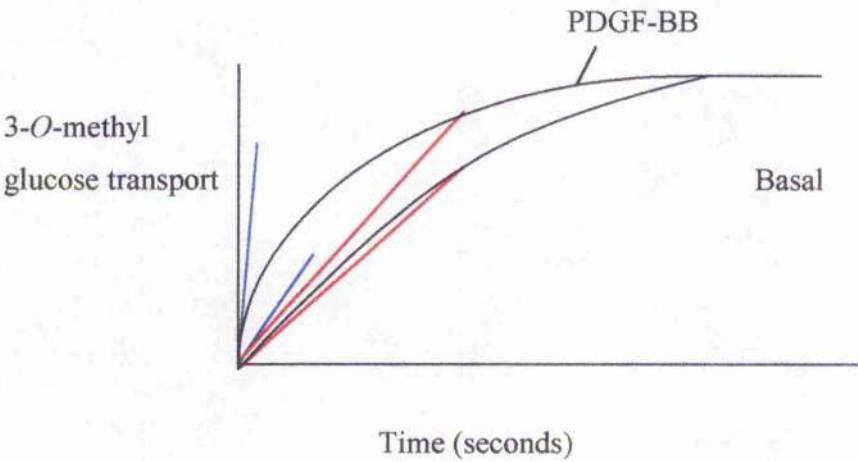
The mechanisms regulating the altered expression of these proteins in this system are unclear. The expression of GLUT-4 is regulated by a number of factors *in vivo*, including diet and exposure of cells to insulin (Gould, *et al* 1997). The most plausible explanation for such a rapid loss of GLUT-4 expression is that there is some factor that the VSMCs are exposed to in intact aorta, perhaps from the endothelium, which normally maintains the expression of GLUT-4. When the VSMCs are isolated away from the endothelium this factor is removed and GLUT-4 expression declines. GLUT-3 expression may then increase with passage to compensate for the loss of GLUT-4 expression. This is, of course, speculation, and what such a factor may be is unclear.

#### **3.4.2 PDGF-BB-stimulated glucose transport in VSMC**

Little is known about glucose transport in VSMC. To date the only work on glucose transport in VSMC has looked at the effects of IGF-1, insulin and angiotensin II (Sowers, 1996, Fujiwara & Nakai, 1996, Quinn & McCumbee, 1998). There has been no work published on the effects of PDGF-BB (one of the growth factors believed to play a major role in regulating VSMC proliferation in atherosclerotic plaque development (Bobik & Campbell, 1993, Ross, 1993)) in regulating glucose transport in VSMCs. We were interested in determining the effects of PDGF-BB on glucose transport in VSMC. PDGF-BB stimulated a biphasic increase in glucose transport in VSMCs (Figure 3.3), with an acute phase that was maximal within 1 hour of exposure of cells to PDGF-BB and independent of new protein synthesis, as determined by use of the inhibitor cycloheximide (Figure 3.4). The maximum increase in the acute phase of PDGF-BB-stimulated 2-deoxyglucose transport in VSMC was ~ 6-fold. This value for PDGF-BB-stimulated acute-phase glucose transport was rather high when compared to the increases that this and other mitogens can stimulate in other cell lines, typically two-fold (Thomson & Gould, 1997). It is unclear why this may be the case. One possible explanation is presence of the GLUT isoform, GLUT-3, in this cell line (see section 3.3.1) as well as GLUT-1. This may mean that the cell has a larger pool of glucose transporters available for transport. Upon appropriate stimulation, the cell may be able to translocate/activate more glucose transporters, and therefore be able to stimulate a greater increase in rates of transport than cells which do not contain GLUT-3. However,

it should be noted that the rate of PDGF-BB-stimulated glucose transport in the VSMCs used could be somewhat variable (typically between 2- and 5-fold). The chronic phase of PDGF-BB-stimulated 2-deoxyglucose transport became apparent after about two hours (Figure 3.3), with an increase in transport of ~10-fold over basal. The chronic phase of PDGF-BB-stimulated 2-deoxyglucose transport plateaued after ~ 6 hours and was dependent on synthesis of new proteins (Figure 3.4). The biphasic pattern of glucose transport in VSMCs in response to PDGF-BB is consistent with previous work on mitogen-stimulated glucose transport in other cell lines (Thomson & Gould, 1997). Dose-response studies suggest that PDGF-BB induces these effects via its cognate receptor.

The 3-*O*-methyl glucose transport rate reported for PDGF-BB stimulated transport was only 1.5 fold that of basal 3-*O*-methyl glucose transport. This does not correlate well with the 6-fold increase in 2-deoxyglucose transport seen with PDGF-BB in VSMCs. As 3-*O*-methyl glucose is not a substrate for hexokinase it is not phosphorylated once it enters the cell, unlike 2-deoxyglucose, and so remains a substrate for glucose transporters and is transported out of, as well as in to, the cell. Ideally, 3-*O*-methyl glucose transport would be measured over time points as low as 5 seconds when the amount of glucose in the cells is still low and the degree of flux out of the cell is minimal. At early time points the difference between basal and stimulated transport rates is greatest (see figure below). However, this is practically very difficult to do.



The differences between the gradients of the curves are largest at the lowest time points (blue lines), and as time progresses the differences in the gradients of the two curves becomes less (red lines). As the time points I was able to measure were further along the curve, the differences between basal and stimulated rates of transport,  $k$ , were smaller. Therefore I obtained a low value for PDGF-BB-stimulated 3-*O*-methyl glucose transport, 1.5-fold.

### **3.4.3 Characterisation of signalling mechanisms involved in mediating PDGF-BB-stimulated glucose transport in VSMC**

#### *PI3' kinase*

Wortmannin and LY 294002 effectively inhibited PDGF-BB-stimulated 2-deoxyglucose transport. Wortmannin completely inhibited PDGF-BB-stimulated glucose transport at doses of ~100 nM, with an  $IC_{50}$  of ~20 nM (Figure 3.9). LY 294002 was also effective at inhibiting PDGF-BB-stimulated glucose transport, with an  $EC_{50}$  of ~1.3  $\mu$ M (Figure 3.9). These figures for  $IC_{50}$  are consistent with those previously published for inhibition of glucose transport via specific inhibition of PI3' kinase (Gould *et al.*, 1994, Thomson *et al.*, 1996). Therefore PI3' kinase activity is necessary for mediating PDGF-BB-stimulated 2-deoxyglucose transport.

Immunoblotting of VSMC whole cell lysates demonstrated that there was p85 but no p55 PI3' kinase regulatory subunit present in VSMCs (Figure 3.8). As only the p85 regulatory subunit is present in VSMCs, then this isoform of PI3' kinase must be responsible for mediating PDGF-BB-stimulated 2-deoxyglucose transport in VSMC.

#### *MAP kinase*

To determine the role that MAP kinases may play in mediating PDGF-BB-stimulated 2-deoxyglucose transport in VSMC, it was first determined which of the MAP kinases were stimulated by PDGF-BB in VSMCs. Both p38 and p42/44 were strongly phosphorylated, therefore activated, by 10 ng/ml PDGF-BB in VSMCs. The stimulation

was greatest within 5 minutes of stimulation with PDGF-BB. After fifteen minutes the phosphorylation of p42/44 and p38 was beginning to decrease, and after 60 minutes the levels of phosphorylation had returned to basal levels (Figure 10). JNK was not significantly phosphorylated in response to 10 ng/ml PDGF-BB (Figure 10), however the anti-phospho JNK antibody cross-reacted with phospho-p42/44, making analysis of PDGF-BB-stimulated JNK activation difficult.

To determine the role of p38 and p42/44 activation in PDGF-BB-stimulated 2-deoxy glucose transport in VSMCs, the specific inhibitors SB 203580 (p38 inhibitor) and PD 98059 (p42/44 inhibitor) were used. As can be seen in Figure 3.11, both SB 203580 and PD 98059 were effective at inhibiting 2-deoxyglucose transport. SB 203580 was capable of inhibiting PDGF-BB-stimulated glucose transport at lower doses than PD 98059. The approximate  $IC_{50}$  values for SB 203580 and PD 98059 were 10  $\mu$ M and 30  $\mu$ M respectively. From this we can see that both p38 and p42/44 are required for PDGF-BB-stimulated 2-deoxyglucose transport in VSMC. To ensure that the inhibitors were working in a specific manner, and not cross-reacting with other MAP kinases, immunoblot analysis was carried out to determine the levels of phosphorylation, and activation, of the p38 and p42/44 in the presence of these inhibitors. It was seen that SB 203580 only inhibited the phosphorylation of p38 and had no effect on the levels of phosphorylation, and therefore activation of p42/44. Conversely, PD 98059 only inhibited the phosphorylation and activation of p42/44 and had no effect on p38 activation.

This is a very interesting observation, as previous work had indicated that p38 was involved in cytokine-stimulated glucose transport, but had no role in tyrosine kinase receptor activated transport (Gould *et al.*, 1995). Similarly, it was shown that p42/44 was involved in mediating glucose transport stimulated by IGF-1 (a tyrosine kinase receptor agonist), but there was no role for p38 here (Gould *et al.*, 1995). Here, however we appear to have a pathway, activated by an agonist acting at a tyrosine kinase receptor, that activates both p38 and p42/44, and activation of both these MAP kinases is necessary for stimulation of glucose transport.



### 3.5 SUMMARY

Cultured rat aortic vascular smooth muscle cells express the glucose transporters GLUT-1 and GLUT-3, but not the insulin responsive glucose transporter, GLUT-4. This is in contrast to fresh rat aortic vascular smooth muscle cells that express GLUT-1 and GLUT-4, but no GLUT-3. It is currently unclear why the VSMCs down-regulate the expression of one glucose transporter and increase the expression of another when they are cultured. It is however, clear that culture of VSMC can result in diminished expression of several proteins (i.e. PKG down-regulation in cultured VSMC, Cornwell *et al.*, 1994). It is possible that the cell up-regulates GLUT-3 expression to compensate for the loss of GLUT-4 in these cells.

In rat aortic VSMCs PDGF-BB is capable of stimulating cell growth, as measured by increased [ $^3\text{H}$ ] thymidine incorporation, and a biphasic increase in glucose transport in VSMCs. The acute phase of this transport is maximal within ~1 hour and is independent of new protein synthesis. The maximum rate of 2-deoxyglucose transport attained in the acute phase is ~500 pmol/min/mg protein, and the  $\text{EC}_{50}$  is ~10 ng/ml. The chronic phase of PDGF-BB-stimulated transport occurs after ~2 hours and is maximal after ~6 hours. The chronic phase of PDGF-BB-stimulated 2-deoxyglucose transport is dependent on the synthesis of new protein. The increase in acute phase of PDGF-BB-stimulated glucose transport in VSMC is not limited by the rate of glucose phosphorylation as determined by measuring the rate of PDGF-BB-stimulated 3-*O*-methyl glucose transport, an analogue of glucose that is not a substrate for phosphorylation. The  $K_m$  for basal and PDGF-BB stimulated 3-*O*-methyl glucose transport are  $0.36 \text{ min}^{-1}$  and  $0.55 \text{ min}^{-1}$  respectively. Therefore the rate of PDGF-BB-stimulated 3-*O*-methyl glucose transport is ~1.6 fold that of basal 3-*O*-methyl glucose transport.

Both PI3' kinase and the MAP kinases p38 and p42/44 are involved in mediating the acute phase of PDGF-BB-stimulated glucose transport, as determined by the use of specific inhibitors of these signalling molecules.

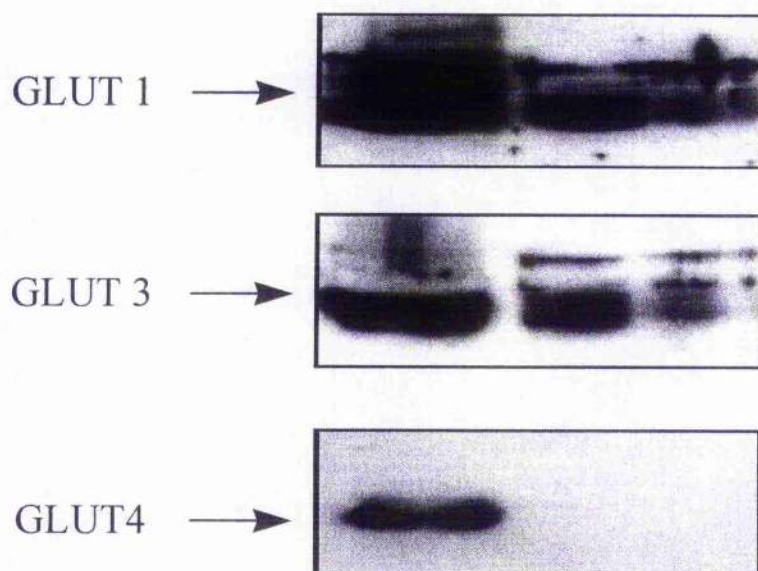
All further work in this thesis concentrates on the acute phase of glucose transport in VSMCs.

### **Figure 3.1 Analysis of glucose transporters in cultures VSMCs**

Whole cell lysates were prepared from flasks of VSMCs (passage 12) as described in section 2.9. 5 and 15  $\mu$ g of protein were loaded on a 10 % SDS-PAGE gel and subjected to electrophoresis and immunoblotting as described in section 2.8. Positive controls were samples of rat brain lysate for GLUTs 1 and 3, and a whole cell lysates from 3T3-L1 adipocytes for GLUT-4. Blots were developed using antibodies to the C-terminal of GLUT-1, -3 and -4 respectively (see section 2.1.2).

GLUT-1 and -3 were present in VSMCs, as determined by the presence of an immunoreactive band of approximately 49 kDa, however there was no detectable GLUT-4. This blot is representative of three such experiments.

+ve  
Cont. 15 $\mu$ g 5  $\mu$ g



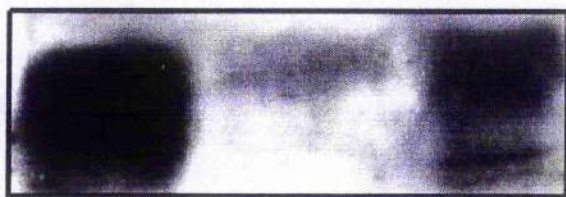
### **Figure 3.2 Analysis of glucose transporters in fresh aortic VSMCs**

Whole cell lysates were prepared from freshly isolated VSMCs as described in section 2.9. 20 and 40  $\mu$ g of protein were loaded on a 10 % SDS-PAGE gel and subjected to electrophoresis and immunoblotting as described in section 2.8. Positive controls were samples of rat brain lysate for GLUTs 1 and 3, and whole cell lysates from 3T3-L1 adipocytes for GLUT-4. Blots were developed using antibodies to the C-terminal of GLUT-1, -3 and -4 respectively (see section 2.1.2).

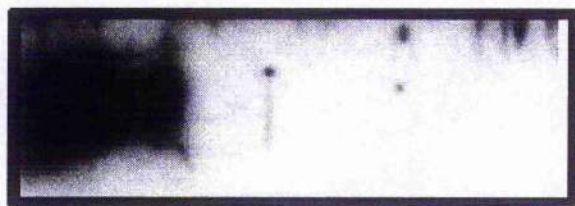
GLUT-1 and -4 were present in VSMCs, as determined by the presence of an immunoreactive band of approximately 49 kDa, however there was no detectable GLUT-3. This blot is representative of three such experiments.

+ve cont.      20 $\mu$ g      40 $\mu$ g

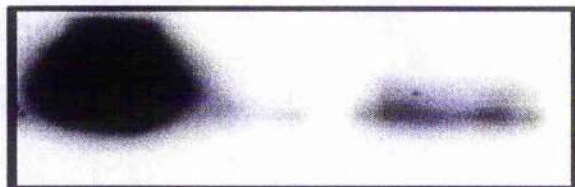
GLUT 1 →



GLUT 3 →



GLUT 4 →



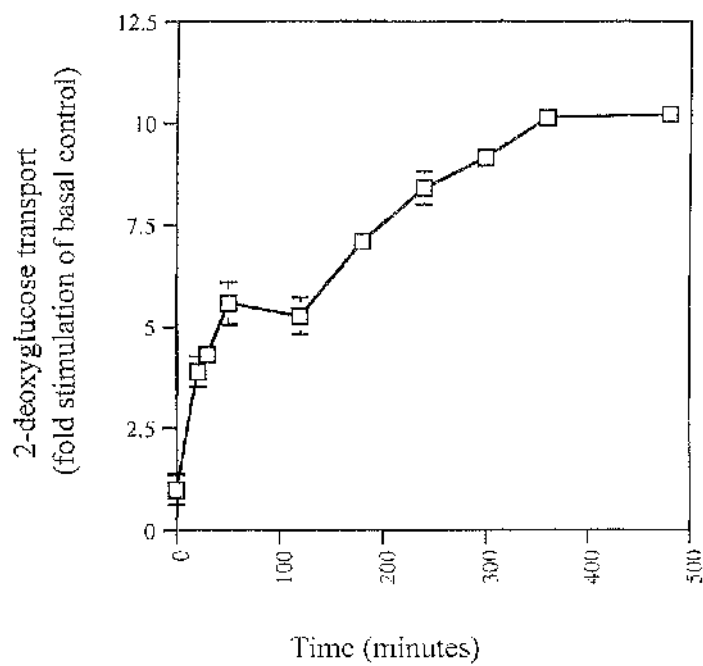
### **Figure 3.3 Time-course of 2-deoxyglucose transport in VSMCs in response to PDGF**

2-deoxyglucose transport assay was carried out as described in section 2.5.

Cells were quiesced for 36-48 hours, then treated with PDGF (10 ng/ml) for the times indicated, prior to 2-deoxyglucose transport assay. Data from a representative experiment is shown, repeated three times with similar results.

Each point represents the mean of triplicate determinations  $\pm$  S.E.M. Data is expressed as a fold stimulation of basal (unstimulated) transport rates.

Time course of 2-deoxyglucose transport in VSMCs in response to PDGF (10 ng/ml)





### **Figure 3.4 2-deoxyglucose transport in VSMCs in response to PDGF in the presence or absence of cycloheximide**

2-deoxyglucose transport assay was carried out as described in section 2.5.

Cells were quiesced for 36-48 hours, then treated with PDGF (10 ng/ml) for the times indicated, in the presence or absence of the inhibitor of protein synthesis, cycloheximide (50  $\mu$ M), prior to 2-deoxyglucose transport assay. Data from a representative experiment is shown, repeated three times with similar results.

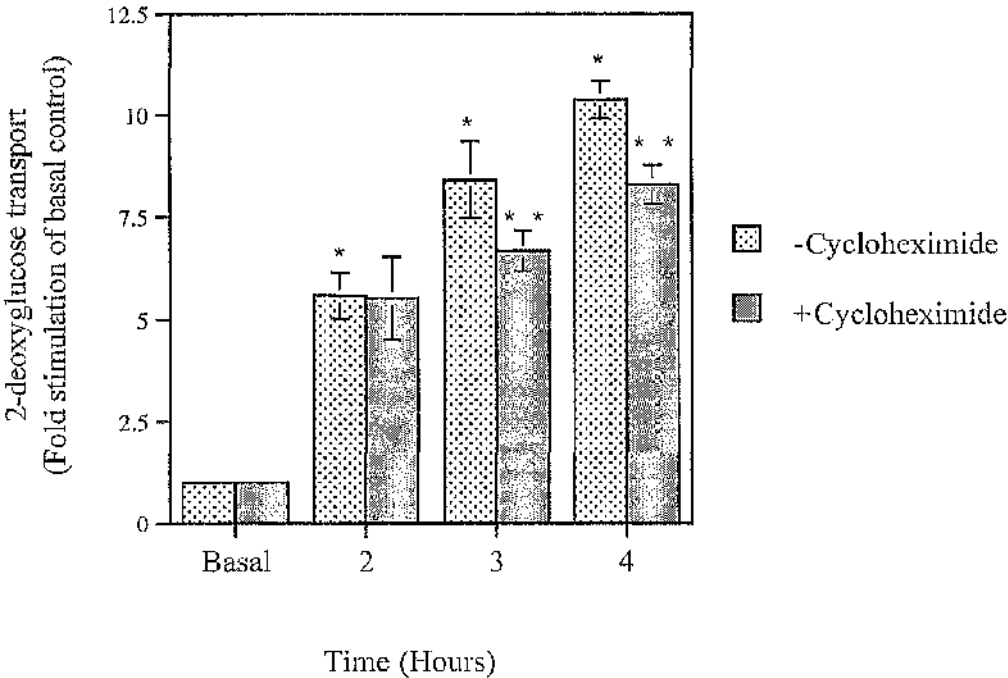
Each point represents the mean of triplicate determinations  $\pm$  S.E.M. Data is expressed as a fold stimulation of basal (unstimulated) transport rates.

\* represents  $P < 0.05$  in cells treated with PDGF alone as compared to basal, untreated cells as determined by Student's t-test.

\*\* represents  $P < 0.05$  as compared to cells treated with PDGF alone for the same time period as determined by Student's t-test.

Cycloheximide has no effect on PDGF-stimulated glucose transport up to two hours. However in cells treated with PDGF for 3 and 4 hours cycloheximide inhibits glucose transport.

2-deoxyglucose transport in VSMCs in response to PDGF in the absence or presence of cycloheximide



### **Figure 3.5 Dose-response curve of 2-deoxyglucose transport in VSMCs in response to PDGF**

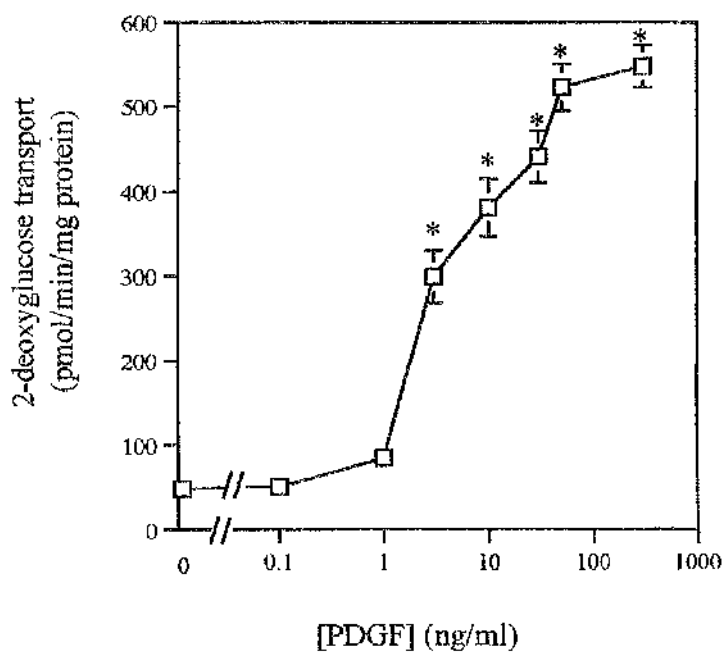
2-deoxyglucose transport assay was carried out as described in section 2.5.

Cells were quiesced for 36-48 hours, then treated with PDGF for 1 hour at the concentrations indicated, prior to 2-deoxyglucose transport assay. Data from a representative experiment is shown, repeated three times with similar results.

Each point represents the mean of triplicate determinations  $\pm$  S.E.M. Data is expressed as rate of transport in pmoles of 2-deoxyglucose transported/minute/mg of protein.

\* represents  $P < 0.05$  in cells treated with PDGF as compared to basal, untreated cells, as determined by Student's t-test.

Dose-response curve of 2-deoxyglucose transport in VSMCs in response to PDGF



### **Figure 3.6 3-*O*-methyl glucose transport in VSMCs in response to PDGF**

3-*O*-methyl glucose transport assay was carried out as described in section 2.6.

Cells were quiesced for 36-48 hours, then treated with PDGF (10 ng/ml) for 1 hour and 3-*O*-methyl glucose transport measured for the times indicated. Data from a representative experiment is shown, repeated three times with similar results.

#### **A.**

Each point represents the mean of triplicate determinations  $\pm$  S.E.M. Data is expressed as cpm of 3-*O*-methyl glucose transported/well.

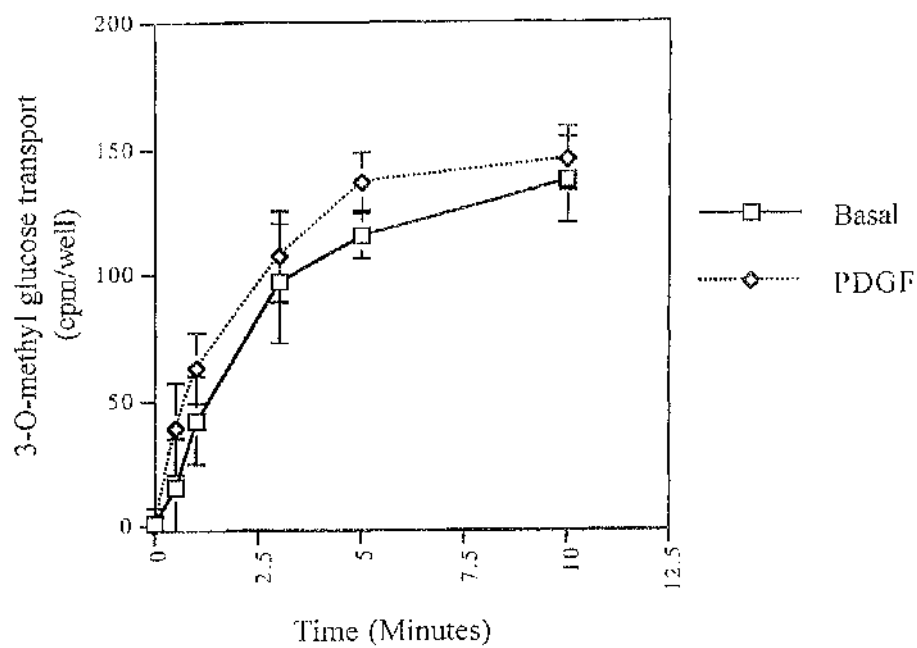
#### **B.**

The mean cpm/well values were converted using the equation:

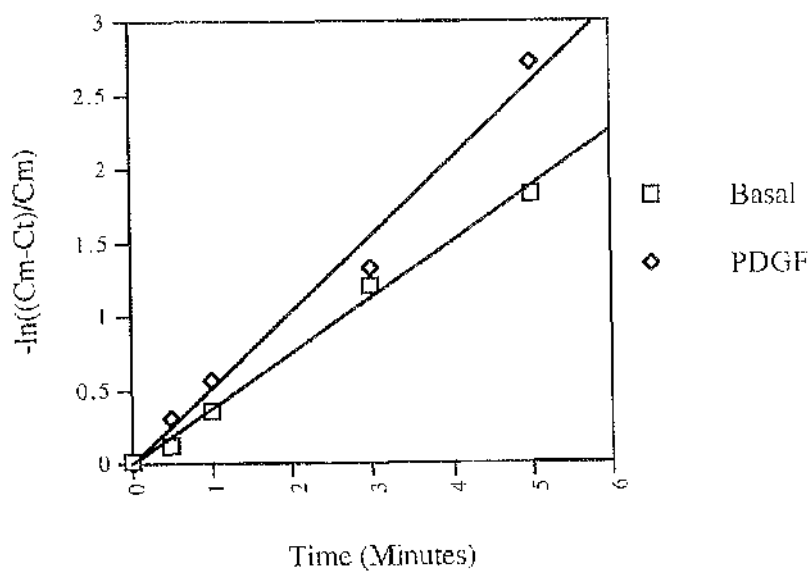
$$-\ln((C_m - C_t)/C_m)$$

where  $C_m$  was the maximum cpm/well and  $C_t$  was the cpm/well at a given time point,  $t$ . This gives a straight line, where the gradient of each line represents the rate constant,  $k$ , for 3-*O*-methyl glucose transport.

A.



B.

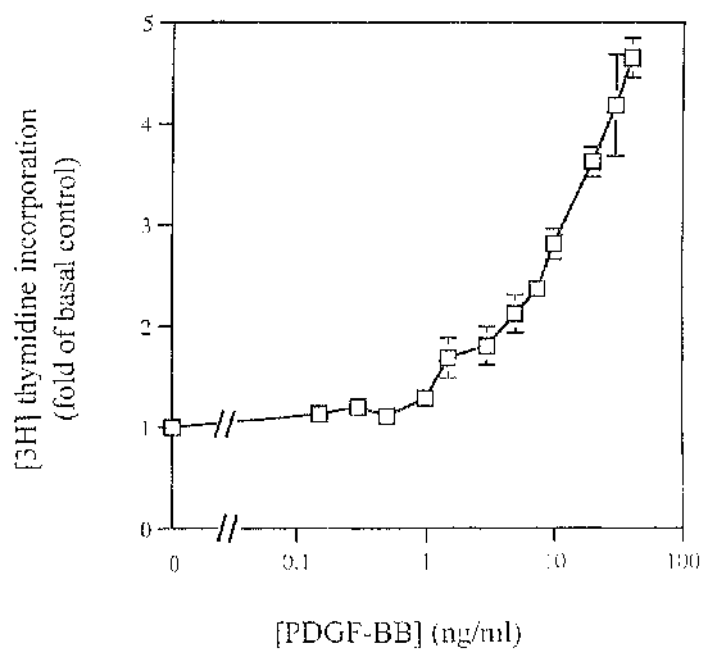


### **Figure 3.7 [<sup>3</sup>H] thymidine incorporation in VSMCs in response to PDGF**

[<sup>3</sup>H] thymidine incorporation was determined as described in section 2.11. Cells were quiesced for 12-24 hours, then treated with PDGF at the concentrations indicated for a further 24 hours. 0.5 µCi of [<sup>3</sup>H] thymidine is added per well for the final 6 hours of the incubation with PDGF. Data from a representative experiment is shown, repeated three times with similar results.

Each point represents the mean of triplicate determinations ± S.E.M. Data is expressed as a fold stimulation over basal (unstimulated) rates of [<sup>3</sup>H] thymidine incorporation.

$^3\text{H}$  Thymidine incorporation in  
VSMCs in response to PDGF

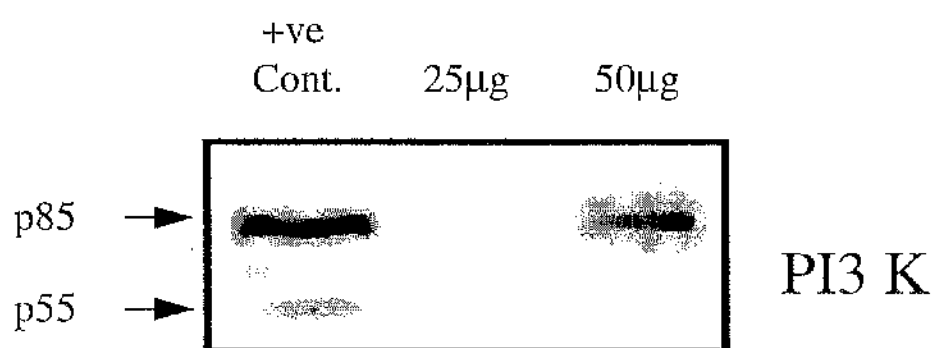




### **Figure 3.8 Analysis of PI3' kinase isoforms in VSMCs**

Whole cell lysates were prepared from flasks of VSMCs as described in section 2.9. 25 and 50 µg of protein were loaded in each lane of a 10 % SDS-PAGE gel and subjected to electrophoresis and immunoblotting as described in section 2.8. Positive controls were samples from the manufacturer of the antibody. Blots were developed using antibodies to p85, p55 PI3' kinase from Upstate Biotechnology

PI3' kinase p85 was present in VSMCs, as determined by the presence of an immunoreactive band of approximately 85 kDa, however there was no detectable p55. This blot is representative of two such experiments.



### **Figure 3.9 Effect of PI3' kinase inhibitors on PDGF-stimulated 2-deoxyglucose transport in VSMCs**

2-deoxyglucose transport assay was carried out as described in section 2.5.

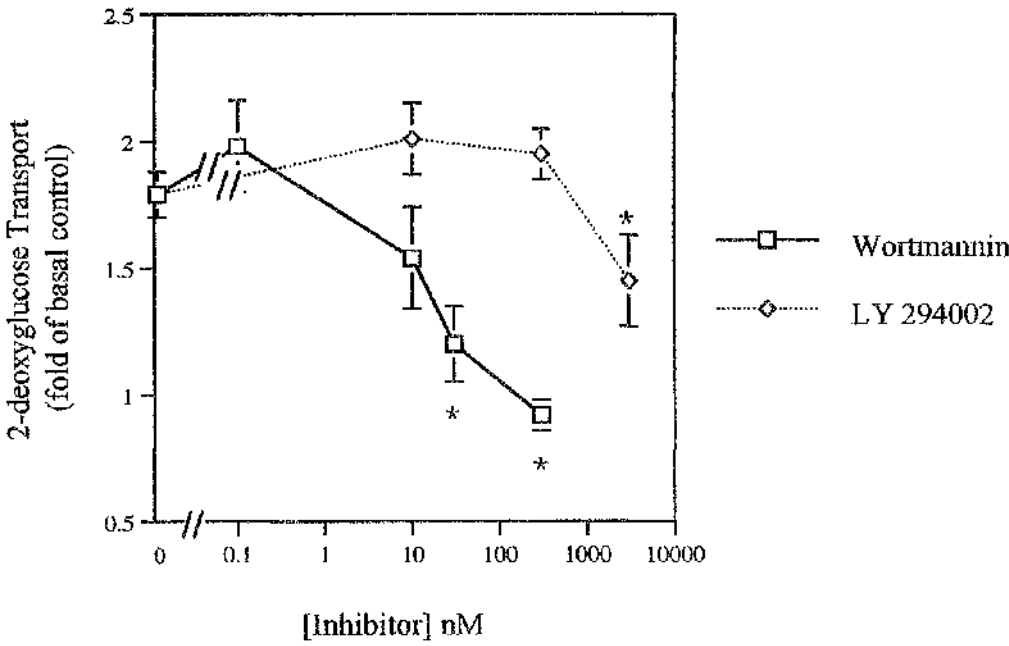
Cells were quiesced for 36-48 hours, treated with wortmannin or LY 294002 for 30 minutes, then with PDGF (10 ng/ml) for a further hour, prior to 2-deoxyglucose transport assay. Data from a representative experiment is shown, repeated three times with similar results.

Each point represents the mean of triplicate determinations  $\pm$  S.E.M. Data is expressed as a fold stimulation of basal (unstimulated) transport rates.

Both LY 294002 and wortmannin inhibited PDGF-stimulated 2-deoxyglucose transport.

\* represents  $P < 0.05$  when compared to cells treated with PDGF alone as determined by Student's t-test.

Effect of PI3' kinase inhibitors on PDGF-stimulated  
2-deoxyglucose transport in VSMCs

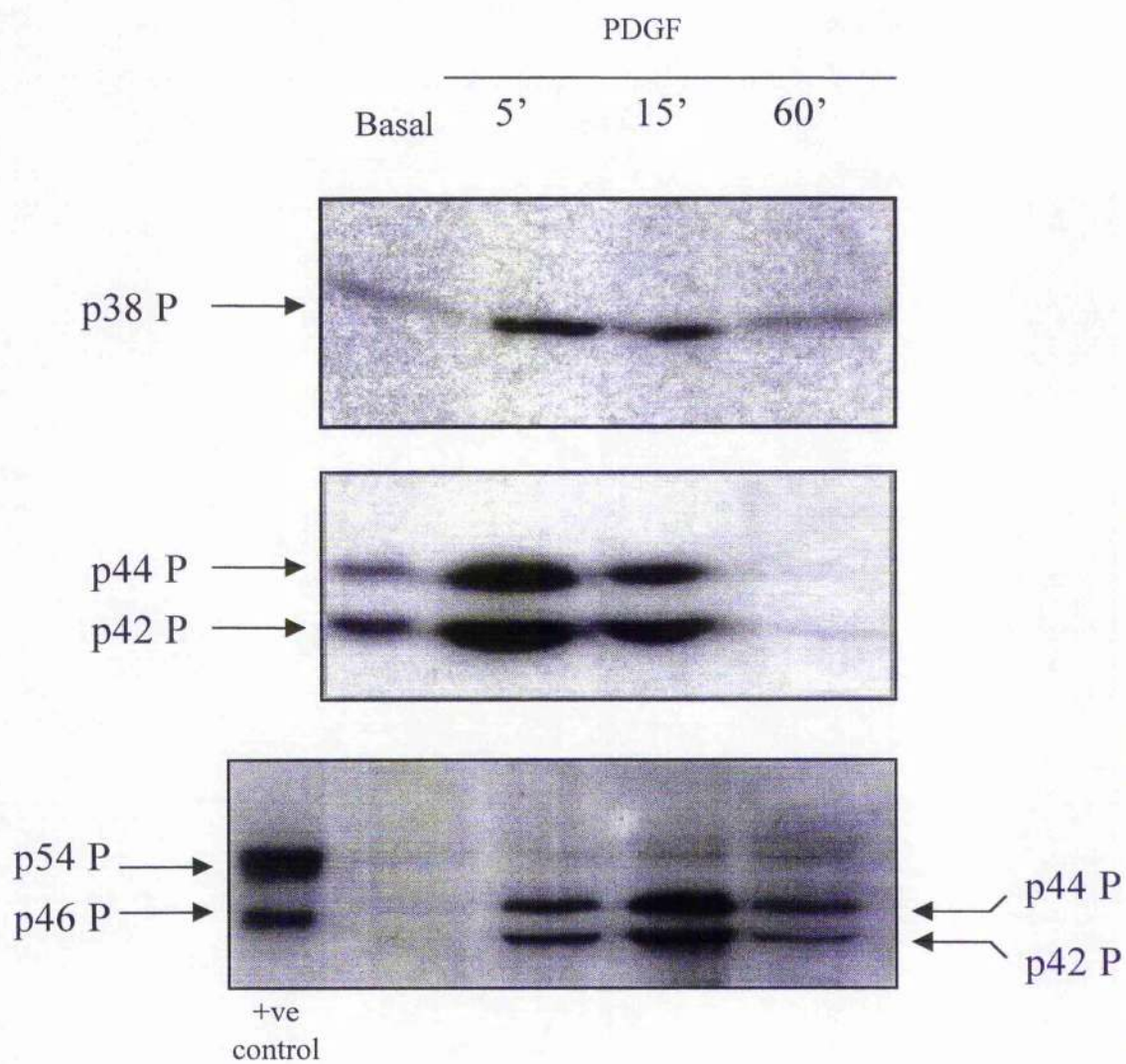


### **Figure 3.10 Effects of PDGF on the phosphorylation/activation of MAP kinases**

VSMCS were grown to confluency in 6-well plates and quiesced in serum-free DMEM for 36-48 hours. Cells were treated with or without PDGF (10 ng/ml) for 5, 15 or 60 minutes and then whole cell lysates were prepared as described in section 2.9. 50µl of each lysate was loaded in each lane of a 10 % SDS-PAGE gel and subjected to electrophoresis and immunoblotting as described in section 2.8. Blots were developed using phospho-specific antibodies to p38, p42/44 and JNK MAP kinases, respectively, which only recognise the phosphorylated, therefore activated, kinase. The positive control on the JNK blot is UV treated HEK cell lysates provided from the manufacturers of the antibody (New England Biolabs).

PDGF stimulated phosphorylation, and activation, of both p38 and p42/44, but had no effect on the phosphorylation of JNK (although the cross-reactivity of the JNK antibody with p42/44 did not allow accurate analysis of this).

These blots are representative of three such experiments.



### **Figure 3.11 Effects of inhibitors of MAP kinases, p38 and p42/44, on PDGF-stimulated 2-deoxyglucose transport**

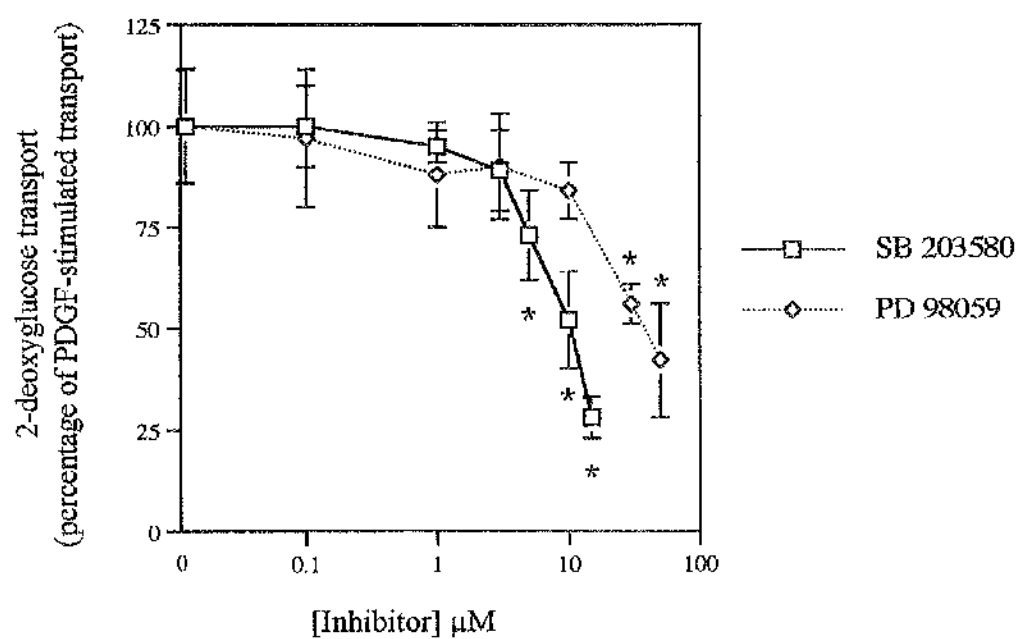
2-deoxyglucose transport assay was carried out as described in section 2.5.

Cells were quiesced for 36-48 hours, treated with SB 203580 or PD 98059 for 1 hour, then with PDGF (10 ng/ml) for a further hour, prior to 2-deoxyglucose transport assay. Data from a representative experiment is shown, repeated three times with similar results.

Each point represents the mean of triplicate determinations  $\pm$  S.E.M. Data is expressed as a percentage of PDGF-stimulated 2-deoxyglucose transport.

\* represents  $P < 0.05$  as compared to cells treated with PDGF alone as determined by Student's t-test.

Effect of p38 and p42/44 inhibitors on  
PDGF-stimulated 2-deoxyglucose transport



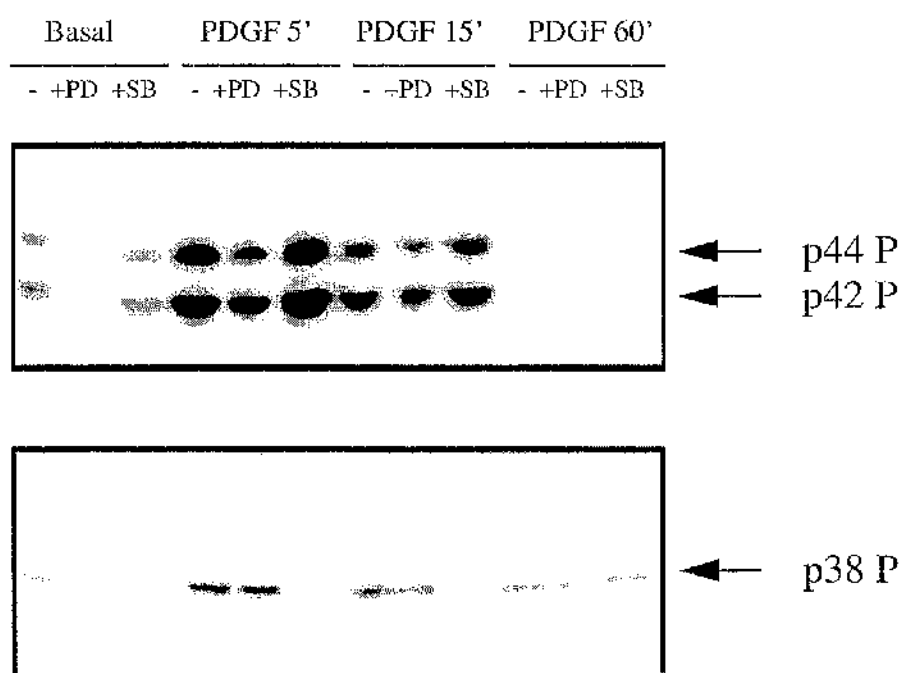


### **Figure 3.12 Analysis of the specificity of the MAP kinase inhibitors SB 203580 and PD 98059**

VSMCS were grown to confluency in 6-well plates and quiesced in serum-free DMEM for 36-48 hours. Cells were pre-treated nothing, 25  $\mu$ M SB 203580 or 50  $\mu$ M PD98059 for 1 hour, followed by PDGF (10 ng/ml) for 5, 15 or 60 minutes. Whole cell lysates were prepared as described in section 2.9. 50 $\mu$ l of each lysate was loaded in each lane of a 10 % SDS-PAGE gel and subjected to electrophoresis and immunoblotting as described in section 2.8. Blots were developed using phospho-specific antibodies to p38 and p42/44 MAP kinases, respectively, which only recognise the phosphorylated kinase.

PDGF stimulated phosphorylation, and activation, of both p38 and p42/44. PD 98059 inhibited the phosphorylation/activation of p42/44 by PDGF but had no effect on p38 activation by PDGF. Conversely, SB 203580 had no effect on p42/44 activation by PDGF. Therefore the inhibitors SB 203580 and PD 98059 do act in a specific manner, with regard to MAP kinase activity.

- Cells were not pretreated with any MAP kinase inhibitor
- +PD Cells were pretreated with 50  $\mu$ M PD 98059
- +SB Cells were pretreated with 25  $\mu$ M SB 203580



## **CHAPTER 4**

# **THE ROLE OF CYCLIC NUCLEOTIDES IN REGULATING GLUCOSE TRANSPORT IN RAT AORTIC VASCULAR SMOOTH MUSCLE CELLS**

## **4.1 AIMS**

The aims of this chapter are:

1. To determine what effect, if any, cAMP has on basal and PDGF-stimulated glucose transport in rat aortic vascular smooth muscle cells.
2. To determine what signalling mechanisms are involved in mediating cAMP's effects on glucose transport in rat aortic vascular smooth muscle cells.
3. To determine what mechanisms the cell may use to endogenously increase intracellular [cAMP] and increase glucose transport.
4. To determine if cGMP has any effect on basal or PDGF-stimulated glucose transport in rat aortic vascular smooth muscle cells.

## 4.2 INTRODUCTION

Cyclic nucleotides have been shown to regulate a number of important functions in vascular smooth muscle cells. In terms of atherosclerotic plaque development, the most important functions that cyclic nucleotides regulate in vascular smooth muscle cells are relaxation (Landgraf *et al.*, 1992, Murthy & Mahklouf, 1995, Toyoshima *et al.*, 1998) and proliferation (Kronemann *et al.*, 1999, Ciche *et al.*, 1998).

In vascular smooth muscle cells, contraction occurs when phospholipase C $\beta$  activity is stimulated. This results in the production of inositol triphosphate (IP<sub>3</sub>) and diacylglycerol (DAG). IP<sub>3</sub> then binds to and activates specialised Ca<sup>2+</sup> channels in the sarcoplasmic reticulum, a specialised intracellular Ca<sup>2+</sup> storage organelle found in muscle cells. Upon activation of the IP<sub>3</sub> gated channels, Ca<sup>2+</sup> floods into the cytosol of the cell, increasing the intracellular levels of Ca<sup>2+</sup>. The calcium associates with calmodulin and activates myosin light chain kinase, which then phosphorylates and activates myosin, resulting in contraction of the cell (reviewed in Horowitz *et al.*, 1996).

Both cAMP and cGMP have been shown to be able to reduce intracellular levels of Ca<sup>2+</sup> and cause relaxation of smooth muscle (Landgraf *et al.*, 1992, Murthy & Mahklouf, 1995, Toyoshima *et al.*, 1998). cAMP and cGMP can reduce the levels of intracellular Ca<sup>2+</sup> by two main mechanisms. Firstly PKA and PKG can phosphorylate and inhibit the activity of PLC  $\beta$ . This inhibits the production of IP<sub>3</sub> and ultimately the release of calcium from the sarcoplasmic reticulum, via activation of the IP<sub>3</sub>-gated calcium channels (Murthy *et al.*, 1993). The second mechanism that allows cAMP and cGMP to inhibit Ca<sup>2+</sup> release and cause smooth muscle relaxation is by direct phosphorylation of the IP<sub>3</sub>-gated Ca<sup>2+</sup> channel itself (Komalavilas & Lincoln, 1994, Komalavilas & Lincoln, 1996). It is believed that this phosphorylation may desensitise the IP<sub>3</sub> receptor to IP<sub>3</sub>, therefore greater levels of IP<sub>3</sub> are required to open the Ca<sup>2+</sup> channel. Through these two mechanisms cAMP and cGMP are capable of reducing intracellular [Ca<sup>2+</sup>], and ultimately cause relaxation of smooth muscle cells. PKA and

PKG can act alone or in concert to mediate smooth muscle cell relaxation (Murthy & Makhoul, 1995).

cAMP and cGMP can also regulate smooth muscle cell proliferation (Kronemann *et al.*, 1999, Chiche *et al.*, 1998). These cyclic nucleotides mediate their inhibitory effects on proliferation by inhibiting the expression of certain cyclins necessary for cell cycle progression (Kronemann *et al.*, 1999). cAMP appears to be more potent in inhibiting VSMC proliferation, but this could be due to the decrease in PKG expression in VSMC which have been passaged in culture. In VSMCs which have had their PKG expression augmented by transfection, the antiproliferative effects of NO/cGMP are enhanced (Chiche *et al.*, 1998).

It is tempting to speculate that, as cAMP and cGMP are major regulators of proliferation and relaxation of vascular smooth muscle cells, perhaps aberrant cAMP and cGMP signalling may be important in atherosclerotic plaque development (see sections 1.1.1 and 1.1.2).

Very little is currently known about the role of cyclic nucleotides in regulating glucose transport. There are various reports of cAMP and cGMP being stimulatory, inhibitory or without effect on glucose transport depending on what tissue or cell lines are used.

The cAMP analogue 8-Br cAMP stimulates glucose transport in 3T3-L1 preadipocytes (Cornelius *et al.*, 1991). In cultured rat thyroid cells glucose transport is increased by thyroid stimulating hormone in a cAMP-dependent manner (Hosaka *et al.*, 1992). In these cells cAMP analogues stimulated an increase in the levels of GLUT-1 mRNA, but caused a decrease in GLUT-4 mRNA. In fat cells cAMP has no effect on basal rates of glucose transport, but is inhibitory with regard to insulin-stimulated glucose transport, mediated via GLUT-4 (Lönnroth *et al.*, 1987). These results suggest that perhaps cAMP's effect on glucose transport depends on the GLUT isoforms expressed, with cAMP being stimulatory with regard to GLUT-1 mediated transport but inhibitory with regard to GLUT-4 mediated glucose transport. In pancreatic  $\beta$  cells, phosphorylation of GLUT-2 by PKA results in an inhibition of

glucose transport in these cells (Thorens *et al.*, 1996). In cardiomyocytes cAMP analogues have no effect on glucose transport (Fischer *et al.*, 1996).

Less is known about cGMP's ability to regulate glucose transport. Early reports suggested that cGMP could stimulate glucose transport in cardiomyocytes (Shanahan & Edwards, 1989), however more recent studies have reported that cGMP is without effect on glucose transport in these cells (Fischer *et al.*, 1996). Other work has shown that cGMP is inhibitory with regard to insulin-stimulated glucose transport in rat adipocytes. This effect is thought to be mediated via cGMP's inhibition of PDE 3 in these cells (Eriksson *et al.*, 1994). However, to date the role of cGMP in regulating glucose transport is very poorly understood.

As cAMP and cGMP are important regulators of VSMC proliferation and relaxation, and are also known to be able to regulate glucose transport, I was interested in determining what role, if any, that cAMP and cGMP played in regulating glucose transport in rat aortic vascular smooth muscle cells.

## 4.3 RESULTS

### 4.3.1 Effects of cAMP analogues on basal and PDGF-stimulated glucose transport

To determine what effect, if any, cAMP has on the acute phase of basal and PDGF-stimulated glucose transport, 2-deoxyglucose transport assays were carried out in VSMCs. Cells were treated with 8-Br cAMP (0.1 -1 mM) for 1 hour, either in the absence or presence of PDGF (10 ng/ml) prior to 2-deoxyglucose transport assay. As described in chapter 3, PDGF stimulated an increase in 2-deoxyglucose transport, here a  $2.08 \pm 0.17$  fold increase (n=3 experiments) (Figure 4.1). cAMP had very little effect on PDGF stimulated glucose transport, but did stimulate a  $1.98 \pm 0.07$  fold increase in basal glucose transport (n=3 experiments) (Figure 4.1).

To ensure that the increase in 2-deoxyglucose transport was not due to some peculiar effect of the analogue, the ability of dibutyryl cAMP, another cAMP analogue, to stimulate glucose transport in VSMC was tested. Both cAMP analogues stimulated a ~2 fold increase in 2-deoxyglucose transport, with dibutyryl cAMP stimulating a  $1.96 \pm 0.18$  fold increase and 8-Br cAMP stimulated a  $2.38 \pm 0.4$  fold increase (n=3 experiments), both with an  $EC_{50}$  of ~0.5 mM (Figure 4.2). A time course of 8-Br cAMP stimulated 2-deoxyglucose transport was carried out using treatments of 0.5 mM 8-Br cAMP for 0-2 hours (Figure 4.3). 2-deoxyglucose transport increased within 30 minutes of exposure to 8-Br cAMP, and was still increasing up to two hours after stimulation. All work carried out in this chapter uses a 1 hour stimulation with 8-Br cAMP.

As with PDGF-stimulated glucose transport, it was necessary to ensure that the 8-Br cAMP stimulated transport was not dependent on the rate of phosphorylation of the 2-deoxyglucose. Cells were treated with or without 0.5 mM 8-Br cAMP, and 3-O-methyl glucose transport was measured over varying time points (as described in section 2.6). 8-Br cAMP stimulated an increase in 3-O-methyl glucose transport compared to untreated cells at all time points measured (Figure 4.4). This data can be



converted to give a straight line as described in section 3.3.2, which allows calculation of the rate constant,  $k$ , for transport. The rate constants,  $k$ , for basal and 8-Br cAMP transport were  $0.25 \text{ min}^{-1}$  and  $0.65 \text{ min}^{-1}$  respectively, therefore 8-Br cAMP stimulates an ~2.5 fold increase in the rate of glucose transport in VSMCs. This is very similar to the rate of 2-deoxyglucose transport in response to 8-Br cAMP. PDGF, however, appeared to stimulate a smaller increase in 3-*O*-methyl glucose transport than 2-deoxyglucose transport in VSMCs (see Chapter 3). This is probably just due to experimental variability.

As cAMP analogues were stimulatory with regard to glucose transport in VSMCs, we were interested in determining if they could act as mitogens in these cells. This was achieved by measuring [ $^3\text{H}$ ] thymidine incorporation. 8-Br cAMP was inhibitory with regard to [ $^3\text{H}$ ] thymidine incorporation (Figure 4.5) and therefore was not acting as a mitogen in these cells.

So, analogues of cAMP were stimulatory with regards to glucose transport in VSMCs but were inhibitory with regards to cell growth. The effect of cAMP analogues on glucose transport in VSMCs were not additive to those of PDGF, suggesting that PDGF and cAMP utilise some of the same signalling components in mediating glucose transport.

#### **4.3.2 Cell signalling mechanisms regulating cAMP-stimulated glucose transport in VSMCs**

Next it was of interest to determine which cell signalling pathways may be involved in mediating cAMP-stimulated transport.

##### *PKA*

The most obvious downstream effector for cAMP is PKA. To determine if PKA plays a role in mediating 8-Br cAMP-stimulated glucose transport the PKA inhibitor H-89 was used. Cells were treated for 15 minutes with H-89 (0-500 nM), then 0.5 mM 8-Br cAMP was added and cells incubated for a further 1 hour. H-89 fully inhibited 8-Br

cAMP stimulated glucose transport at doses as low as 50 nM (Figure 4.6). This figure is in keeping with the  $IC_{50}$  for H-89 effects on PKA activity (40 nM).

As 8-Br cAMP's effect on 2-deoxyglucose transport is not additive with PDGF's stimulation of 2-deoxyglucose transport, we were interested in determining if cAMP-PKA were components of the signalling pathway mediating PDGF-stimulated glucose transport. In certain tissues PDGF can stimulate an increase in intracellular [cAMP]. This happens when PDGF stimulates an increase in PKC activity (see section 1.2.3.1) that can phosphorylate and activate certain adenylyl cyclase isoforms (AC II) (see section 1.3.1, table 1.2). First it was determined which adenylyl cyclase isoforms are present in VSMCs by reverse transcription PCR, using primers specific for each isoform studied. The primers used for the RT-PCR are shown in table 4.1. The presence of AC I, II, IV, V, and IX was examined. AC III expression was not examined, as it is expressed solely in the olfactory tissue (see section 1.3.1, Table 1.2), and the presence of the isoforms VII and VIII was not determined as the primers for RT-PCR were not available. RT-PCR showed that the isoforms II, VI, and IX are expressed in VSMCs (Figure 4.7). The primers for AC IV also gives a band but this is also present in the negative control so is most likely a false positive (Figure 4.7).

To determine if cAMP/PKA are components of the signalling pathway involved in mediating PDGF-stimulated glucose transport the effect of the PKA inhibitor, H-89, on PDGF-stimulated glucose transport was tested. Cells were treated for 15 minutes with H-89 and then treated with PDGF (10 ng/ml) for a further 1 hour prior to 2-deoxy glucose transport assay. H-89 had no effect on PDGF-stimulated 2-deoxyglucose transport (Figure 4.8).

As cAMP/PKA are not components of the PDGF-stimulated transport, but cAMP-stimulated transport is not additive with PDGF-stimulated glucose transport, it is possible that these two stimuli utilise some of the same signalling components. The role of PI3' kinase and MAP kinases in mediating 8-Br cAMP-stimulated glucose transport was therefore investigated.

### *PI3' kinase*

To determine the role of PI3' kinase in mediating 8-Br cAMP, cells were treated with 100 nM wortmannin, a PI3' kinase inhibitor, for 30 minutes, then further treated with or without 0.5 mM 8-Br cAMP for 1 hour, prior to 2-deoxyglucose uptake assay. 8-Br cAMP stimulated ~ 2 fold increase in glucose transport (Figure 4.9). Wortmannin had no effect on basal levels of glucose transport, but inhibited the 8-Br cAMP-stimulated glucose transport (Figure 4.9).

### *MAP kinases*

Next, we were interested in determining if there is a role for any of the MAP kinase family, p42/44, p38 or JNK, in mediating 8-Br cAMP-stimulated glucose transport in VSMCs. Firstly the ability of 8-Br cAMP to stimulate the phosphorylation, and therefore the activation of p38, p42/44 and JNK was assessed by using phospho-specific antibodies for the MAP kinases. 1 mM 8-Br cAMP had no effect on the phosphorylation of p42/44 or JNK at all time points looked at, however p38 phosphorylation was stimulated by 1 mM 8-Br cAMP, as determined by the presence of an immunoreactive band of 38 kDa (Figure 4.10). Stimulation was maximal after 5 minutes stimulation with 8-Br cAMP, and was beginning to decline by 15 minutes. After 60 minutes p38 phosphorylation had returned to basal levels.

To determine if p38 plays a role in mediating 8-Br cAMP-stimulated glucose transport, the p38 specific inhibitor SB 203580 was used. SB 203580 completely inhibited 8-Br cAMP stimulated glucose transport at a dose of 10  $\mu$ M (Figure 4.11). This figure for inhibition of glucose transport by inhibition of p38 is consistent with previous results (Gould *et al.*, 1995).

To determine if PKA is upstream of 8-Br cAMP mediated p38 activation, the ability of H-89 to inhibit p38 phosphorylation was measured. Cells were treated with or without H-89 (50nM) for 15 minutes, then treated with 0.5 mM 8-Br cAMP for various times. Whole cell lysates were prepared as described in section 2.9 and subjected to immunoblotting (see section 2.8). H-89 had no effect 8-Br cAMP

stimulated phosphorylation of p38 (Figure 4.12). Therefore, cAMP activation of PKA is not responsible for 8-Br cAMP mediated phosphorylation of p38 in VSMCs.

#### **4.3.3 Endogenous mechanisms of increasing [cAMP] and rates of glucose transport in VSMC**

Next, we were interested in what possible ways the cell may generate intracellular cAMP and increase glucose transport in VSMCs. The most obvious way that muscle cell can increase intracellular cAMP levels is via stimulation of  $\beta_2$  adrenoceptors (Watson & Arkininstall, 1994). These receptors couple to  $G_{\alpha s}$ , which then stimulates adenylyl cyclase activity and increases intracellular [cAMP] (see section 1.3.1). Stimulation of VSMCs with the  $\beta_2$  adrenoceptor agonist, isoprenaline, had no effect on basal levels of glucose transport but did stimulate large increases in the intracellular [cAMP] (Figure 4.13). Other possible endogenous agonists that could raise intracellular [cAMP] and therefore increase the rate of glucose transport in VSMC are agonists of the PGI receptors (Watson & Arkininstall, 1994). The PGI receptor agonist iloprost had little effect on cAMP levels in VSMCs and had no effect on 2-deoxyglucose transport in VSMCs (Figure 4.14).

The inability of agonists that stimulate adenylyl cyclase activity, and cAMP synthesis, to stimulate glucose transport, raised the interesting possibility that it may be necessary to have a very localised increase in [cAMP] to give rise to increased glucose transport rates. One mechanism by which cells can give rise to localised increase in [cAMP] is by decreasing phosphodiesterase activity at specific intracellular sites (see section 1.3.2). In cultured VSMCs the PDEs 1, 3, 4, 5 and, to a lesser extent 2, are expressed (Polson & Strada, 1996). PDEs 1 and 2 hydrolyse both cAMP and cGMP, PDEs 3 and 4 hydrolyse cAMP specifically and PDE 5 hydrolyses cGMP specifically. To determine if a localised increase in [cAMP], caused by decreased PDE activity, can stimulate 2-deoxyglucose transport in VSMCs, inhibitors of PDE activity were used. Unfortunately there are currently no specific inhibitors of PDE1 available, therefore it was not possible to determine a role for PDE 1 here. As PDE 2 constitutes very little of the PDE activity present in VSMCs (Polson & Strada, 1996), the effect of inhibition of PDE 2 activity on 2-deoxyglucose transport was not assessed. Cells were

treated with specific inhibitors of PDE 3 (milrinone), PDE 4 (rolipram) or PDE 5 (zaprinast) for 1 hour prior to 2-deoxyglucose transport assay (see section 2.5). Only the inhibitor of PDE 3, milrinone, had any effect on glucose transport, causing an approximately 2 fold increase in glucose transport in VSMCs at doses as low as 500 nM (Figure 4.15). The inhibitors of PDE 4 and 5 were without effect on 2-deoxyglucose transport in VSMCs (Figure 4.16).

#### **4.3.4 Effects of cGMP on basal and PDGF-stimulated glucose transport in VSMCs**

To determine what effect, if any, cGMP has on glucose transport in VSMCs, the analogue 8-Br cGMP was used. Cells were treated with 8-Br cGMP (0-1 mM) for 1 hour, either in the absence or presence of PDGF (10 ng/ml). PDGF-stimulated a  $2.5 \pm 0.32$  fold increase in 2-deoxyglucose transport and 8-Br cGMP inhibited this transport completely at a dose of 1 mM ( $n=3$  experiments) (Figure 4.17). However, 8-Br cGMP is without effect on basal rates of 2-deoxyglucose transport (Figure 4.17).

cGMP is generated by guanylyl cyclases (see section 1.4.1). Soluble guanylyl cyclases are activated by NO whereas transmembrane guanylyl cyclases are activated upon agonist binding (see section 1.4.1). To determine if activation of transmembrane guanylyl cyclase or soluble guanylyl cyclase can also inhibit PDGF-stimulated glucose transport cells were treated with ANF (atrial natriuretic factor), an agonist of a transmembrane guanylyl cyclase expressed in VSMCs (Garbers & Lowe, 1994), or with sodium nitroprusside (SNP), a nitric oxide donor. ANF was indeed capable of inhibiting PDGF-stimulated glucose transport however SNP had no effect on glucose transport (Figure 4.18).

As described in section 3.3.3, both PI3' kinase and the MAP kinases p38, p42/44 are involved in mediating PDGF-stimulated glucose transport in VSMCs. We were therefore interested in determining if the inhibitory effects of ANF/cGMP on glucose transport are via inhibition of stimulation of MAP kinases. Cells were quiesced in serum-free DMEM for 36-48 hours then treated with ANF (300 nM) for 30 minutes followed by PDGF (10 ng/ml) for various times. Lysates were prepared and subjected

to immunoblotting. To determine the level of phosphorylation, and therefore activation, of the proteins, phospho-specific antibodies to both p38 and p42/44 were used to develop the immunoblots. ANF was not capable of inhibiting PDGF-stimulated phosphorylation and activation of either p38 or p42/44 (Figure 4.19). As yet we have been unable to ascertain the effects of cGMP on PI3' kinase activity.

## 4.4 DISCUSSION

Currently cyclic nucleotides have been reported to affect glucose transport in a variety of ways depending on the cell type used. For example, in 3T3-L1 preadipocytes the cAMP analogue, 8-Br cAMP, stimulates glucose transport (Cornelius *et al.*, 1991), however it is inhibitory with regard to insulin-stimulated glucose transport in fat cells (Lönnroth *et al.*, 1987). In pancreatic  $\beta$  cells, phosphorylation of GLUT-2 by the cAMP stimulated protein kinase, PKA, results in a decrease in the rates of glucose transport (Thorens *et al.*, 1996), however, in cardiomyocytes agents which alter the levels of cAMP had no effect on glucose transport (Fischer *et al.*, 1996). Less is known about the effects of cGMP on glucose transport, with early reports suggesting that cGMP could stimulate transport in cardiomyocytes (Shanahan & Edwards, 1989), however more recent work has shown that cGMP is without effect on glucose transport in cardiomyocytes (Fischer *et al.*, 1996).

Cyclic nucleotides play an important role in regulating vascular smooth muscle cell function. They are involved in regulating smooth muscle cell relaxation and inhibiting proliferation, as described in section 4.2 (Landgraf *et al.*, 1992, Murthy & Mahklouf, 1995, Toyoshima *et al.*, 1998, Kronemann *et al.*, 1999, Ciche *et al.*, 1998). In the work of this chapter we determined what role, if any, cyclic nucleotides play in regulating glucose transport in rat aortic vascular smooth muscle cells.

### 4.4.1 Effects of cAMP on basal and PDGF-stimulated glucose transport

Analogues of cAMP, 8-Br cAMP and dibutyryl cAMP, both stimulate an approximately two-fold increase in 2-deoxyglucose transport in VSMCs (Figure 4.2). This stimulation of glucose transport was not additive with PDGF stimulated glucose transport (Figure 4.1). This suggests that both PDGF and cAMP use components of the same signalling mechanisms to effect increased glucose transport, or that there was a limited pool of glucose transporters in these cells available for transport, and that this pool is fully active in the presence of 10 ng/ml PDGF. However, although cAMP and PDGF can both stimulate glucose transport in VSMCs, cAMP inhibited

cell growth, as determined by [ $^3\text{H}$ ] thymidine incorporation (Figure 4.5), unlike PDGF which stimulated cell growth (see 3.3.2, Figure 3.7).

As discussed in the introduction (see section 1.2.3.1), increased glucose transport may be achieved by translocation of transporters from an intracellular site to the plasma membrane, increasing the total number of glucose transporters at the cell surface, by an increase in the intrinsic activity of the transporter, or by a combination of the above (Gould & Holman, 1993, Czech *et al.*, 1992). cAMP/PKA has been reported to be able to affect traffic along the exocytic pathway as well as alter the intrinsic activity of glucose transporters. PKA has been shown to play a regulatory role in traffic along the exocytic route. By treating NRK cells (normal rat kidney cells) with the PKA inhibitor H89, it was shown that PKA activity was required for transport along the whole exocytic pathway (Muñiz *et al.*, 1996). By treating these cells with agents that increase PKA activity, such as IBMX or forskolin, transport was increased from the Golgi to the plasma membrane. In hepatocytes, cAMP has been shown to increase translocation of the  $\text{Na}^+/\text{taurocholate}$  cotransport polypeptide (Ntcp) to the plasma membrane resulting in an increase in the  $\text{Na}^+/\text{taurocholate}$  cotransport in these cells (Mukhopadhyay *et al.*, 1998). Protein kinase A has also been shown to be involved in the regulated exocytosis of the transport protein aquaporin-2 from intracellular vesicles to the plasma membrane (Katsura *et al.*, 1997). These examples show that cAMP/PKA is capable of eliciting the movement of proteins from intracellular sites to the plasma membrane by a mechanism which is similar to that used by insulin to increase glucose transport in adipocytes with GLUT-4. Therefore it is possible that cAMP/PKA is increasing glucose transport in VSMC by increasing the number of functional glucose transporters at the plasma membrane. If there is a limited pool of glucose transporters available for translocation to the cell surface, it is possible that this pool of transporters is fully translocated to the cell surface in response to PDGF (10 ng/ml). Therefore, when cells are treated with 8-Br cAMP in addition to PDGF no increase in the rates of glucose transport are seen, as there are no further transporters available for translocation.

As well as possibly being able to cause translocation of transporter proteins to the cell surface, cAMP/PKA is capable of altering the activity of glucose transporters. In



pancreatic  $\beta$  cells, protein kinase A rapidly phosphorylates GLUT-2 after activation of adenylyl cyclase. This results in a decrease in the rate of 3-*O*-methyl glucose transport (Thorens *et al.*, 1996). In brown adipocytes noradrenaline can increase the rate of glucose transport in a cAMP dependant manner. This is not due to an increase in the total amount of immunoreactive GLUT-1 present in the plasma membrane, however there is an increase in photoaffinity labelling with the reagent 2-*N*-[4-(1-azitrifluoroethyl)benzoyl]-[2-<sup>3</sup>H]1,3-bis-(D-mannose-4-yl)oxyl)-2-propylamine (ATB-[<sup>3</sup>H]BMPA) of cell surface GLUT-1 (Shimizu *et al.*, 1998). This indicates that noradrenaline's effects on glucose transport in these cells are through an increase in the functional activity of GLUT-1. Therefore we can see that cAMP can alter the functional activity of glucose transporters.

These examples demonstrate that cAMP/PKA could increase the rate of glucose transport either by an increase in the number of transporters at the cell surface, by altering the intrinsic activity of the transporter or by a combination of both of these mechanisms.

#### **4.4.2 Cell signalling mechanisms involved in mediating cAMP-stimulated glucose transport**

##### *PKA*

The most obvious downstream effector of cAMP is the cAMP-stimulated protein kinase, PKA. By using the PKA inhibitor H89, we showed that cAMP-stimulated 2-deoxyglucose transport did indeed require PKA activity (Figure 4.6). As PDGF and cAMP stimulation of glucose transport are not additive with each other, we were interested in determining if cAMP/PKA were components of the PDGF signalling pathway leading to increased glucose transport. In cells expressing adenylyl cyclase II (see table 1.2), PDGF can elevate cAMP levels in a PKC dependant manner (Smit *et al.*, 1998). In airway smooth muscle, protein kinase C activity can stimulate adenylyl cyclase II activity and results in an increase in [cAMP] (Pyne *et al.*, 1994, Moughal *et al.*, 1995). Therefore it was possible that stimulation of VSMCs with PDGF resulted in activation of adenylyl cyclase II and an increase in [cAMP].

We determined by RT-PCR that type II adenylyl cyclase was indeed expressed in VSMCs (Figure 4.7). Therefore it was possible that PDGF could be stimulating an increase in [cAMP] and that this could be a component of the signalling pathway responsible for increased glucose transport in VSMCs. However, when cells are pre-treated with the PKA inhibitor H89 before treatment with PDGF there was no inhibition of glucose transport, indicating that cAMP and PKA are not components of the signalling mechanism mediating PDGF-stimulated glucose transport.

### *PI3' kinase*

Wortmannin (100 nM) was capable of fully inhibiting 8-Br cAMP stimulated glucose transport in VSMCs (Figure 4.9). 100 nM is the concentration of wortmannin capable of eliciting a 100% inhibition of PDGF-stimulated glucose transport, as determined in chapter 3 (section 3.3.3). Therefore PI3' kinase activity is required to mediate cAMP-stimulated glucose transport in VSMCs. The role of PI3' kinase plays in mediating cAMP-stimulated glucose transport is unclear. It is possible that PI3' kinase acts as a signalling molecule downstream of cAMP/PKA. However, PI3' kinase activation is also involved in regulating a variety of vesicular trafficking events (Corvera & Czech, 1998, Wumser, *et al.*, 1999) and may therefore be important in recruiting GLUT1 to the plasma membrane.

### *MAP kinases*

To determine if there was a role for MAP kinases in cAMP-stimulated glucose transport it was first assessed which MAP kinases were stimulated in response to 8-Br cAMP in VSMCs. Only p38 MAP kinase is phosphorylated, and activated, in response to 8-Br cAMP (Figure 4.10). The specific inhibitor of p38, SB 203580, was used to determine if p38 activity was necessary for cAMP-stimulated glucose transport. SB 203580 fully inhibited cAMP-stimulated glucose transport at doses as low as 10  $\mu$ M (figure 4.11). This dose is consistent with that from previous work on p38's role in glucose transport (Gould *et al.*, 1995). Therefore p38 activity is required to mediate cAMP-stimulated glucose transport.

There are several reports of cAMP being able to stimulate the activity of p38. In rat epididymal fat cells, isoproterenol and cAMP analogue chlorophenylthio-cAMP will stimulate a rapid and sustained increase in p38 activity (Moule & Denton, 1998), and in T-cells PKA can mediate the release of MAP kinases from proteins which inhibit their activity (Saxena *et al.*, 1999). These reports state that cAMP's effects on p38 activity are mediated via activation of PKA. However, we have showed that stimulation of p38 phosphorylation and activation in response to 8-Br cAMP is not dependent on PKA activity (by the use of the PKA inhibitor H89) in VSMCs (Figure 4.12). It is unclear how cAMP could be stimulating p38 activity independent of PKA activity. Recent work has shown that cAMP can directly bind and activate certain guanine nucleotide exchange factors (GEFS) (de Rooij *et al.*, 1998). It is therefore possible that cAMP could activate small G-proteins, by activation of GEFS, which are upstream from p38 activation. However, this is as yet speculation.

So, overall, cAMP requires protein kinase A, PI3' kinase and p38 MAP kinase activity to stimulate glucose transport in VSMCs.

#### **4.4.3 Endogenous mechanisms for generating cAMP and stimulating glucose transport**

From section 4.3.1 it was shown that cAMP analogues could stimulate an increase in glucose transport in VSMCs (Figure 4.2). We were therefore interested in determining what endogenous ligands could stimulate an increase in intracellular [cAMP] and glucose transport. Two obvious candidates were agonists of the  $\beta 2$  adrenoceptor and of the PGI receptor. Both of these receptors are expressed in vascular smooth muscle tissue and couple predominantly to G $\alpha$ s to stimulate the production of cAMP (Watson & Arkininstall, 1994). However agonists of both receptors failed to stimulate any increase in glucose transport in VSMCs, at doses which did stimulate an increase in cAMP production in the cells (Figures 4.13 and 4.14). Therefore stimulation of cAMP production by activation of adenylyl cyclase is not sufficient to stimulate glucose transport in VSMCs.

This raised the possibility that it was a very localised increase in [cAMP] that may be necessary to stimulate glucose transport. There are several reports on the importance of the spatial distribution of cAMP in eliciting specific cellular effects (Hempel *et al.*, 1996, Aass *et al.*, 1988, Jurevicius & Fischmeister, 1996). By inhibition of specific PDEs at specific subcellular locations a small, very localised increase in cAMP concentration can be achieved (see section 1.3.2 for information on PDEs). These small increases in local cAMP concentration can then stimulate PKAII isoforms held at specific sites by AKAPs (A Kinase Anchoring Proteins) (see section 1.3.3 for overview). This tailoring of cAMP signalling is reviewed in Houslay & Milligan, 1997. VSMCs express PDEs 1, 2, 3, 4 & 5 (Polson & Strada, 1996). We determined that by inhibiting PDE 3 activity an increase in glucose transport rates, similar to that seen with cAMP analogues, is achieved (Figure 4.15), however no effect is seen on glucose transport rates when inhibitors of PDE 4 and 5 are used (Figure 4.16). This supports the idea that a localised increase in [cAMP], caused by a decrease in PDE activity, could stimulate glucose transport in VSMCs.

#### **4.4.4 Effect of cGMP on basal and PDGF-stimulated glucose transport in VSMCs**

Very little is known about cGMP's ability to regulate glucose transport. An early report suggested that cGMP could stimulate glucose transport in rat cardiomyocytes (Shanahan & Edwards, 1989), however a more recent report has shown that agents that increase levels of cGMP have no effect on glucose transport in these cells (Fischer *et al.*, 1996). We used the cGMP analogue, 8-Br cGMP, to determine if cGMP could affect glucose transport in VSMCs. 8-Br cGMP had no effect on basal rates of glucose transport but was able to inhibit PDGF-stimulated glucose transport (Figure 4.17). This was a surprising result, as cAMP and cGMP often work in concert to elicit their effects in VSMCs, i.e. their effects on proliferation and relaxation (see section 4.2).

cGMP is generated by guanylyl cyclase. There are two types of guanylyl cyclase; soluble guanylyl cyclase that is activated by nitric oxide (NO), and transmembrane

guanylyl cyclase, which is activated upon binding of an appropriate agonist (see section 1.4.1). We determined if agents that can raise intracellular cGMP, can also inhibit PDGF-stimulated glucose transport in VSMCs. Treatment of cells with ANF, an agonist of transmembrane guanylyl cyclase, did inhibit PDGF-stimulated glucose transport, whereas sodium nitroprusside (SNP), an NO donor, had no effect on PDGF-stimulated glucose transport (Figure 4.18). It is intriguing that both agents should result in an increase in intracellular [cGMP], but apparently have different effects on glucose transport in VSMCs. It is possible that perhaps the spatial distribution of cGMP within the cell could play an important role in determining the effects seen, or perhaps soluble guanylyl cyclase isoforms are not expressed in cultured VSMCs.

As was shown in section 3.3.3 the MAP kinases, p42/44 and p38 are involved in mediating PDGF-stimulated glucose transport. cGMP has been shown to inhibit activation of MAP kinases in BHK cells (baby hamster kidney cells). We were therefore interested in determining if the inhibitory effects of cGMP on PDGF-stimulated glucose transport were via inhibition of MAP kinase activity. We determined, however, that neither 8-Br cGMP nor ANF had any effect on PDGF's ability to stimulate either p42/44 or p38 (Figure 4.19). Therefore cGMP's inhibitory effects on PDGF-stimulated glucose transport are not mediated via inhibition of MAP kinases. As yet we have not looked at the effect of cGMP on PI3'kinase, but as MAP kinases and PI3' kinase are the only two signalling mechanisms known to be involved in mediating PDGF-stimulated glucose transport, this is the next most obvious target for cGMP's effects.

## 4.5. SUMMARY

Cyclic nucleotides play an important role in regulating a number of VSMC functions, including proliferation and relaxation (Murthy & Makhlouf, 1995, Kronemann *et al.*, 1999, Chiche *et al.*, 1998). cAMP and cGMP have been shown to be stimulatory, inhibitory or without effect on glucose transport depending on what cells are studied. However, although cyclic nucleotides are important second messengers in VSMCs and are known to affect glucose transport, no work has been done on the role of cyclic nucleotides in regulating glucose transport in VSMCs.

Here we showed that analogues of cAMP could stimulate an approximately two-fold increase in glucose transport in VSMCs. This stimulation of glucose transport by cAMP analogues is not additive with PDGF-stimulated glucose transport, indicating that both cAMP and PDGF must use some of the same signalling components to mediate the increase in glucose transport. The stimulation of glucose transport by cAMP analogues requires PKA, however, cAMP/PKA are not components of the PDGF-stimulated signalling pathway mediating glucose transport in VSMCs (as the PKA inhibitor, H89, has no effect on PDGF-stimulated glucose transport). As well as PKA, both p38 and PI3' kinase are necessary for cAMP-stimulated glucose transport.

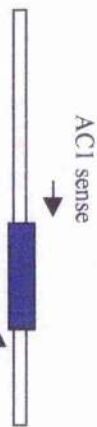

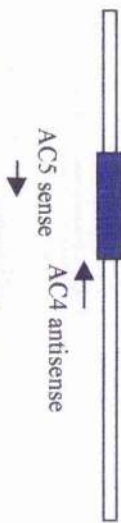
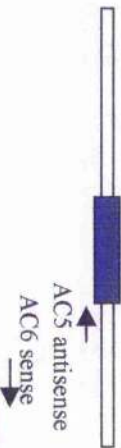
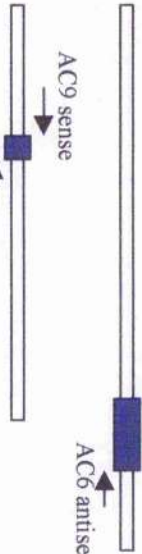

Ligands that stimulated adenylyl cyclase activity and an increase in intracellular [cAMP] in VSMCs, such as isoprenaline and iloprost, had no effect on glucose transport in VSMCs, however by inhibiting PDE 3 activity, to give a small localised increase in [cAMP], an increase in glucose transport similar to that seen with cAMP analogues was seen (approximately two-fold). This indicates that it is the spatial distribution of cAMP in the cell rather than the overall amount of cAMP that is important in the stimulation of glucose transport in VSMCs.

Analogues of cGMP are without effect on basal glucose transport rates in VSMCs but are inhibitory with regard to PDGF-stimulated glucose transport. ANF, a ligand of transmembrane guanylyl cyclase, is also inhibitory with regard to PDGF-stimulated glucose transport, whereas SNP, an NO donor (NO stimulates soluble guanylyl

cyclase activity), is without effect on glucose transport in VSMCs. The ability of cGMP to inhibit PDGF-stimulated glucose transport is not via an inhibition of MAP kinase activity. The effects of cGMP on PI3' kinase activity have not yet been determined.

Table 4.1 Products and primers for RT-PCR analysis of adenylyl cyclase isoforms

Primers were as follows:

	AC 1 Product 800 bp	AC1 sense GATCCTGCTCTCCGGGCTCA	AC1 antisense CTTCTCAGCAGCCGGTGGACT
	AC 2 Product 1000 bp	AC2 sense CACGGATCTCCCTCACAATCGTCA	AC2 antisense GCCCATGGTTGATACCCACTCGCA
	AC 4 Product 1000 bp	AC4 sense CAGGAGCACCTCCTCTTGCTAT	AC4 antisense GTTGTTGGAATGACCTGGAAGAAGAAC
	AC 5 Product 800 bp	AC5 sense CTACAACCACCTTGGGTGGCAAC	AC5 antisense TATGGCAATTGGCGGTGACCAG
	AC 6 Product 600 bp	AC6 sense CGGAAAGTAGACCCCTCGTTTCGGA	AC6 antisense GCCAAGCCATGAGACGCTAAGCA
	AC 9 Product 350 bp	AC9 sense CGCTGCTTCCGCAGACCCAG	AC9 antisense GTGGCCGTGAGAGTATGATTGGAGCTGTC



#### **Figure 4.1 2-deoxyglucose transport in VSMCs in response to 8-Br cAMP with and without PDGF**

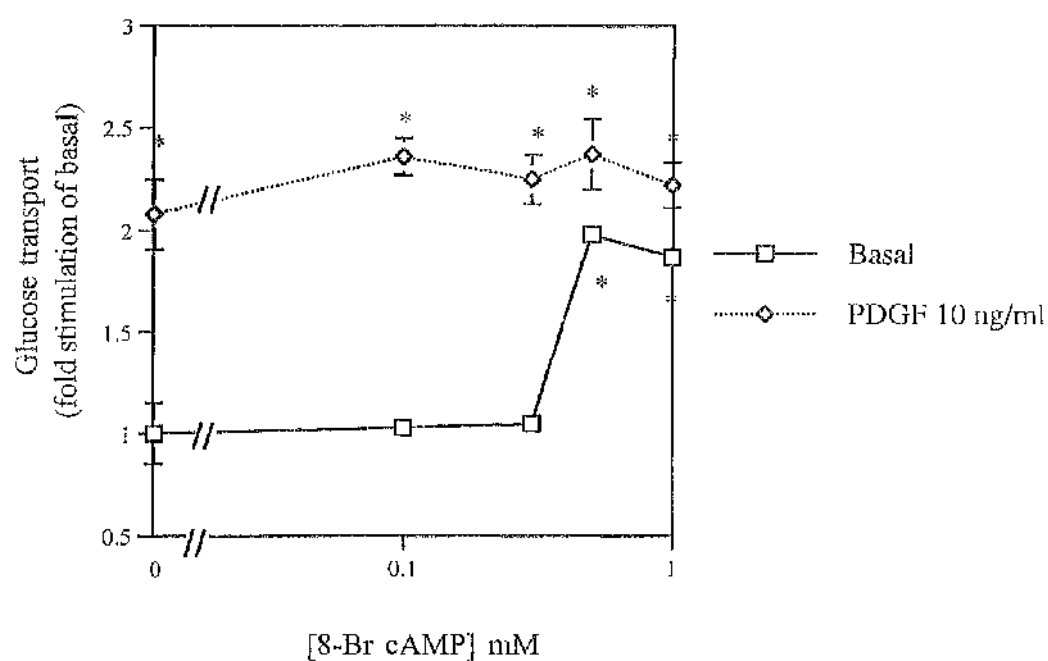
2-deoxyglucose transport assay was carried out as described in section 2.5.

Cells were quiesced for 36-48 hours, then treated with 8-Br cAMP for 1 hour at the concentrations shown followed by PDGF (10 ng/ml) a further hour, prior to 2-deoxyglucose transport assay. Data from a representative experiment is shown, repeated three times with similar results.

Each point represents the mean of triplicate determinations  $\pm$  S.E.M. Data is expressed as a fold stimulation of basal (unstimulated) transport rates.

\* represents  $P < 0.05$  when compared to untreated cells as determined by Student's t-test..

2-deoxy glucose transport in VSMC in response to 8-Br cAMP  
with and without PDGF



## **Figure 4.2 Effect of cAMP analogues on 2-deoxyglucose transport in VSMCs**

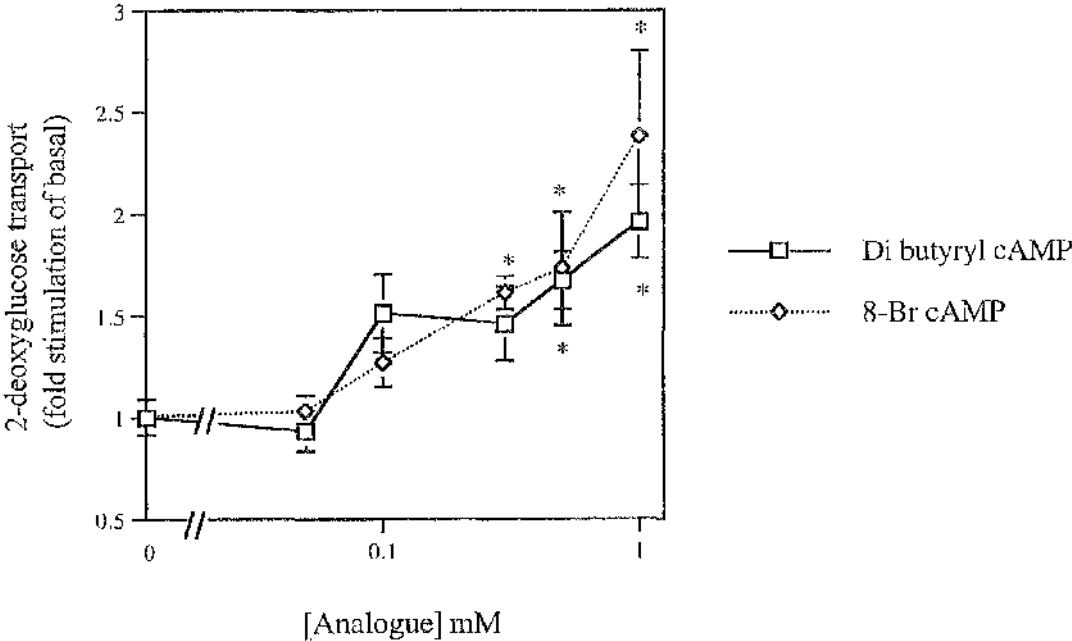
2-deoxyglucose transport assay was carried out as described in section 2.5.

Cells were quiesced for 36-48 hours, then treated with 8-Br cAMP or dibutyryl cAMP for 1 hour at the concentrations shown, prior to 2-deoxyglucose transport assay. Data from a representative experiment is shown, repeated three times with similar results.

Each point represents the mean of triplicate determinations  $\pm$  S.E.M. Data is expressed as a fold stimulation of basal (unstimulated) transport rates.

\* represents  $P < 0.05$  as compared to basal/untreated cells as determined by Student's t-test.

Stimulation of 2-deoxyglucose transport in VSMCs in response to cAMP analogues



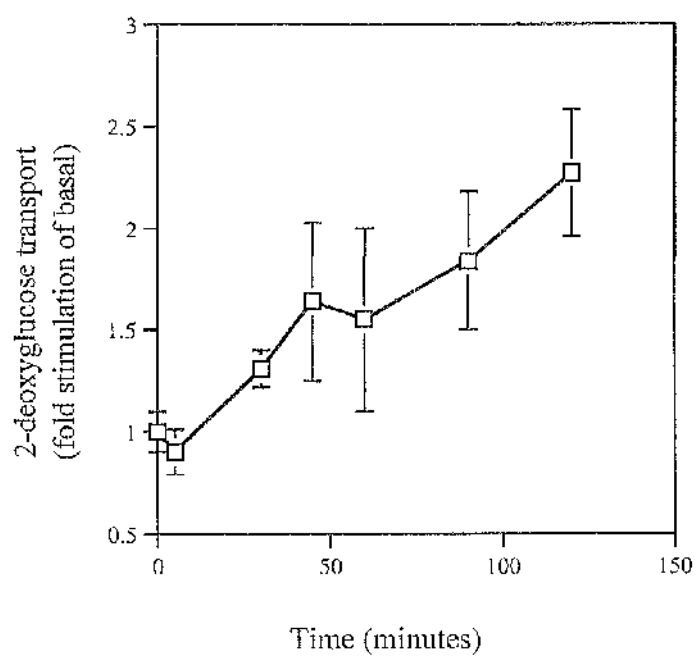
### **Figure 4.3 Time-course of 2-deoxyglucose transport in VSMCs in response to 8-Br cAMP**

2-deoxyglucose transport assay was carried out as described in section 2.5.

Cells were quiesced for 36-48 hours, then treated with 8-Br cAMP (0.5 mM) for the times indicated, prior to 2-deoxyglucose transport assay. Data from a representative experiment is shown, repeated three times with similar results.

Each point represents the mean of triplicate determinations  $\pm$  S.E.M. Data is expressed as a fold stimulation of basal (unstimulated) transport rates.

Time-course of 2-Deoxyglucose transport in  
VSMCs in response to 8-Br cAMP



#### **Figure 4.4 3-*O*-methyl glucose transport in VSMCs in response 8-Br cAMP**

3-*O*-methyl glucose transport assay was carried out as described in section 2.6.

Cells were quiesced for 36-48 hours, then treated with 8-Br cAMP (0.5 mM) for 1 hour and 3-*O*-methyl glucose transport measured for the times indicated. Data from a representative experiment is shown, repeated three times with similar results.

##### **A.**

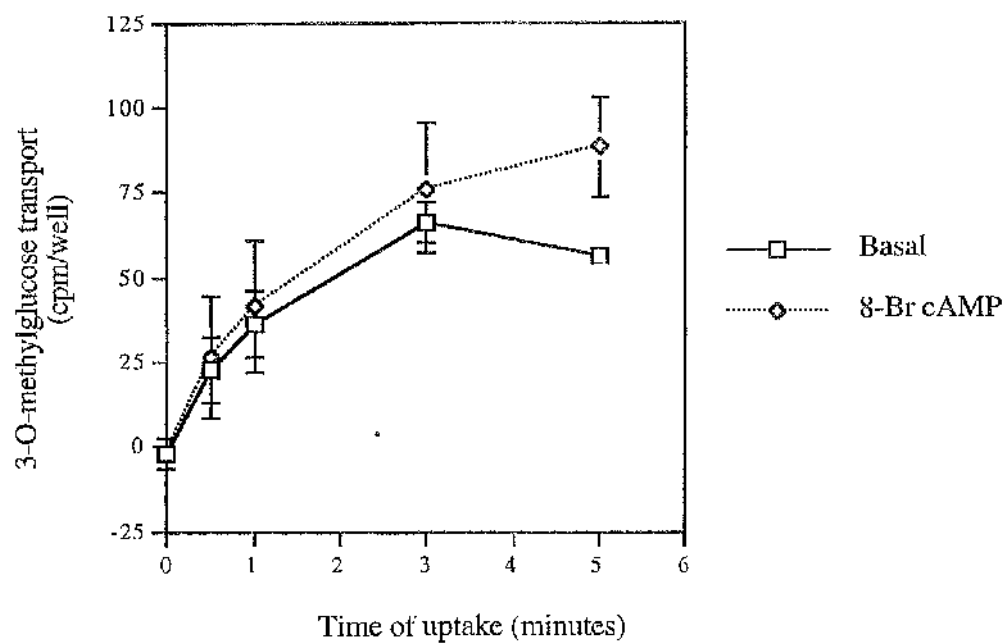
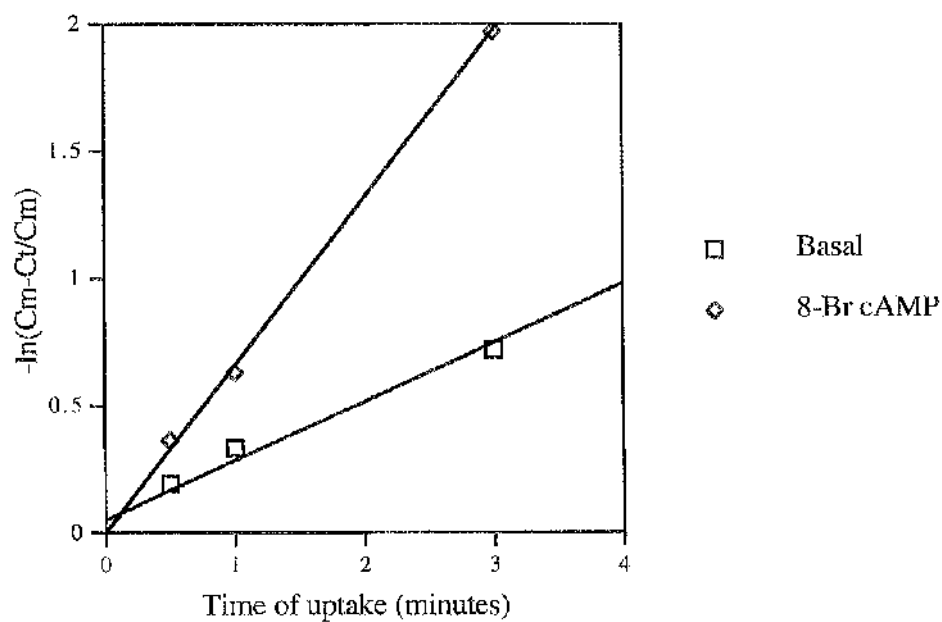
Each point represents the mean of triplicate determinations  $\pm$  S.E.M. Data is expressed as cpm of 3-*O*-methyl glucose transported/well.

##### **B.**

The mean cpm/well values were converted using the equation:

$$-\ln((C_m - C_t)/C_m)$$

where  $C_m$  was the maximum cpm/well and  $C_t$  was the cpm/well at a given time point,  $t$ . This gives a straight line, where the gradient of each line represents the rate constant,  $k$ , for 3-*O*-methyl glucose.

**A****B**



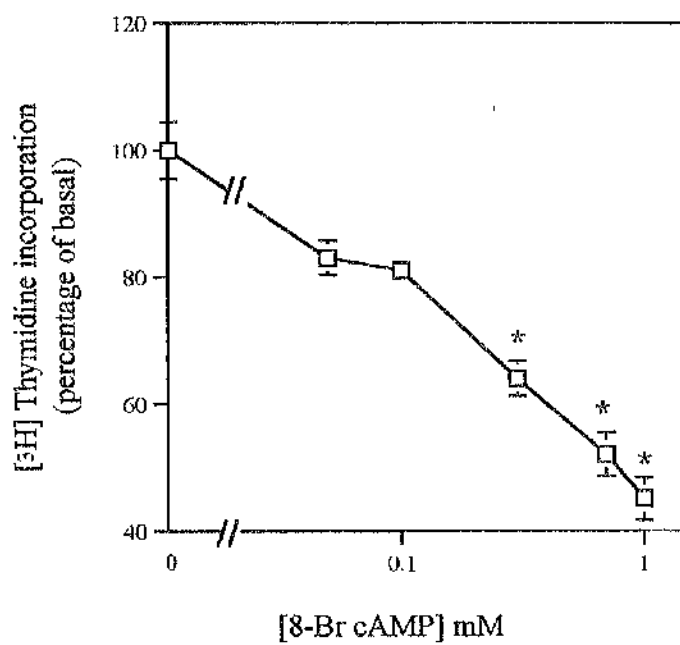
## Figure 4.5

[<sup>3</sup>H] thymidine incorporation was determined as described in section 2.11. Cells were quiesced for 12-24 hours, then treated with 8-Br cAMP at the concentrations indicated for a further 24 hours. 0.5 µCi of [<sup>3</sup>H] thymidine was added per well for the final 6 hours of the incubation with PDGF. Data from a representative experiment is shown, repeated three times with similar results.

Each point represents the mean of triplicate determinations ± S.E.M. Data is expressed as a fold stimulation over basal (unstimulated) rates of [<sup>3</sup>H] thymidine incorporation.

\* represents  $P < 0.05$  when compared to basal/untreated cells as determined by Student's t-test.

[<sup>3</sup>H] Thymidine incorporation in  
VSMCs in response to 8-Br cAMP



#### **Figure 4.6 Effect of PKA inhibitor, H 89, on basal and 8-Br cAMP-stimulated 2-deoxyglucose transport**

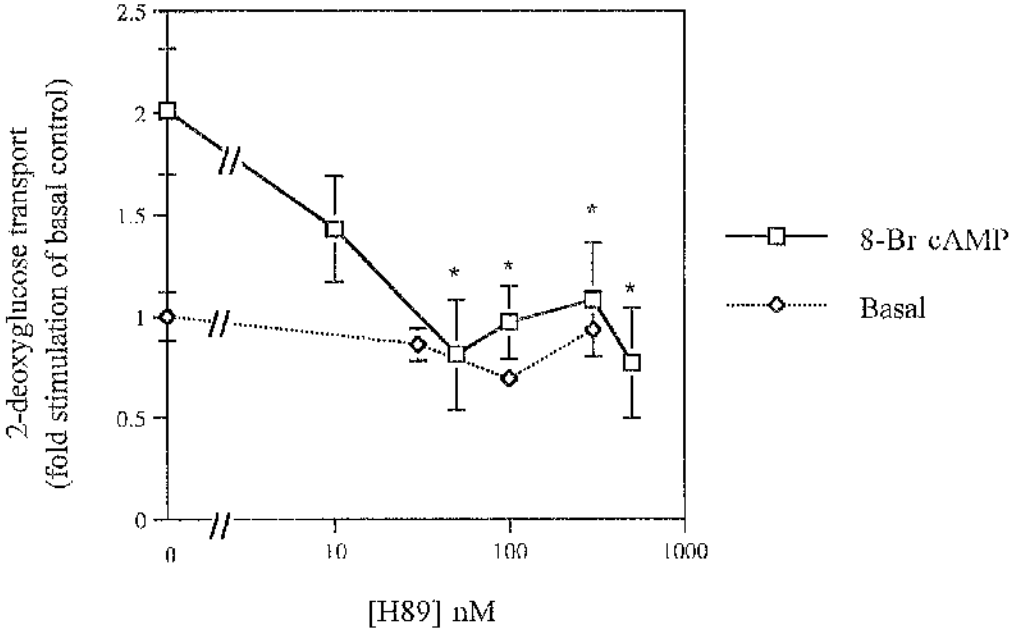
2-deoxyglucose transport assay was carried out as described in section 2.5.

Cells were quiesced for 36-48 hours, then treated with the PKA inhibitor, H-89 for 15 minutes, followed by 8-Br cAMP (0.5 mM) for a further hour, prior to 2-deoxyglucose transport assay. Data from a representative experiment is shown, repeated three times with similar results.

Each point represents the mean of triplicate determinations  $\pm$  S.E.M. Data is expressed as a fold stimulation of basal (unstimulated) transport rates.

\* represents  $P < 0.05$  when compared to cells treated with 8-Br cAMP alone as determined by Student's t test.

Effect of H89 on basal and 8-Br cAMP-stimulated  
2-deoxyglucose transport



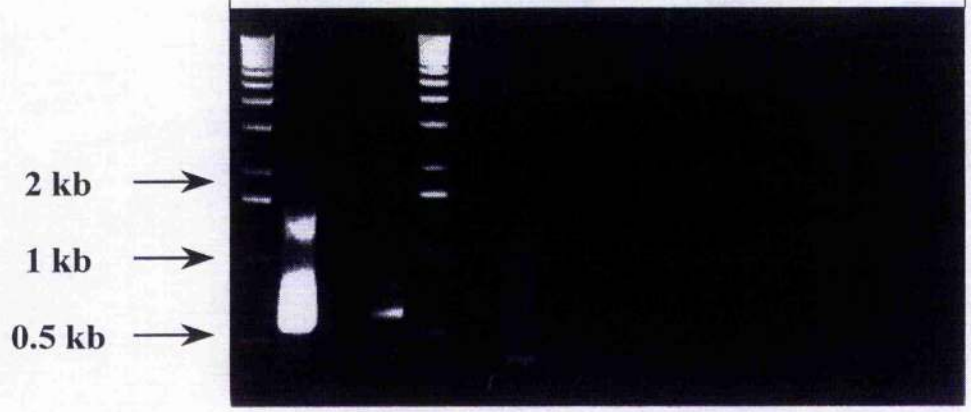
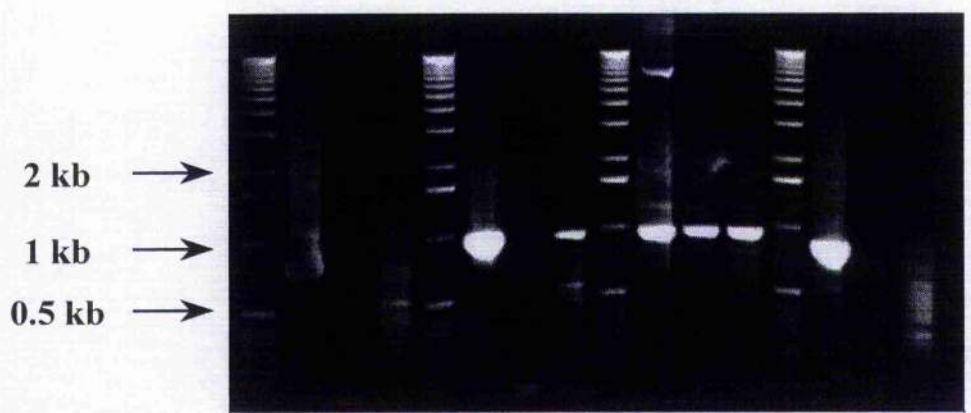
**Figure 4.7 RT-PCR analysis of adenylyl cyclase isoforms expressed in VSMCs**

RT-PCR was carried out to determine which adenylyl cyclase isoforms were expressed in VSMCs.

mRNA was extracted from cultured VSMCs and reverse transcription was carried out using the Wizard RT-PCR kit from Promega as described in section 2.17.11. The products of reverse transcription were the used in PCR reactions using the primers defined in Table 4.1 and PCR conditions are described in section 2.17.11.

AC I	adenyl cyclase I	AC V	adenyl cyclase V
AC II	adenyl cyclase II	AC VI	adenyl cyclase VI
AC IV	adenyl cyclase IV	AC IX	adenyl cyclase IX
M	1 kb ladder		
+	RT-PCR positive control		
-	RT-PCR negative control		
S	RT-PCR of VSMC mRNA		

<u>AC I</u>				<u>AC II</u>				<u>AC IV</u>				<u>AC V</u>			
M	+	-	S	M	+	-	S	M	+	-	S	M	+	-	S



M	+	-	S	M	-	S
<u>AC VI</u>				<u>AC IX</u>		

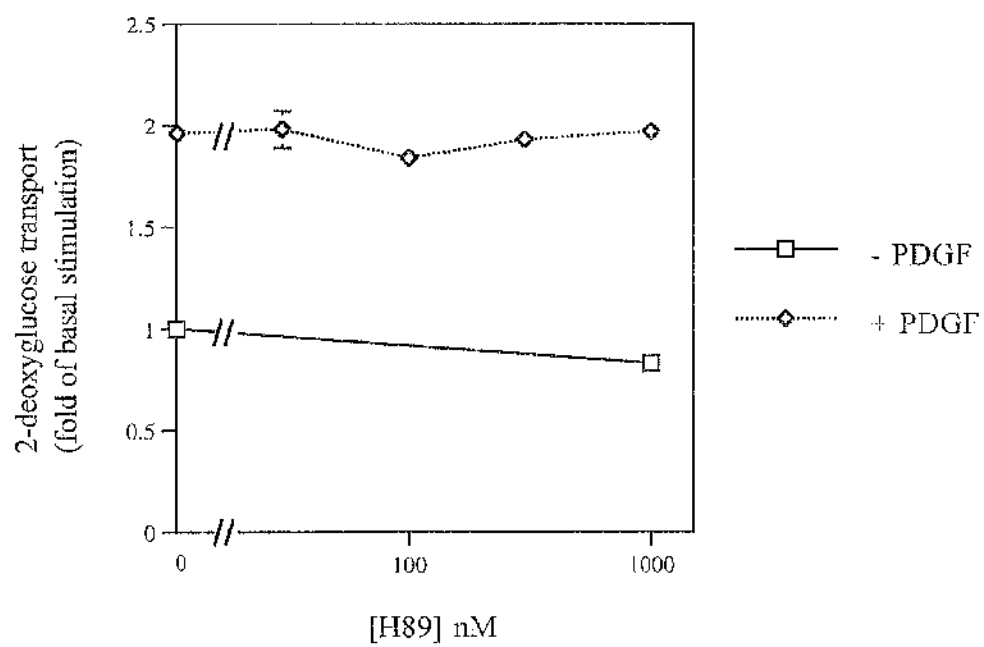
### **Figure 4.8 Effect of H89 on basal and PDGF-stimulated 2-deoxyglucose transport**

2-deoxyglucose transport assay was carried out as described in section 2.5.

Cells were quiesced for 36-48 hours, then treated with the PKA inhibitor, H-89 for 15 minutes, followed by PDGF (10 ng/ml) for a further hour, prior to 2-deoxyglucose transport assay. Data from a representative experiment is shown, repeated three times with similar results.

Each point represents the mean of triplicate determinations  $\pm$  S.E.M. Data is expressed as a fold stimulation of basal (unstimulated) transport rates.

Effect of H89 of basal and PDGF-stimulated  
2-deoxyglucose transport





### **Figure 4.9 Effect of wortmannin on 8-Br cAMP-stimulated 2-deoxyglucose transport**

2-deoxyglucose transport assay was carried out as described in section 2.5.

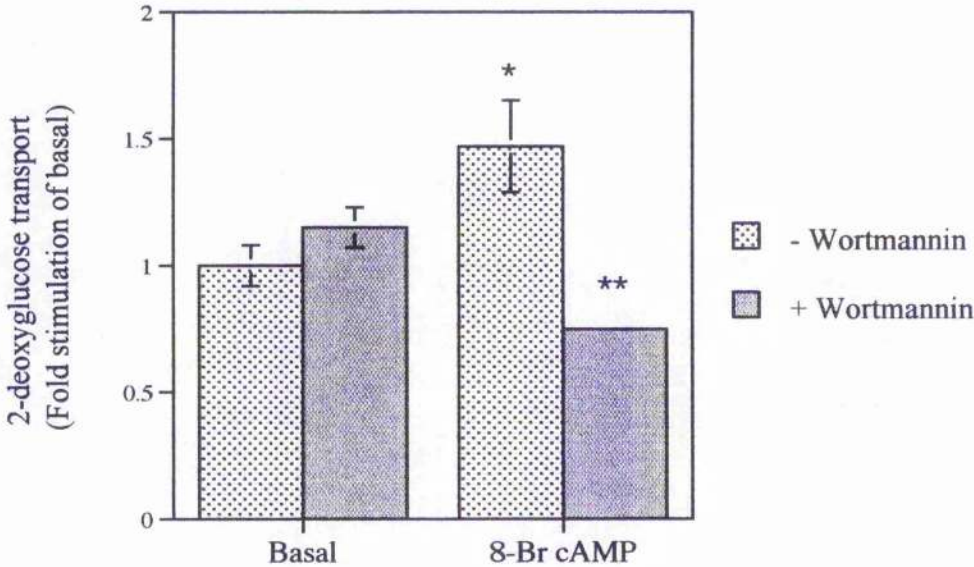
Cells were quiesced for 36-48 hours, then treated with or without wortmannin (100 nM) for 30 minutes followed by 8-Br cAMP (0.5 mM) for a further hour, prior to 2-deoxyglucose transport assay. Data from a representative experiment is shown, repeated three times with similar results.

Each point represents the mean of triplicate determinations  $\pm$  S.E.M. Data is expressed as a fold stimulation of basal (unstimulated) transport rates.

\* represents  $P < 0.05$  when compared to basal untreated cells as determined by Student's t test.

\*\* represents  $P < 0.05$  when compared to cells treated with 8-Br cAMP alone as determined by Student's t test.

Effect of wortmannin on 8-Br cAMP-stimulated  
2-deoxy glucose transport

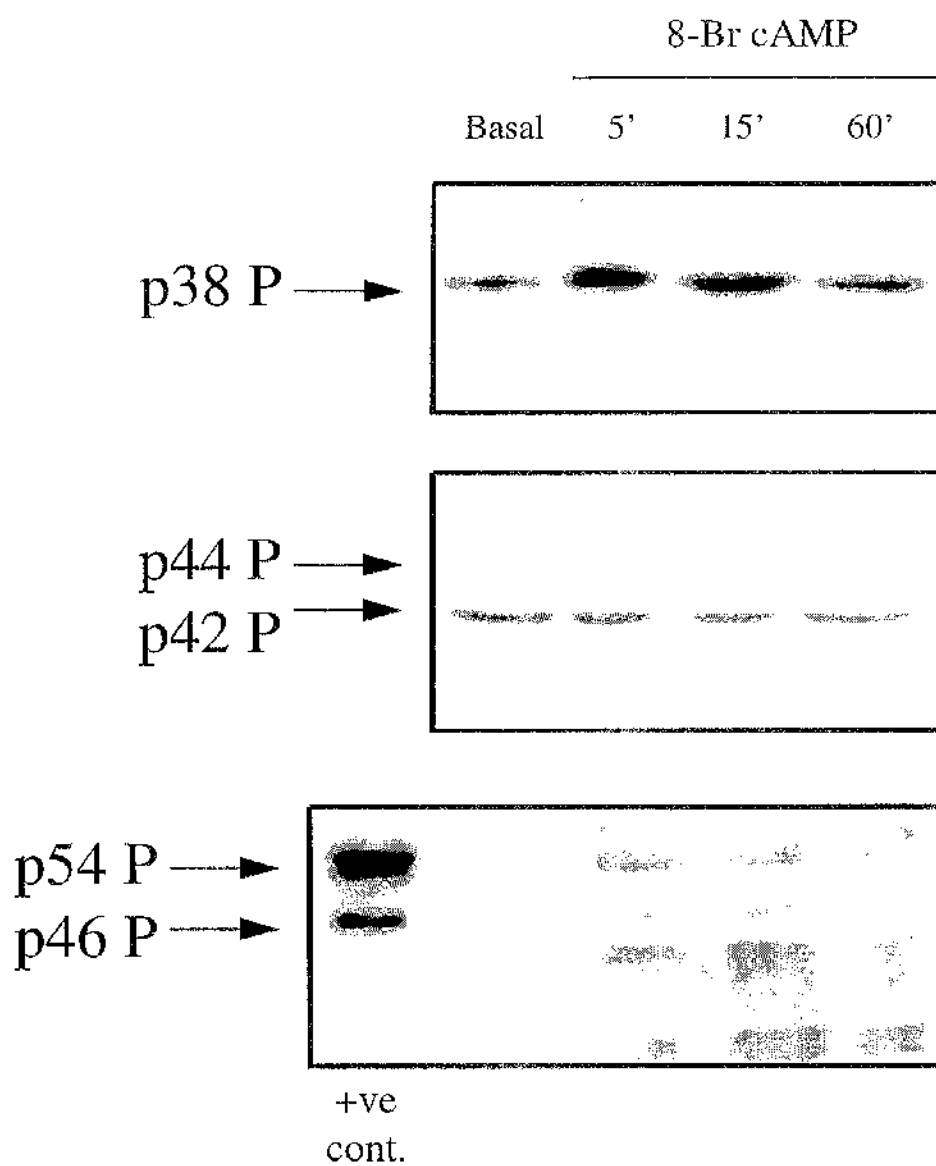


### **Figure 4.10 Effects of 8-Br cAMP on the activation/phosphorylation of MAP kinases**

VSMCS were grown to confluency in 6-well plates and quiesced in serum-free DMEM for 36-48 hours. Cells were treated with or without 8-Br cAMP (0.5 mM) for 5, 15 or 60 minutes and then whole cell lysates were prepared as described in section 2.9. 50µl of each lysate was loaded in each lane of a 10 % SDS-PAGE gel and subjected to electrophoresis and immunoblotting as described in section 2.8. Blots were developed using phospho-specific antibodies to p38, p42/44 and JNK MAP kinases, respectively, which only recognise the phosphorylated, therefore activated, kinase. The positive control on the JNK blot is from the manufacturers of the antibody (New England Biolabs).

8-Br cAMP stimulated phosphorylation, and activation of p38, but had no effect on the phosphorylation of p42/44 or JNK (although the cross-reactivity of the JNK antibody with p42/44 did not allow accurate analysis of this).

These blots are representative of three such experiments.



### **Figure 4.11 Effects of SB 203580 on basal and 8-Br cAMP-stimulated 2-deoxyglucose transport**

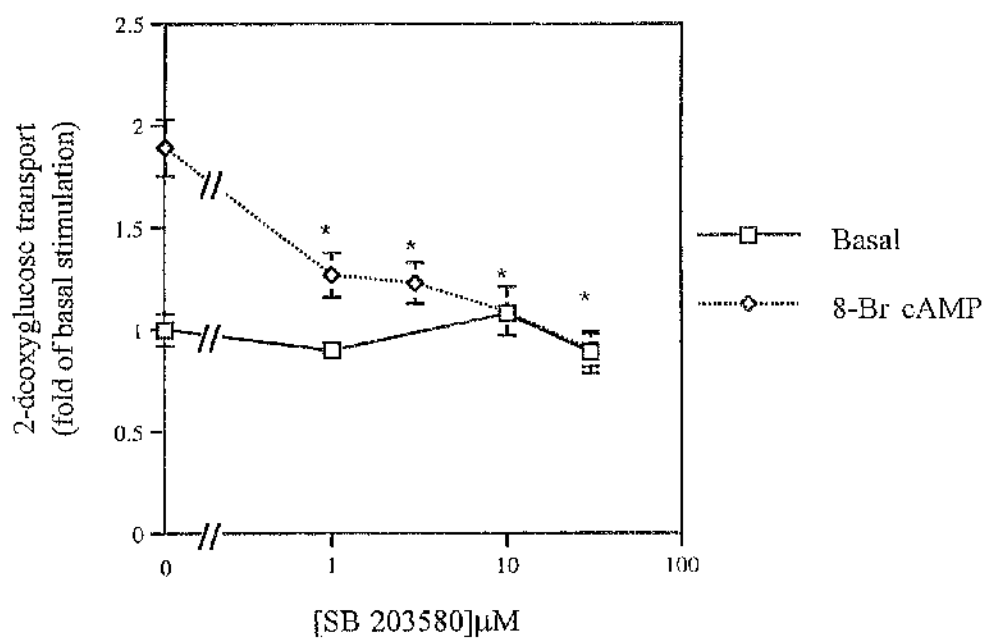
2-deoxyglucose transport assay was carried out as described in section 2.5.

Cells were quiesced for 36-48 hours, then treated with or without SB 203580 for 1 hour followed by 8-Br cAMP (0.5 mM) for a further hour, prior to 2-deoxyglucose transport assay. Data from a representative experiment is shown, repeated three times with similar results.

Each point represents the mean of triplicate determinations  $\pm$  S.E.M. Data is expressed as a fold stimulation of basal (unstimulated) transport rates.

\* represents  $P < 0.05$  when compared to cells treated with PDGF alone as determined by Student's *t* test.

# Effect of SB 203580 on basal and 8-Br cAMP-stimulated 2-deoxyglucose transport



### **Figure 4.12 Effect of H89 on 8-Br cAMP-stimulated p38 phosphorylation/activation**

VSMCS were grown to confluency in 6-well plates and quiesced in serum-free DMEM for 36-48 hours. Cells were treated with or without H-89 (50 nM) for 15 minutes followed by 8-Br cAMP (0.5 mM) for 5, 15 or 60 minutes and then whole cell lysates were prepared as described in section 2.9. 50 $\mu$ l of each lysate was loaded in each lane of a 10 % SDS-PAGE gel and subjected to electrophoresis and immunoblotting as described in section 2.8. Blots were developed using phospho-specific antibodies to p38, which only recognise the phosphorylated, therefore activated, kinase.

H-89 has no effect on the ability of 8-Br cAMP to phosphorylate, therefore activate p38.

These blots are representative of three such experiments.

8-Br cAMP

Basal

5'

15'

60'

H89

-

+

-

+

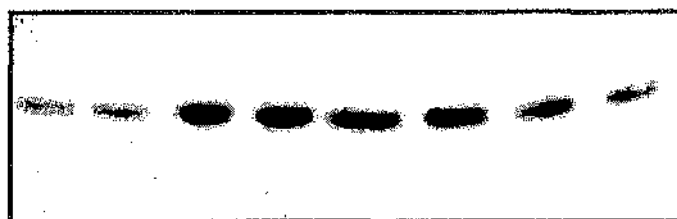
-

+

-

+

p38 P





## **Figure 4.13 Isoprenaline-stimulated cAMP generation and 2-deoxyglucose transport in VSMCs**

### **Upper panel**

Adenyl cyclase assay was carried out as described in section 2.16.

Cells were quiesced for 36-48 hours, 24 hours prior to assay the cells were labelled with [ $^3\text{H}$ ] adenine at 1  $\mu\text{Ci/ml}$ . Cells were treated with isoprenaline for 30 minutes, prior to adenyl cyclase assay. Data from a representative experiment is shown, repeated three times with similar results.

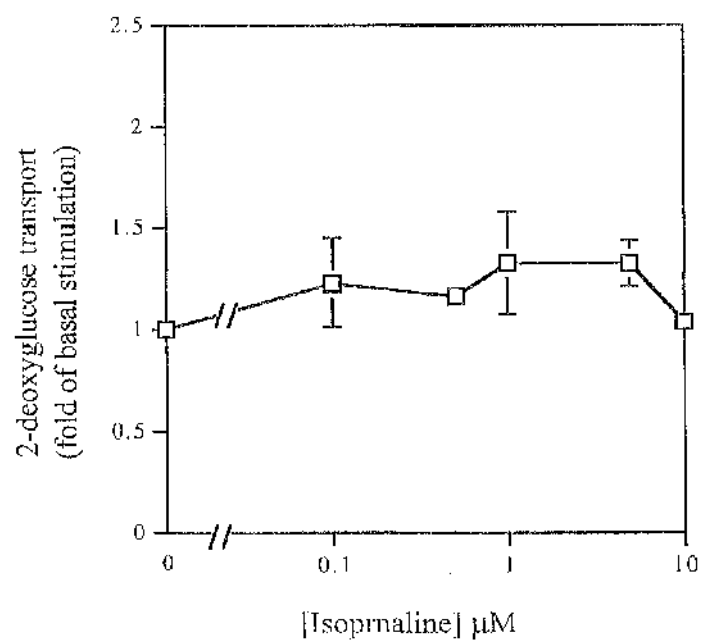
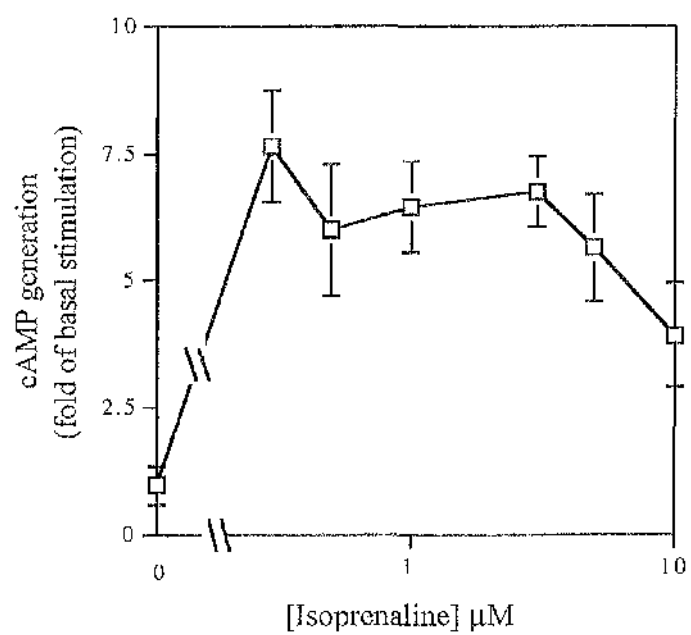
Each point represents the mean of triplicate determinations  $\pm$  S.E.M. Data is expressed as a fold stimulation of basal (unstimulated) transport rates.

### **Lower Panel**

2-deoxyglucose transport assay was carried out as described in section 2.5.

Cells were quiesced for 36-48 hours, then treated with isoprenaline for 30 minutes prior to 2-deoxyglucose transport assay. Data from a representative experiment is shown, repeated three times with similar results.

Each point represents the mean of triplicate determinations  $\pm$  S.E.M. Data is expressed as a fold stimulation of basal (unstimulated) transport rates.



## **Figure 4.14 Iloprost-stimulated cAMP generation and 2-deoxyglucose transport in VSMCs**

### **Upper panel**

Adenyl cyclase assay was carried out as described in section 2.16.

Cells were quiesced for 36-48 hours, 24 hours prior to assay the cells were labelled with [<sup>3</sup>H] adenine at 1 µCi/ml. Cells were treated with iloprost or PGE1 for 30 minutes, prior to adenyl cyclase assay. Data from a representative experiment is shown, repeated three times with similar results.

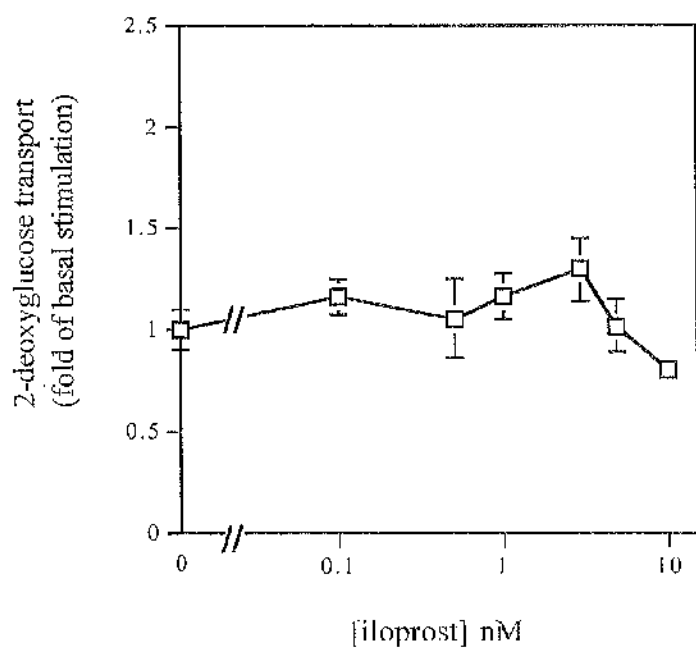
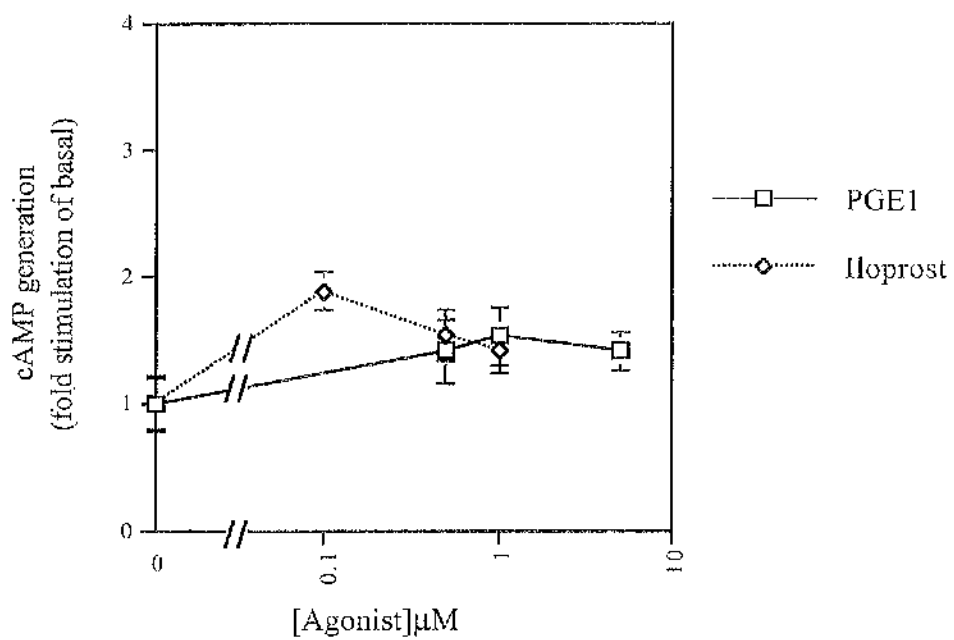
Each point represents the mean of triplicate determinations ± S.E.M. Data is expressed as a fold stimulation of basal (unstimulated) transport rates.

### **Lower Panel**

2-deoxyglucose transport assay was carried out as described in section 2.5.

Cells were quiesced for 36-48 hours, then treated with iloprost for 30 minutes prior to 2-deoxyglucose transport assay. Data from a representative experiment is shown, repeated three times with similar results.

Each point represents the mean of triplicate determinations ± S.E.M. Data is expressed as a fold stimulation of basal (unstimulated) transport rates.



### **Figure 4.15 Effect of PDE 3 inhibitor, milrinone, on 2-deoxyglucose transport in VSMCs**

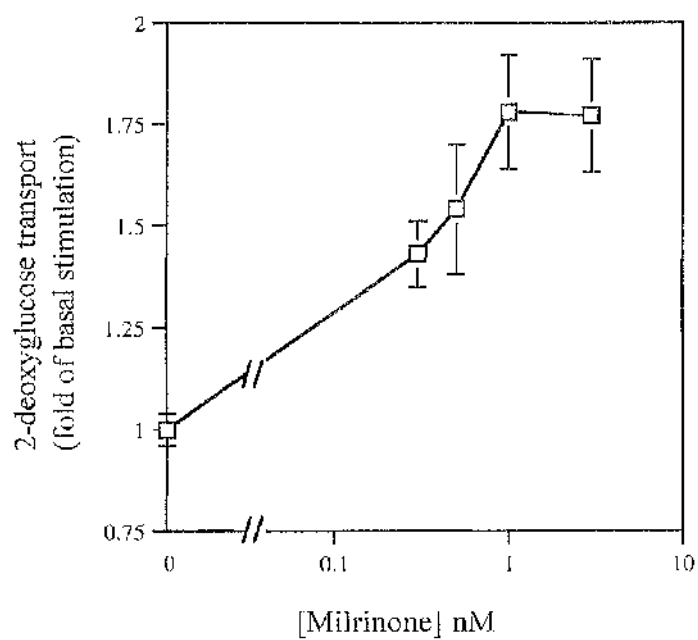
2-deoxyglucose transport assay was carried out as described in section 2.5.

Cells were quiesced for 36-48 hours, then treated with milrinone for 1 hour prior to 2-deoxyglucose transport assay. Data from a representative experiment is shown, repeated three times with similar results.

Each point represents the mean of triplicate determinations  $\pm$  S.E.M. Data is expressed as a fold stimulation of basal (unstimulated) transport rates.

\* represents  $P < 0.05$  when compared to basal/untreated cells as determined by Student's t-test.

2-deoxyglucose transport in VSMCs in  
response to milrinone

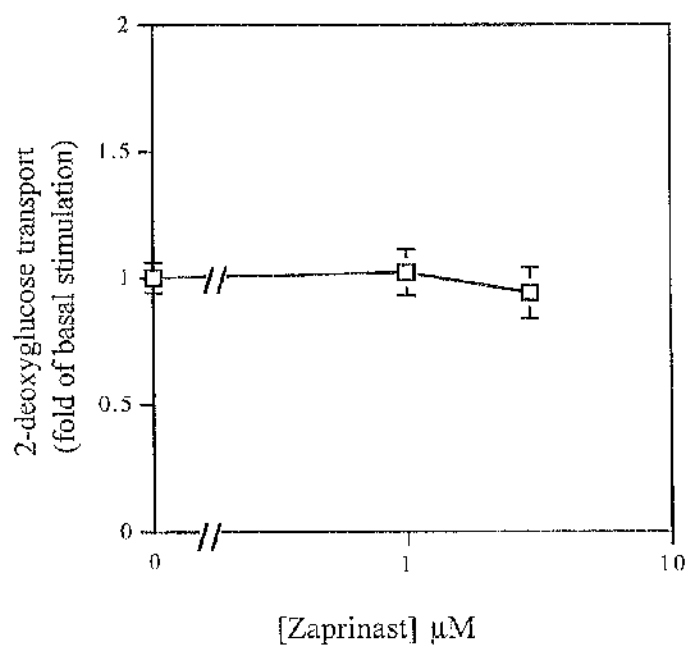
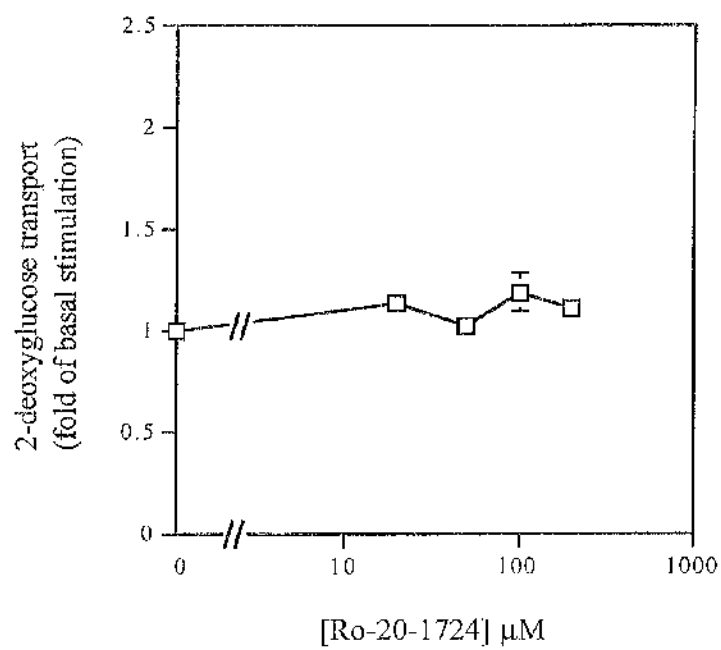


**Figure 4.16 Effects of PDE inhibitors, zaprinast and Ro-20-1724, on 2-deoxyglucose transport in VSMCs**

2-deoxyglucose transport assay was carried out as described in section 2.5.

Cells were quiesced for 36-48 hours, then treated with Ro-20-1724 (upper panel), or zaprinast (lower panel) for 1 hour prior to 2-deoxyglucose transport assay. Data from a representative experiment is shown, repeated three times with similar results.

Each point represents the mean of triplicate determinations  $\pm$  S.E.M. Data is expressed as a fold stimulation of basal (unstimulated) transport rates.





### **Figure 4.17 Effect of 8-Br cGMP on basal and PDGF-stimulated 2-deoxyglucose transport**

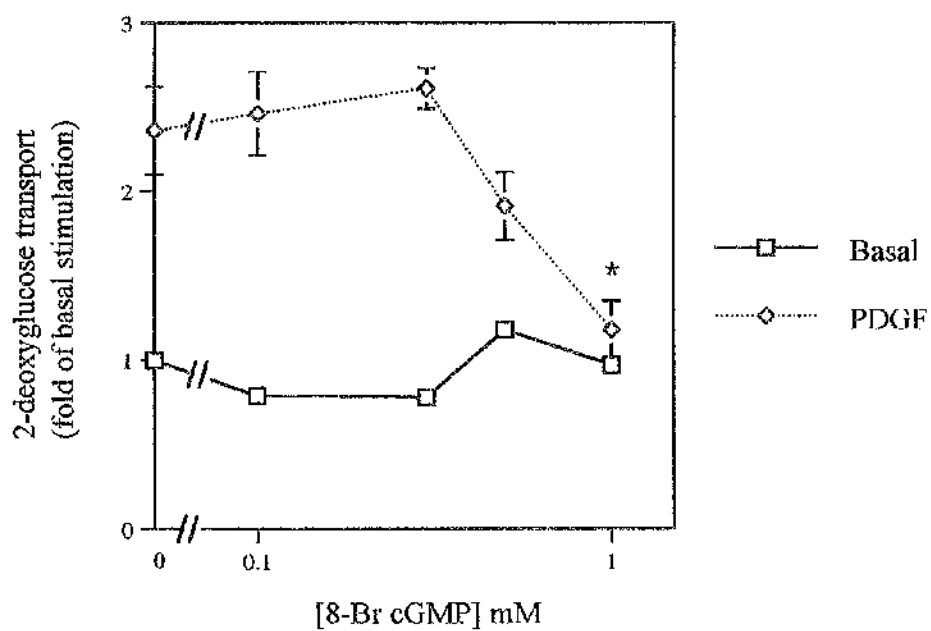
2-deoxyglucose transport assay was carried out as described in section 2.5.

Cells were quiesced for 36-48 hours, then treated with 8-Br cGMP for 1 hour, followed by PDGF (10 ng/ml) for 1 hour, prior to 2-deoxyglucose transport assay. Data from a representative experiment is shown, repeated three times with similar results.

Each point represents the mean of triplicate determinations  $\pm$  S.E.M. Data is expressed as a fold stimulation of basal (unstimulated) transport rates.

\* represents  $P < 0.05$  when compared to cells treated with PDGF alone as determined by Student's t test.

Effect of 8-Br cGMP on basal and PDGF-stimulated 2-deoxyglucose transport



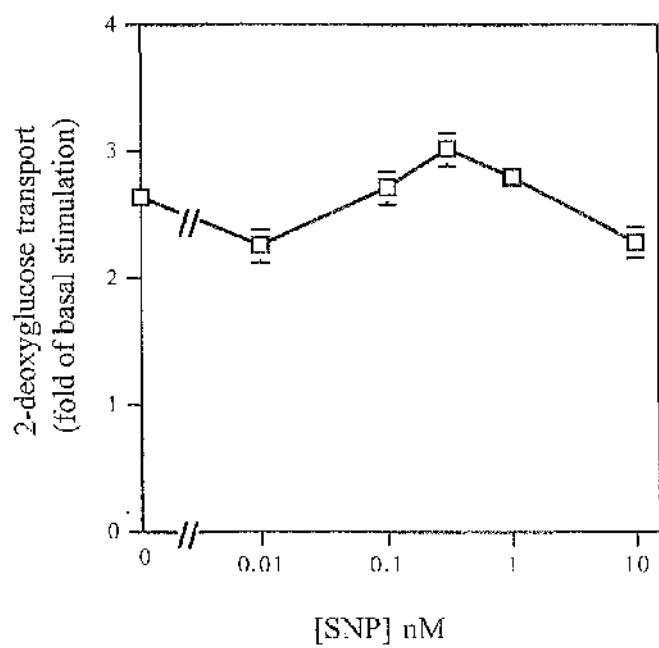
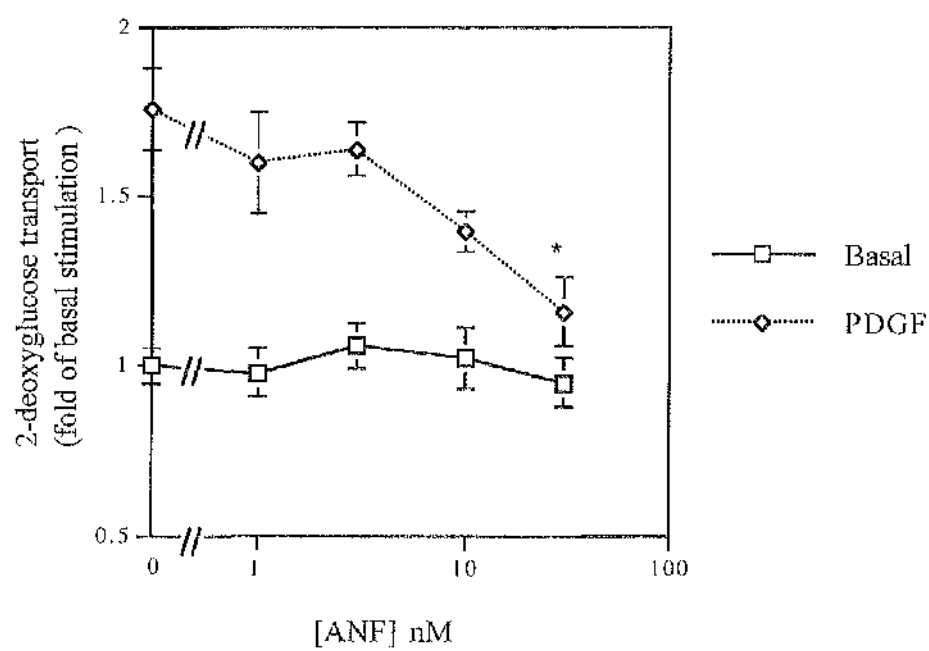
### **Figure 4.18 Effects of ANF and SNP on PDGF-stimulated 2-deoxyglucose transport**

2-deoxyglucose transport assay was carried out as described in section 2.5.

Cells were quiesced for 36-48 hours, then treated with ANF (upper panel) or SNP (lower panel) for 30 minutes, followed by PDGF for 1 hour, prior to 2-deoxyglucose transport assay. Data from a representative experiment is shown, repeated three times with similar results.

Each point represents the mean of triplicate determinations  $\pm$  S.E.M. Data is expressed as a fold stimulation of basal (unstimulated) transport rates.

\* represents  $P < 0.05$  when compared to cells treated with PDGF alone as determined by Student's t test.

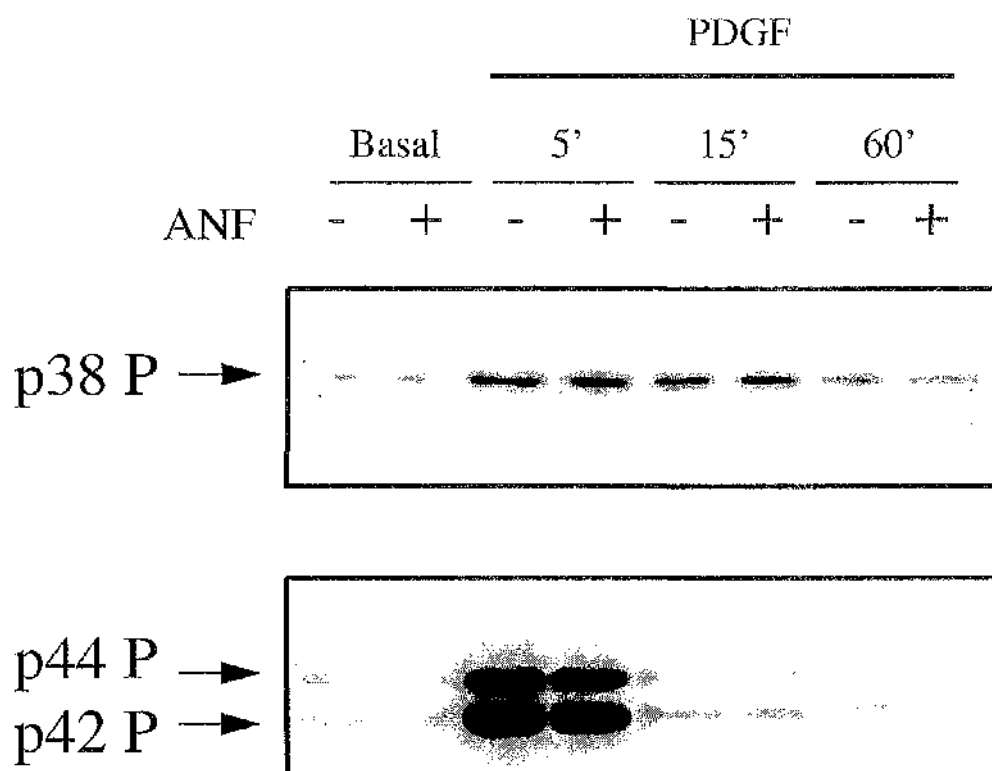


### **Figure 4.19 Effect of ANF on PDGF-stimulated MAP kinase, p38 and p42/44, phosphorylation/activation**

VSMCS were grown to confluency in 6-well plates and quiesced in serum-free DMEM for 36-48 hours. Cells were treated with or without ANF (300 nM) for 30 minutes followed by PDGF (10 ng/ml) for 5, 15 or 60 minutes and then whole cell lysates were prepared as described in section 2.9. 50µl of each lysate was loaded in each lane of a 10 % SDS-PAGE gel and subjected to electrophoresis and immunoblotting as described in section 2.8. Blots were developed using phospho-specific antibodies to p38 and p42/44 which only recognise the phosphorylated, therefore activated, kinase.

ANF had no effect on the ability of PDGF to phosphorylate, therefore activate, p38 or p42/44.

These blots are representative of three such experiments.



## **CHAPTER 5**

### **INVESTIGATION OF THE MECHANISMS LEADING TO INCREASED GLUCOSE TRANSPORT IN RAT AORTIC VASCULAR SMOOTH MUSCLE CELLS**

## 5.1 AIMS

The aims of this chapter were:

1. To generate GLUT-1/green fluorescent protein (GFP) chimeras.
2. To use the GLUT-1/GFP chimeras to follow the movement of GLUT-1 within cells in response to agonists that stimulate an increase in glucose transport.
3. To determine if GLUT-1 and GLUT-3 are phosphorylated in response to either PDGF or cAMP analogues.



## 5.2 INTRODUCTION

Exposure of quiescent cells to mitogens results in the stimulation of numerous intracellular signalling cascades, culminating in cell growth and division several hours later. Due to the increased energy requirements of growing cells, one of the early responses of cells common to all mitogens is an increase in the rate of glucose uptake. GLUT-1 is thought to be the glucose transporter responsible for the increase in glucose transport (Thomson & Gould, 1997).

The acute phase of growth factor-stimulated glucose transport occurs within minutes. This is thought to occur by a movement of GLUT-1 from the recycling endosomal system to the plasma membrane, therefore increasing the number of functional transporters at the plasma-membrane, and also possibly via an increase in the intrinsic activity of the transporters (Gould and Holman, 1993, Czech *et al.*, 1992). However the molecular mechanisms underlying these effects are poorly understood.

As yet, it is unclear what contribution increased transporter activity and increased translocation of glucose transporters play in increased glucose transport in response to mitogens. In adipose tissue, for example, which expresses the glucose transporter GLUT-4, the increase in glucose transport in response to insulin is mediated entirely by a translocation of GLUT-4 to the cell surface (Holman & Kasuga, 1997). In platelets, thrombin has been shown to stimulate the translocation of the glucose transporter GLUT-3 from an intracellular location to the cell surface resulting in increased glucose transport (Sorbara *et al.*, 1997). In other work, however, it is thought that alteration of the intrinsic activity of the transporter itself can regulate the rate of glucose transport. For example, in pancreatic  $\beta$  cells, phosphorylation of GLUT-2 by PKA reduces the rate of glucose transport in these cells (Thorens *et al.*, 1996), and in CHO cells phosphorylation of GLUT-4 inhibits glucose transport (Piper *et al.*, 1993).

It is of interest, therefore, to determine what role each of these two possible mechanisms play in mediating mitogen-stimulated glucose transport.

As discussed above it is likely that mitogen-stimulated transport is mediated via the glucose transporter GLUT-1. To study the translocation of GLUT-1 within the cell green fluorescent protein (GFP) can be utilised. GFP, from the jellyfish *Aequora victoria*, is a protein of 238 amino acids in a single polypeptide chain (reviewed in Tsien, 1998). The chromophore, the part of the protein that confers the fluorescent properties on the protein, is formed from residues 65-67, which are Ser-Tyr-Gly in the native protein. These residues undergo a series of reactions during protein folding to form a *p*-hydroxybenzylideneimidazolinone, the chromophore. The protein forms a  $\beta$ -barrel from eleven  $\beta$ -strands through which an  $\alpha$ -helix is threaded bearing the chromophore. GFP fluoresces when the chromophore is hit by photons of the appropriate wavelength (in this case 395-397 nm), this causes excitation of electrons within the chromophore. When these electrons return to their basal, non-excited state, they emit light, the green fluorescence, of wavelength 504 nm (reviewed in Tsien, 1998). GFP retains its fluorescent properties when recombinantly expressed in both prokaryotic and eukaryotic living cells and is therefore a powerful tool for following the movement of recombinant proteins within a cell, for example along the secretory pathway and membrane traffic pathways (Kaether & Gerdes, 1995, Girotti & Banting, 1996, Niwa *et al.*, 1996, Rizzuto *et al.*, 1995).

In this chapter, chimeras of GFP and GLUT-1 were constructed to be used to follow the movement of the glucose transporter in live cells in response to mitogens. As well as this, the phosphorylation state of both GLUT-1 and GLUT-3 in cultured vascular smooth muscle cells in response to 8-Br cAMP and PDGF (see chapters 3 and 4) was determined.

## 5.3 RESULTS

### 5.3.1 Generation of GLUT-1/GFP chimeras

To help study the movement of GLUT-1 in response to mitogens within living cells GLUT-1/GFP chimeras were made. Both N- and C-terminal tagged GLUT-1/GFP were made. Chimeras were made using a PCR-based technique. PCR primers were designed to incorporate restriction sites to allow subcloning of products into the vector pcDNA 3 (Figure 5.1). The PCR reactions, restrictions, gel extractions of DNA and ligations were carried out as described in section 2.17. Restriction analysis and DNA sequencing (as described in section 2.17) confirmed the structure of the chimeras.

To determine which transient transfection method would be most effective in the expression of the chimeras different techniques were used. 3T3-L1 fibroblasts were grown to the appropriate confluency on coverslips and transiently transfected with the N-terminal tagged GLUT-1/GFP using Qiagen's "Superfect transfection reagent" and with Invitrogen's "Calcium Phosphate transfection kit" according to manufacturer's directions. The cells were incubated with the DNA/transfection reagent mix for varying times to optimise the transfections. Cells were examined using confocal microscopy as described in section 2.18 (Figure 5.2). Transfection using Qiagen's "Superfect transfection reagent" with an incubation of 3 hours, and Invitrogen's "Calcium phosphate transfection kit" with an incubation of 20 hours were the most effective methods for transient expression of GLUT-1/GFP chimeras, with each technique giving a higher number of cells expressing the chimera (Figure 5.2 A & D). Cells transfected with QIAGEN's "Superfect reagent" appeared slightly less stressed than those transfected with the calcium phosphate kit, with the cells showing less stress fibres. All further transient transfections were carried out using the QIAGEN "Superfect transfection kit" with an incubation period of 3 hours.

Next the expression of the N- and C-terminal chimeras was compared. 3T3-L1 fibroblasts were transiently transfected using Qiagen's "Superfect transfection reagent" with both the N- and C-terminal GLUT-1/GFP chimeras. Cells were

examined using confocal microscopy, and the distribution of the N- and C-terminal chimeras compared (Figure 5.3). The N-terminal chimera shows an even intracellular distribution, with a degree of plasma membrane association. The amount of N-terminal GLUT-1/GFP seen at the cell surface appeared to vary depending on the level of expression of the chimera i.e. high expression levels give rise to an increase in the amount of chimera at the cell surface (Figure 5.3 A & B). In contrast the C-terminal GLUT-1/GFP chimera showed a very punctate distribution within the cell (Figure 5.3 C & D). The chimera formed small rings clumped together at intracellular sites, and no C-terminal GLUT-1/GFP could be seen at the cell surface.

As the C-terminal GLUT-1/GFP chimera showed a punctate intracellular distribution, it was possible that the addition of GFP at the C-terminal resulted in mis-targeting of the chimera. To determine if the C-terminal GLUT-1/GFP chimera was indeed trapped in the recycling endosomes, colocalisation of the chimera with transferrin (labelled with Texas-Red). Cells were transiently transfected with C-terminal GLUT-1/GFP and 1 hour prior to visualisation of cells, transferrin Texas-Red (20 µg/ml) is added to the cells. The transferrin receptor is a well-established prototypic marker for the endosomal recycling system, therefore colocalisation of the C-terminal GLUT-1/GFP chimera with transferrin Texas-Red would indicate that the chimera is indeed trapped in the endosomal network. The C-terminal GLUT-1/GFP chimera was completely co-localised with the transferrin Texas-Red (Figure 5.4), indicating that the C-terminal chimera was indeed trapped in the recycling endosomes. It is possible that as well as being trapped in the endosomal system the chimera disrupts the recycling endosomal system as a whole.

All further work using the GLUT-1/GFP chimeras used only the N-terminally tagged chimera.

### **5.3.2 Stimulation of movement of GLUT-1/GFP with PDGF in 3T3-L1 fibroblasts**

3T3-L1 fibroblasts were transiently transfected with N-terminal GLUT-1 GFP, using Qiagen's "Superfect transfection reagent", as described above. Cells were then

quiesced for ~2-3 hours, then treated with PDGF (10 ng/ml) for a further 1 hour. Cells were visualised both before and after treatment with PDGF (Figure 5.5).

Prior to treatment with PDGF the N-terminal GLUT-1 GFP chimera was predominantly localised intracellularly, with a small degree of plasma membrane association (Figure 5.5 A & B). After treatment with PDGF the degree of plasma membrane association appeared to have increased. However, after treatment with PDGF, the cell's overall morphology appeared to change, with the cells becoming longer and thinner (Figure 5.5 C & D), therefore it was difficult to conclusively interpret any changes in the cellular distribution of GLUT-1/GFP in these cells.

Other reagents, such as LPA, insulin and IGF-1, were used to try and stimulate the movement of GLUT-1/GFP in these cells, and although they did appear to stimulate a degree of translocation of the chimera within the cell the results were variable (results not shown). As discussed above, the degree of association of the chimera with the plasma membrane is rather variable, depending on the level of expression. This meant that in cells expressing a high level of chimera, there was already a high degree of plasma membrane association even in quiescent cells, therefore upon treatment with PDGF it was difficult to see any increase in plasma membrane association.

### **5.3.3 Analysis of phosphorylation state of GLUT-1 and GLUT-3 in VSMCs**

Firstly I wished to determine if GLUTs 1 and 3 were substrates for PKA, as PKA is required for mediating 8-Br cAMP's stimulation of glucose transport (see section 4.3.2). Both GLUT-1 and GLUT-3 contain consensus motifs for PKA phosphorylation (phosphorylation on serine/threonine residues presented in the sequences RRXS/T or RXS/T or KRXXS/T (reviewed by Kemp & Pearson, 1990)). GLUTs 1 and 3 were immunoprecipitated (IP) from VSMC lysates using anti-GLUT-1, anti-GLUT-3 and random IgG as a control, as described in section 2.12. Half of the immunoprecipitates were analysed by immunoblotting, as described in section 2.8, to determine that IP had been successful (blots developed using protein A-HRP instead of secondary antibody, to stop cross reactivity of secondary antibodies with denatured GLUT-1 and GLUT-3 antibodies in IP samples. Protein A will only recognise antibodies in native

structure) (Figure 5.6). The other half of the IP was then subjected to *in vitro* phosphorylation using PKA, as described in section 2.13. Samples were then run on SDS-PAGE (section 2.7) and the gels were fixed in 14% acetic acid, 7% methanol, dried and exposed to X-ray film to identify proteins that had been phosphorylated (Figure 5.7). Although the bands from the IPs using GLUT-1 and GLUT-3 were more intense than IPs carried out using random IgG, there were no bands phosphorylated in the GLUT-1 and GLUT-3 IPs of the appropriate molecular weight (47-50 kDa) that could represent phosphorylated GLUT-1 and GLUT-3.

Next, it was considered that perhaps the GLUTs in these cells already had a basal level of phosphorylation, as the cells from which the lysates were prepared were not quiesced, meaning that no increase in phosphorylation could be seen. To overcome this potential problem, immunoprecipitated GLUTs were first dephosphorylated (see section 2.13), then subjected to *in vitro* phosphorylation, as above (Figure 5.8). Again the intensity of the bands in the lanes from the GLUT-1 and GLUT-3 immunoprecipitates was far greater than in the lanes from immunoprecipitates carried out using random IgG. However, like the previous experiment, there were no bands present of the appropriate molecular weight (48-50 kDa) to represent specific phosphorylation of GLUT-1 or GLUT-3.

Next, the effects of treating the VSMCs with PDGF and 8-Br cAMP (two reagents that can stimulate glucose transport in VSMCs, see chapters 3 and 4) on phosphorylation of GLUT-1 and -3 was investigated. *In vivo* phosphorylation was carried out as described in section 2.14. Cells were grown to confluency in 6 well plates and quiesced for 36-48 hours, cells labelled with 0.2 mCi/ml [ $^{32}$ P] orthophosphoric acid for 90 minutes at 37°C to allow the intracellular pool of ATP to become  $^{32}$ P labelled. After the 90-minute labelling the cells were treated with or without PDGF (10 ng/ml) or 8-Br cAMP (1 mM) for 1 hour. Two wells from each 6-well plate were used for each condition. After this time immunoprecipitation of GLUT-1 and GLUT-3 was carried out as described in section 2.12, and the phosphorylation of each GLUT analysed (Figure 5.9). No specific phosphorylation of either GLUT-1 or GLUT-3 was observed in response to either PDGF or 8-Br cAMP.

## 5.4 DISCUSSION

Currently, the mechanism(s) responsible for increased glucose transport in response to mitogens is poorly understood. It is believed that an increase in the intrinsic activity of the glucose transporters and/or an increase in the number of functional glucose transporters at the cell surface are responsible for increased glucose transport (Thomson & Gould, 1997).

In some cell systems it is clear that only increased translocation of glucose transporters to the cell surface is responsible for increased glucose transport (i.e. GLUT-4 translocation in response to insulin in adipocytes (Holman & Kasuga, 1997)). In other systems, however, it appears that only altered activity of the transporter is responsible for changes in the rate of glucose transport (i.e. PKA phosphorylation of GLUT-2 in pancreatic  $\beta$ -cells, Thorens *et al.*, 1996).

As very little is understood about the mechanisms mediating increased glucose transport in response to mitogens, two strategies were adopted to address this question. Firstly, green fluorescent protein (GFP) was used to tag the glucose transporter GLUT-1 to allow visualisation of its movement through the cell, and to determine what role, if any, translocation of GLUT-1 plays in mediating mitogen-stimulated increases in glucose transport. And secondly, as phosphorylation has been shown to be able to alter the intrinsic activity of glucose transporters (Thorens *et al.*, 1996, Piper *et al.*, 1993), the degree of phosphorylation of the glucose transporters GLUT-1 and GLUT-3 was assessed under various conditions.

### 5.4.1 Generation of GLUT-1/GFP chimeras

Both N and C terminally tagged GLUT-1/GFP chimeras were made. However it was found that the C-terminal tagged chimera was mis-targetted within the cell and appeared to be trapped in the recycling endosomes (Figure 5.4). There is evidence that the C-terminal tail of glucose transporters is very important with regard to correct targetting of the transporter to the plasma membrane (Verhey *et al.*, 1993). It is

possible therefore that due to the presence of the GFP moiety on the C-terminal tail that the GLUT-1/GFP chimera is being mistargetted within the cell, and is unable to exit the recycling endosomes to reach the plasma membrane. Another possible explanation for the punctate distribution of the C-terminal GLUT-1/GFP chimera, is that the chimera is misfolding and forming an aggresome structure (Johnston *et al.*, 1998, Garcia-Mata *et al.*, 1999). Aggresomes are a novel structure, that have been proposed to represent a general cellular response to misfolded proteins (Johnston *et al.*, 1998), therefore this chimera was not pursued.

The N-terminal chimera showed a much more even intracellular distribution in membranes association (Figure 5.3). The degree of chimera associated with the plasma membrane appeared to vary depending on the levels of GLUT-1/GFP expressed. In cells expressing a high level of chimera there was a greater level of membrane association (Figure 5.3 B), whereas in cells with a low level of chimera expression (Figure 5.3 A). This is the kind of expression pattern expected if the GFP was not altering the pattern of GLUT-1 expression and targetting.

#### **5.4.2 Stimulation of movement of GLUT-1/GFP with PDGF in 3T3-L1 fibroblasts**

The movement of the N-terminally tagged GLUT-1/GFP was studied in response to PDGF and various other agonists known to stimulate glucose transport in 3T3-L1 fibroblasts. Treatment of quiesced cells for 1 hour with PDGF resulted in a redistribution of the chimera, from diffuse intracellular expression to a more membrane associated pattern. However, during incubation of cells with PDGF, the cells appeared to undergo a morphology change. When cells were first visualised they had an even rounded shape, however after a period of time they became elongated and occasionally extended stress fibres. (Figure 5.5). The change in cell morphology made analysis of GLUT-1/GFP translocation very difficult, and it was difficult to determine if it was the change in morphology or the agonist that was causing redistribution of the chimera to the cell surface (stress will also stimulate an increase in glucose transport).



In addition to the reshaping of the cells, further problems were encountered in that the level of plasma membrane association of the chimera varied greatly depending on the levels of expression of the chimera (Figure 5.3 A & B). Even in cells that had not been treated with agonist there could be a high degree of chimera at the cell surface if there was a high level of expression of the chimera (Figure 5.3 B). This meant that in these cells it was difficult to see any increase in the amount of chimera at the cell surface in the presence of agonist.

A number of other agonists known to stimulate glucose transport in 3T3-L1 fibroblasts, such as LPA and IGF-1, were also used, and although they did appear to stimulate a degree of translocation of the chimera within the cell the results were variable (results not shown). Similar problems were encountered using these agonists as were encountered with PDGF.

#### **5.4.3 Analysis of phosphorylation state of GLUT-1 and GLUT-3 in VSMCs**

cAMP analogues were able to stimulate an increase in 2-deoxyglucose transport in a PKA dependant manner (see section 4.3). It was interest therefore to determine if either GLUT-1 or GLUT-3 are substrates for PKA, as this is a potential mechanism for mediating the increase in glucose transport. Both GLUT-1 and -3 contain a number of potential PKA phosphorylation sites (serine/threonine residues presented in the sequences RRXS/T or RXS/T or KRXXS/T, reviewed by Kemp & Pearson, 1990). However neither immunoprecipitated GLUT-1 nor GLUT-3 were phosphorylated *in vitro* by PKA (Figure 5.6). To ensure that the GLUTs 1 and 3 were not phosphorylated prior to *in vitro* phosphorylation the immunoprecipitated GLUTs were dephosphorylated before *in vitro* phosphorylation. Dephosphorylation of the immunoprecipitated GLUTs had no effect on PKA's ability to phosphorylate GLUT-1 or GLUT-3 (Figure 5.7). Therefore it is very unlikely that the ability of cAMP analogues to stimulate glucose transport in VSMCs is mediated by direct phosphorylation of glucose transporters by PKA.

Next, it was determined if GLUT-1 and GLUT-3 were phosphorylated *in vivo* in response to either PDGF or 8-Br cAMP (both agents which have been shown to

stimulate increased glucose transport in VSMCs, see Chapters 3 and 4). As with the *in vitro* phosphorylation there were no specific bands present in cells treated with PDGF or 8-Br cAMP as compared to control cells (Figure 5.8). It is unlikely therefore that either PDGF or 8-Br cAMP mediates increased 2-deoxyglucose transport via phosphorylation of GLUT-1 or GLUT-3 resulting in altered glucose transporter activity.

## 5.5 SUMMARY

GLUT-1/GFP chimeric proteins were utilized to analyse the movement of GLUT-1 in response to mitogens. The C-terminally tagged GLUT-1/GFP showed a punctate intracellular distribution that colocalised with transferrin-Texas-Red. This indicated that the C-terminal GLUT-1/GFP was trapped in the recycling endosomal system. There is evidence that the C-terminal tail of GLUT-1 contains motifs that are very important for its correct targetting to the plasma membrane (Verhey *et al.*, 1993). It is likely therefore that the C-terminally tagged GLUT-1/GFP is trapped in the recycling endosomes because of the presence of the GFP moiety on the C-terminal tail of the transporter interfering with the targetting signals.

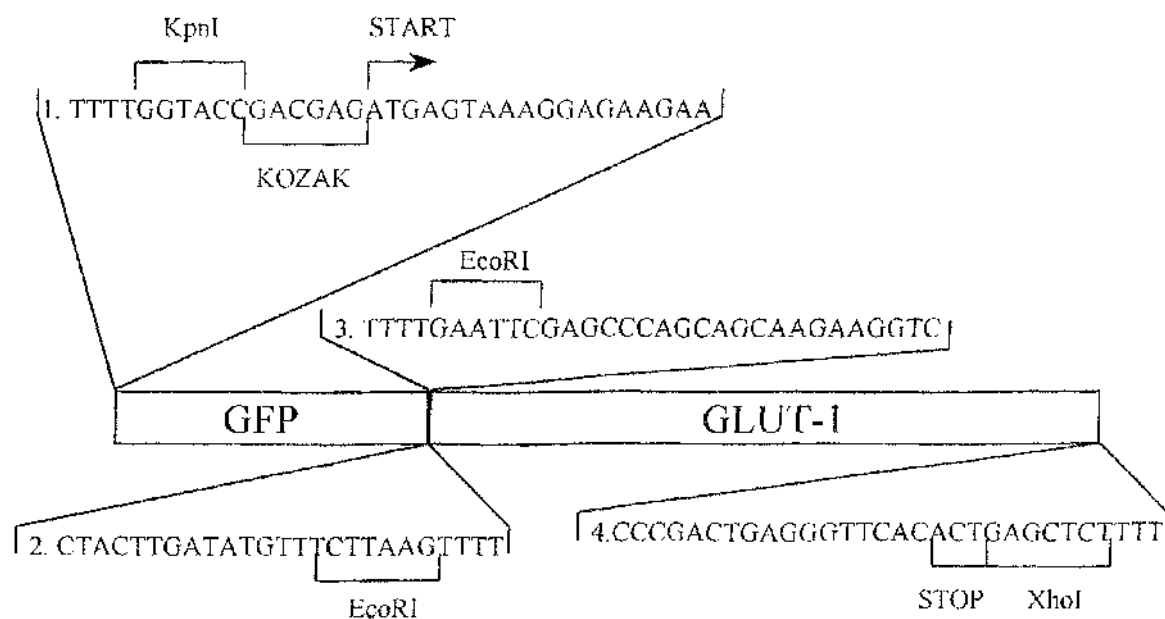
The N-terminal GLUT-1/GFP chimera showed a much more even intracellular distribution with a degree of membrane association. Treatment of cells expressing the N-terminal GLUT-1/GFP chimera resulted in movement of the chimera from this intracellular location to the plasma membrane. However the degree GLUT-1/GFP associated with the plasma membrane in untreated cells was very variable making analysis of any movement of GLUT-1/GFP difficult.

The phosphorylation state of the glucose transporters GLUT-1 and GLUT-3 was investigated. Neither GLUT-1 nor GLUT-3 was a substrate for PKA *in vitro*. There was no increase in the phosphorylation of GLUT-1 and GLUT-3 *in vivo* in response to either PDGF or 8-Br cAMP. Therefore it seems unlikely that increased glucose transport in VSMCs in response to mitogens is mediated by altered activity of glucose transporters via phosphorylation of GLUTs.

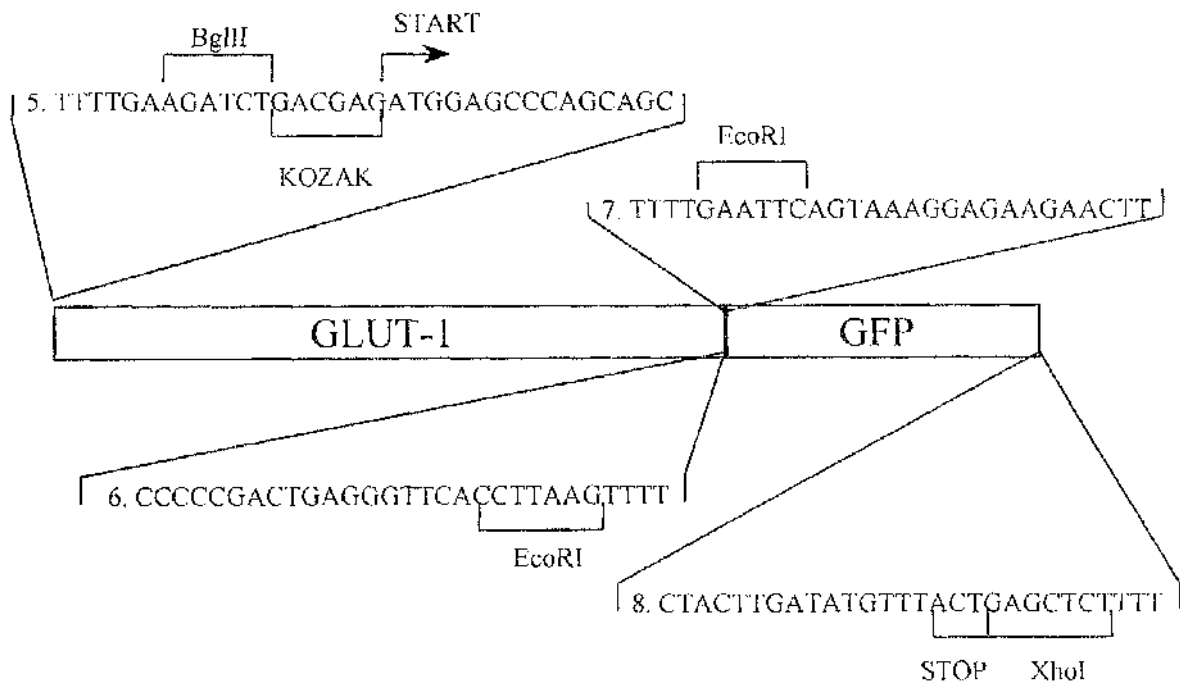
### **Figure 5.1 PCR based method used to synthesize GLUT-1/GFP chimeras**

PCR reactions were carried out as described in section 2.17.1. PCR primers were designed to incorporate restriction sites that would allow subcloning of products into pcDNA 3, and to remove stop and start codons that would occur in the middle of the chimera. Once PCR products were generated they were restricted (see section 2.17.7) and cloned into the appropriate restriction sites of the expression vector pcDNA3 (ligations described in section 2.17.8). Restriction analysis and DNA sequencing (section 2.17.7 and 2.17.11) confirmed the structure of the chimeras.

## N-terminally tagged GLUT-1



## C-terminally tagged GLUT-1



## **Figure 5.2 Optimising transient transfection method for expression of GLUT-1/GFP chimeras**

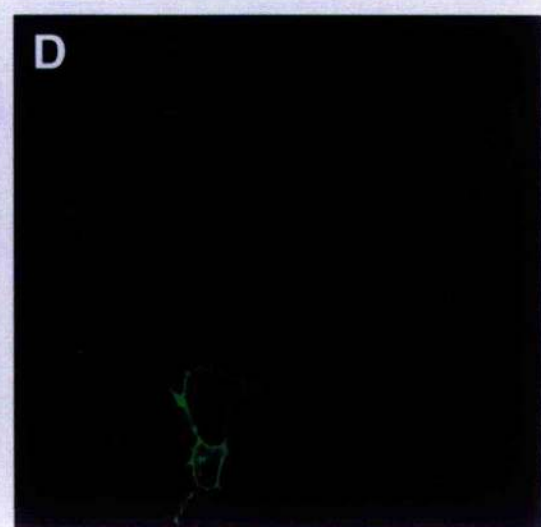
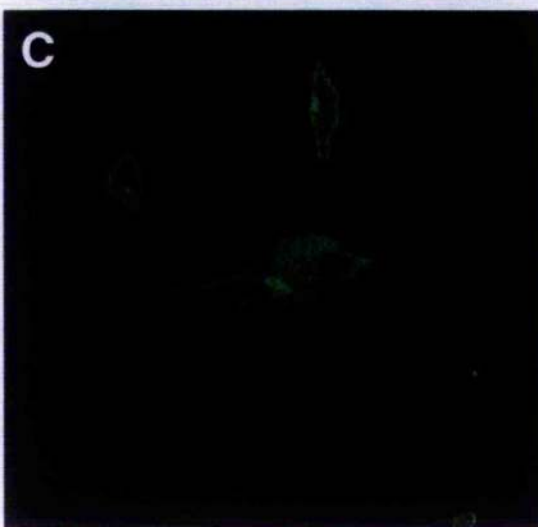
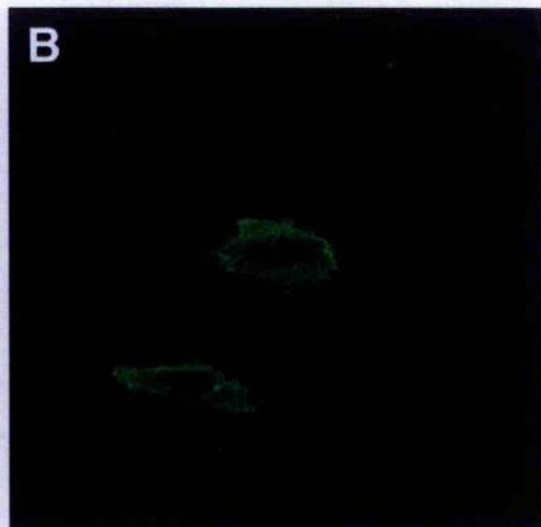
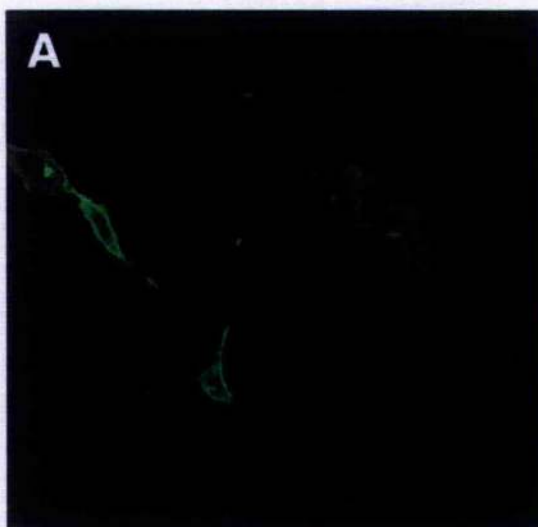
3T3-1.1 fibroblasts were transiently transfected with the N-terminal GLUT-1/GFP chimera using a variety of methods to determine the most effective technique for transient transfection, and visualised using confocal microscopy as described in section 2.18.

**A & B** Cells transfected using QIAGEN's "Superfect transfection reagents" with incubations of 3 and 6 hours respectively.

**C & D** Cells transfected using Invitrogen's "Calcium phosphate transfection kit" with incubations of 6 and 20 hours respectively.

Shown are images representative of three such experiments with similar results.

Transfection using Qiagen's "Superfect transfection reagent" with an incubation of 3 hours, and with Invitrogen's "Calcium phosphate transfection kit" both gave the highest rate of transfection (A & D). Cells transfected with Qiagen's "Superfect reagent" looked less stressed than those transfected with the calcium phosphate reagent, therefore all further transfections were carried using Qiagen's "Superfect transfection reagent" with an incubation of 3 hours.



### **Figure 5.3 Comparison of distribution of N-terminal and C-terminal tagged GLUT-1/GFP chimeras**

3T3-L1 fibroblasts were transiently transfected with both the N- and C-terminal GLUT-1/GFP chimera using Qiagen's "Superfect transfection reagent" with an incubation of 3 hours. Cells were visualised using confocal microscopy as described in section 2.18.

**A & B** 3T3-L1 fibroblasts expressing the N-terminal GLUT-1/GFP chimera.

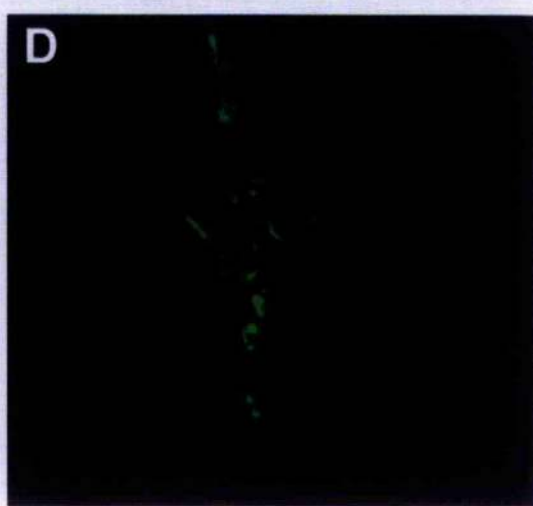
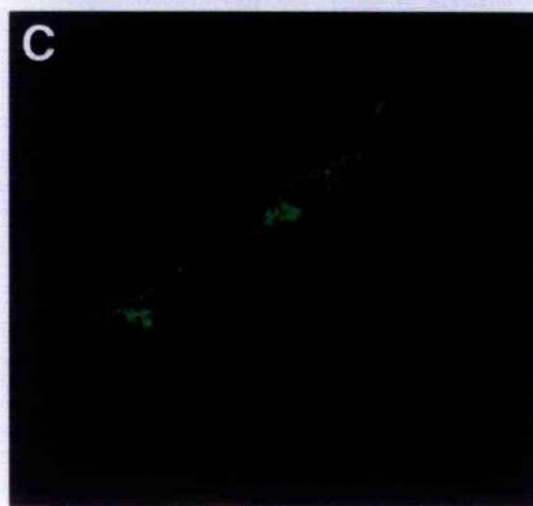
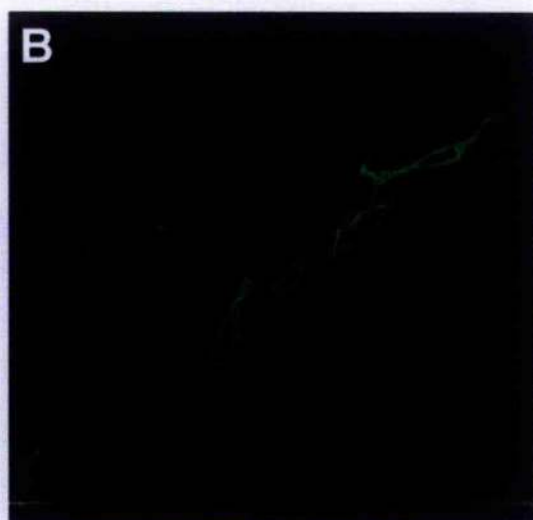
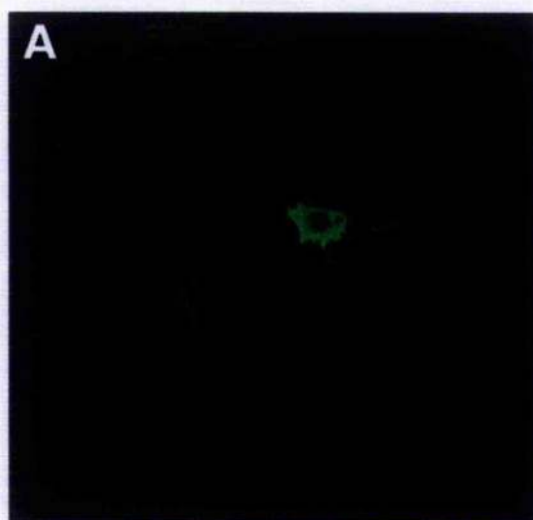
**C & D** 3T3-L1 fibroblasts expressing the C-terminal GLUT-1/GFP chimera.

Shown are images representative of three such experiments.

The N-terminal chimera shows an even intracellular distribution with a degree of membrane association. The degree of plasma membrane association appears to increase as the level of expression of the chimera increases.

The C-terminal chimera shows a punctate intracellular distribution with no membrane association at all.





**Figure 5.4 Colocalisation of C-terminal GLUT-1/GFP with transferrin-texas red**

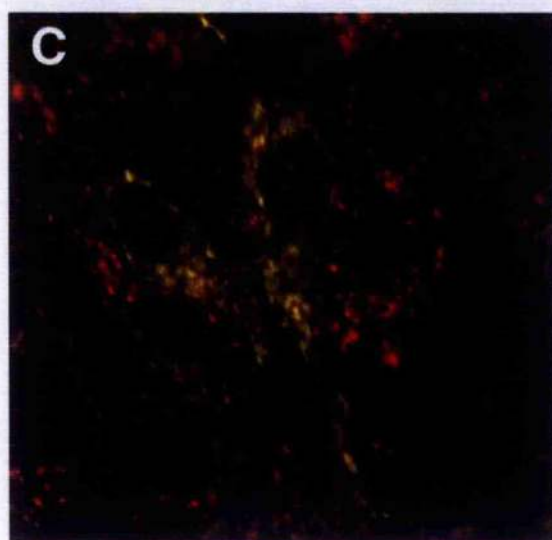
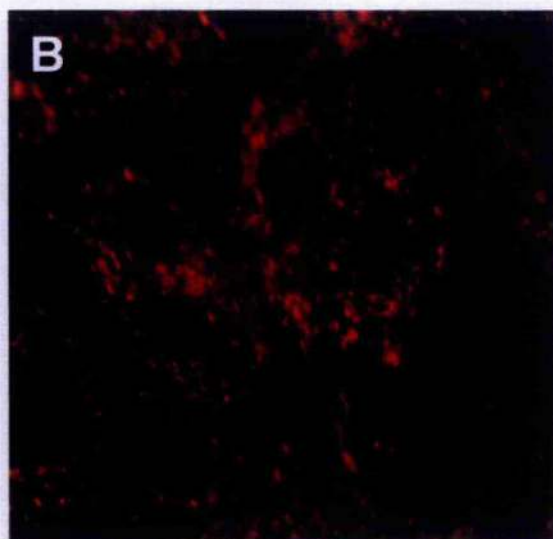
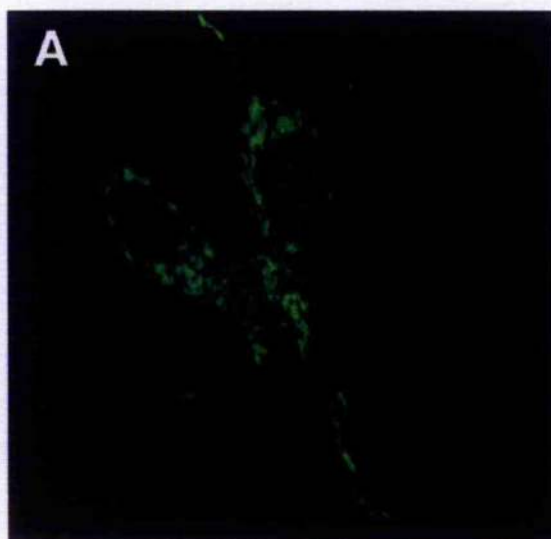
3T3-L1 fibroblasts were transiently transfected with the c-terminal GLUT-1/GFP using the QIAGEN's "Superfect transfection reagent". 1 hour prior to visualisation cells were treated with transferrin Texas-Red (20 µg/ml). Cells were visualised using confocal microscopy and images were merged using Metamorph software as described in section 2.18.

**A** GLUT-1/GFP localisation within cells.

**B** Transferrin Texas-Red localisation within 3T3-L1 fibroblasts.

**C** Colocalisation of GLUT-1/GFP and transferrin texas red.

Shown are images representative of three such experiments.



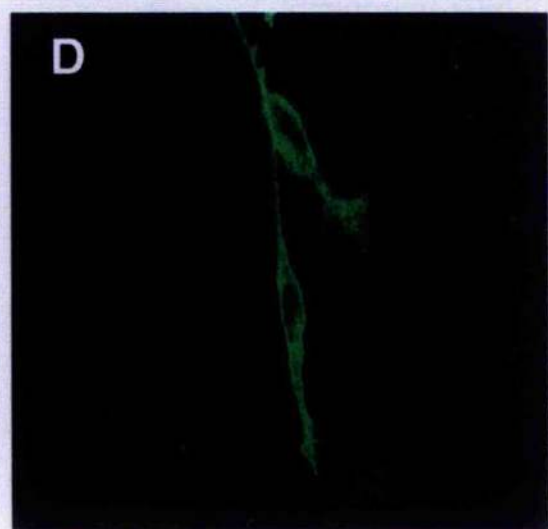
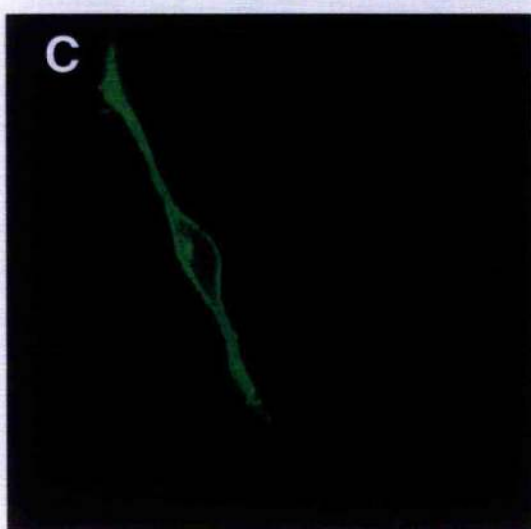
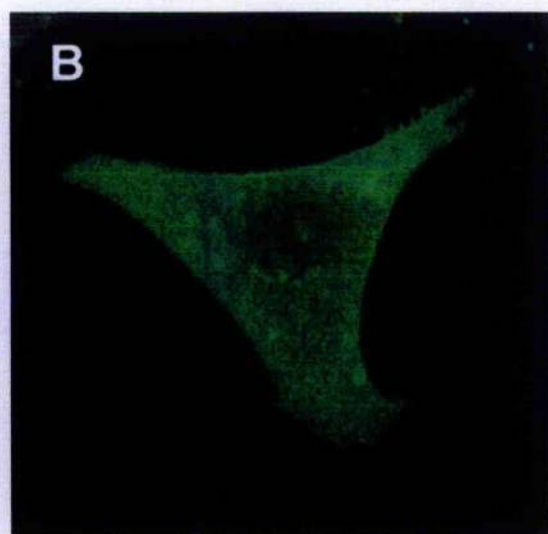
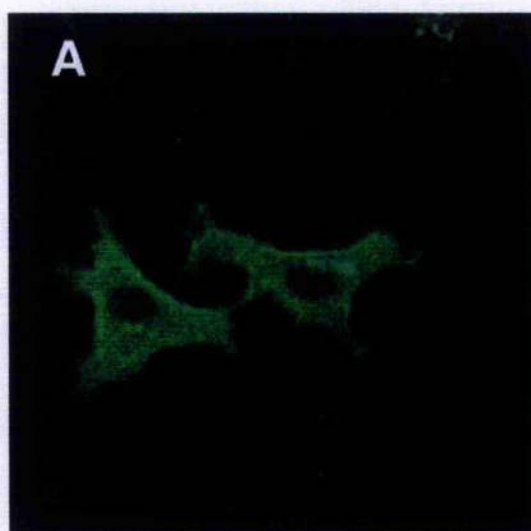
### **Figure 5.5 Translocation of N-terminal GLUT-1/GFP in response to PDGF**

3T3-L1 fibroblasts were transiently transfected using QIAGEN's "superfect transfection reagent". Cells were quiesced for 2-3 hours, then treated with PDGF (10 ng/ml). Cells were visualised using confocal microscopy as described in section 2.18, before and after treatment with PDGF.

**A & B** 3T3-L1 fibroblasts expressing the N-terminal GLUT-1/GFP chimera which have been quiesced for 2 hours.

**C & D** 3T3-L1 fibroblasts expressing the N-terminal GLUT-1/GFP chimera which have been quiesced for 2 hours and treated with PDGF for a further 1 hour.

Shown are images representative of three such experiments.



## Figure 5.6 Immunoprecipitation of GLUTs 1 and 3 from VSMCs

Whole cell lysates were prepared from VSMCs as described in section 2.9 and GLUTs 1 and 3 were immunoprecipitated from the lysates (as described in section 2.12). As a control the immunoprecipitations were carried out using random IgG as well as antibodies to GLUT-1 and GLUT-3.

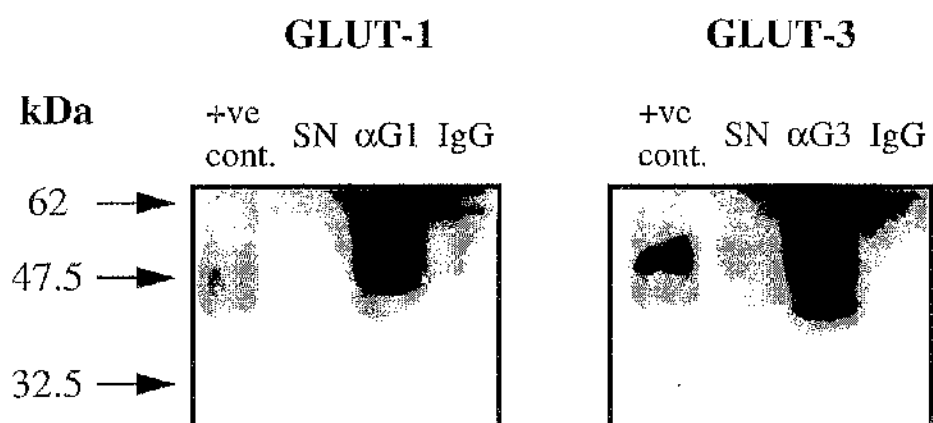
Samples from the immunoprecipitations, using either the GLUT-1 or GLUT-3 antibodies as indicated, were run on a SDS-PAGE and subjected to immunoblotting. Immunoblots were developed using protein A-HRP instead of a secondary antibody, as secondary antibodies would cross react with denatured GLUT-1 and GLUT-3 antibodies within the immunoprecipitated samples, whereas protein A only recognises antibodies in their native structure.

The position of molecular weight markers are illustrated on the left side of the figure in kilo Daltons (kDa).

+ve control	Sample of rat brain whole cell lysate
SN	Supernatant left after immunoprecipitation of GLUTs
$\alpha$ G1, G3	Immunoprecipitated GLUT-1 and GLUT-3 respectively
IgG	Immunoprecipitates carried out using random IgG

Shown is a representative blot. There is very little GLUT-1 or GLUT-3 left in the supernatant from the immunoprecipitates and virtually all the GLUT-1 and GLUT-3 has been successfully immunoprecipitated. Random IgG did not immunoprecipitate any significant amount of GLUT-1 or GLUT-3.

All immunoprecipitations were checked in this manner before being used for *in vitro* phosphorylations.



**Figure 5.7 *In vitro* phosphorylation of GLUTs 1 and 3 with PKA**

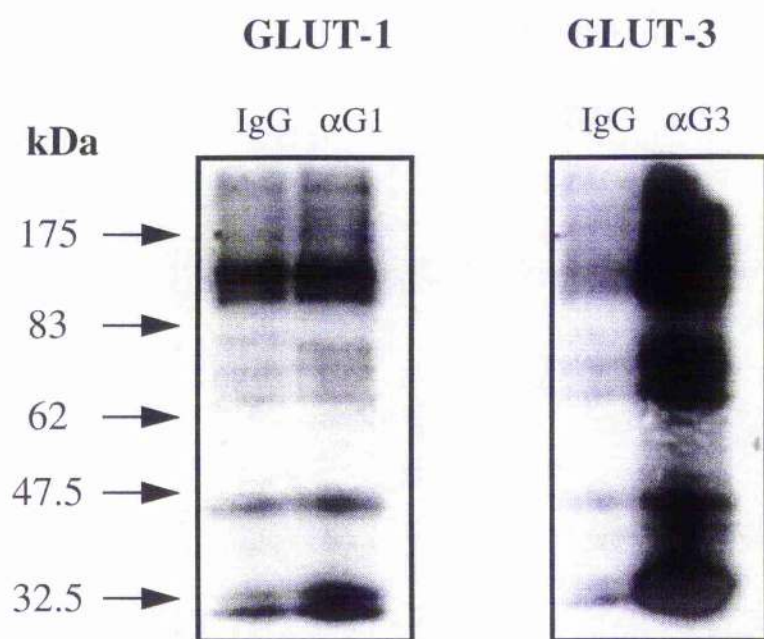
GLUTs 1 and 3 were immunoprecipitated from VSMCs (section 2.12) and subjected to *in vitro* phosphorylation with PKA (see section 2.13). As a control samples were immunoprecipitated with random IgG and subjected to phosphorylation with PKA. Samples were analysed by running on SDS-PAGE, gels were dried and exposed to X-ray film to identify phosphorylated proteins.

The position of molecular weight markers are illustrated on the left side of the figure in kilo Daltons (kDa).

IgG	proteins immunoprecipitated using random IgG
$\alpha$ G1, G3	proteins immunoprecipitated using antibodies to GLUT-1 and GLUT-3 respectively

Shown is a representative figure of three such experiments.





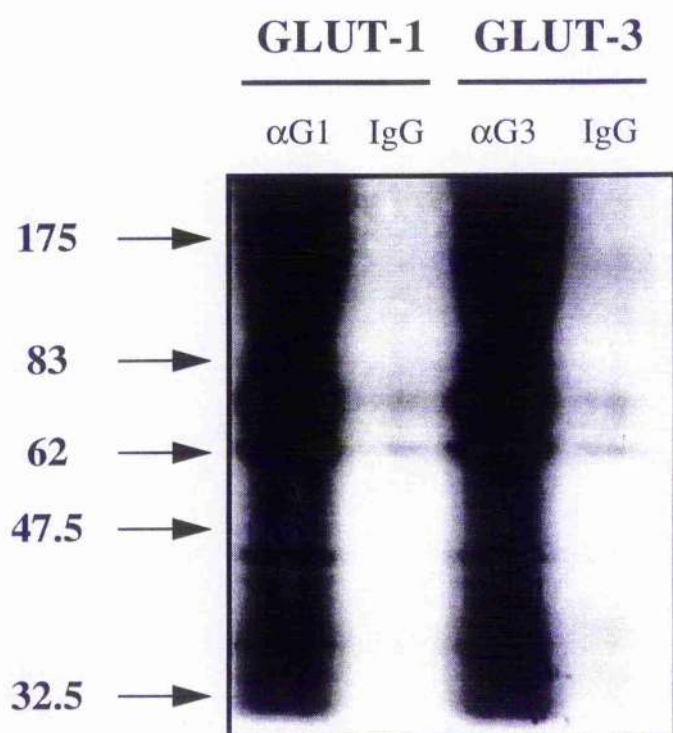
**Figure 5.8 *In vitro* phosphorylation of GLUTs 1 and 3 with PKA after dephosphorylation with PP2A**

GLUTs 1 and 3 were immunoprecipitated from VSMCs (as described in section 2.12). Immunoprecipitates were dephosphorylated with (protein phosphatase 2A) PP2A then subjected to *in vitro* phosphorylation with PKA (see section 2.13). As a control samples were immunoprecipitated with random IgG , dephosphorylated and subjected to *in vitro* phosphorylation with PKA. Samples were analysed by running on SDS-PAGE, gels were dried and exposed to X-ray film to identify phosphorylated proteins.

The position of molecular weight markers are illustrated on the left hand side of the figure in kilo Daltons (kDa).

IgG	proteins immunoprecipitated using random IgG
$\alpha$ G1/G3	proteins immunoprecipitated using antibodies to GLUT-1 and GLUT-3 respectively

Shown is a representative figure of three such experiments.



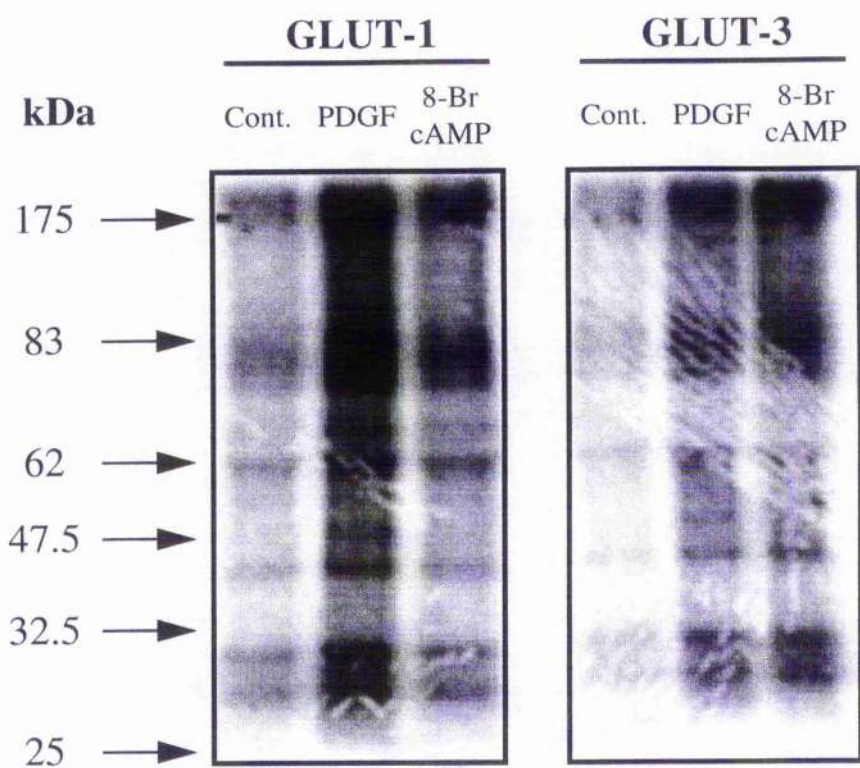
**Figure 5.9 *In vivo* phosphorylation of GLUTs 1 and 3 in VSMCs treated with PDGF and 8-Br cAMP**

Cells were grown to confluency in 6 well plates and quiesced for 36-48 hours, labelled with [ $^{32}$ P], then treated with or without PDGF (10 ng/ml) or 8-Br cAMP (1 mM) for 1 hour, and *in vivo* phosphorylation carried out as described in section 2.14. Two wells from each 6-well plate were used for each condition. After this time immunoprecipitation of GLUT-1 and GLUT-3 was carried out as described in section 2.12, and the phosphorylation of each GLUT analysed.

The position of molecular weight markers are illustrated on the left hand side of the figure in kilo Daltons (kDa).

Shown is a representative figure of three such experiments.

No bands were present at the appropriate size (47-50 kDa) to represent specific phosphorylation of either GLUT-1 or GLUT-3 in response to either PDGF or 8-Br cAMP.



## **CHAPTER 6**

### **DISCUSSION**

Atherosclerosis is an inflammatory disease of the vasculature, and is a major contributor to the progression of coronary heart disease. Fundamental to plaque development is increased proliferation and migration of vascular smooth muscle cells (VSMCs) within the plaque (Ross, 1993). The aberrant proliferation and migration of VSMCs within the plaque is stimulated by the secretion of a number of growth factors and cytokines by endothelial cells, macrophages, lymphocytes and VSMCs themselves within the plaque (Bobik & Campbell, 1993). PDGF is believed to be one of the most important growth factors involved in mediating increased VSMC proliferation in plaque development (Ross, 1993).

Increased glucose transport is an early cellular response common to all mitogens (Thomson & Gould 1997). As increased proliferation of VSMCs is an important factor in atherosclerotic plaque development it is reasonable to assume that this is accompanied by increased glucose transport in VSMCs. However, to date, very little is known about regulation of glucose transport in VSMCs. The work in this thesis investigated the regulation of glucose transport in VSMCs.

It was shown that vascular smooth muscle cells freshly isolated from aorta expressed both GLUT-4 and GLUT-1 glucose transporters. However as the cells were isolated and cultured, GLUT-4 was lost from the cells and the levels of the glucose transporter GLUT-3 increased. The levels of GLUT-1 were unchanged in freshly isolated VSMCs as compared to cells that had been passaged in cell culture.

PDGF (a growth factor believed to be important in regulating VSMC growth in plaque development, Bobik & Campbell, 1993) was able to stimulate a two- to five-fold increase in 2-deoxyglucose transport in VSMCs and this increase in glucose transport was dependent on the activity of both PI3<sup>γ</sup> kinase and the MAP kinases p38 and p42/44.

Cyclic nucleotides are important regulators of smooth muscle cell function, regulating such things as proliferation and relaxation (Landgraf *et al.*, 1992, Murthy & Makhlouf,

1995, Toyoshima *et al.*, 1998, Kronemann *et al.*, 1999, Chiche *et al.*, 1998), and as such their role in regulating glucose transport in VSMCs was studied. Like PDGF, analogues of cAMP were able to stimulate a two-fold increase in 2-deoxyglucose transport in VSMCs. This cAMP-stimulated increase in glucose transport was not additive with PDGF-stimulated glucose transport. cAMP-stimulated glucose transport, like PDGF-stimulated glucose transport, was dependent on the activity of PI3'kinase and the MAP kinase p38, however MAP kinase p42/44 was not activated in response to cAMP analogues. As well as p38 and PI3' kinase, cAMP-stimulated 2-deoxyglucose transport was dependent on protein kinase A (PKA) activity. Although cAMP analogues can stimulate an increase in 2-deoxyglucose transport, agonists that stimulate a large increase in intracellular [cAMP] are unable to stimulate an increase in 2-deoxyglucose transport in VSMCs. However, by using inhibitors of PDE 3, which would result in a small but very localised increase in [cAMP], a two-fold increase in 2-deoxyglucose transport can be achieved. This suggests that the subcellular localisation of any increase in [cAMP] is vital to increase glucose transport rates, rather than the overall concentration of intracellular cAMP.

Analogues of cGMP had no effect on basal glucose transport rates, but was inhibitory with regard to PDGF-stimulated 2-deoxyglucose transport in VSMCs. This was an unexpected result as cAMP and cGMP often work in concert to mediate their effects in VSMCs. Treating the cells with ANF, which will stimulate transmembrane guanylyl cyclase activity, and increase intracellular [cGMP], could mimic the effect of cGMP analogues on PDGF-stimulated 2-deoxyglucose transport, but SNP, which will stimulate soluble guanylyl cyclase activity and increase intracellular [cGMP] was without effect on PDGF-stimulated glucose transport rates.

Attempts were made to understand the mechanisms responsible for increased glucose transport, in terms of translocation and altered activity of glucose transporters. Work using chimeric proteins of GLUT-1 and GFP were of limited use. The degree of plasma membrane association of the chimera was very variable making it difficult to interpret any



movement of the chimera from intracellular sites to the plasma membrane. Work analysing the phosphorylation states of the glucose transporters in VSMCs indicated that neither GLUT-1 nor GLUT-3 were phosphorylated in response to either PDGF or cAMP analogues. It is therefore unlikely that phosphorylation of glucose transporters is responsible for altered rates of glucose transport in VSMCs in response to PDGF or cAMP analogues.

The work carried out in thesis has touched on several interesting areas that could be further investigated in the future. For example, the possibility that a small localised increase in [cAMP] is required to increase 2-deoxyglucose transport in VSMCs, rather than a large increase in the overall [cAMP]. Recent work on the translocation of the transporter protein, aquaporin, has illustrated that it is indeed the subcellular localisation of cAMP, and the PKAs that can be activated at this location, that are important for increased translocation of aquaporin to the cell surface (Klussmann *et al.*, 1999). By treating cells with a peptide which prevents the binding of regulatory subunits of PKA and AKAPs (proteins to which PKA regulatory subunits bind, conferring a specific subcellular localisation upon the PKA) the ability of agents which increase intracellular [cAMP] to cause translocation of aquaporin to the cell surface was lost. If possible, it would be valuable to carry out similar work in VSMCs, to determine if the increase in glucose transport seen in response to the PDE 3 inhibitor, milrinone, was lost if the subcellular localisation of the appropriate PKAs was disrupted. This would allow us to determine if it is indeed a small localised increase in [cAMP] that is required to increase glucose transport in VSMCs.

Other work of interest to pursue is to investigate the mechanisms by which cGMP inhibit PDGF-stimulated glucose transport. It is known that VSMCs in culture do not express PKG, the cGMP activated kinase (Cornwell *et al.*, 1994). Therefore the effects of cGMP on PDGF-stimulated glucose transport must be mediated via some other mechanism, perhaps by direct inhibition of some of the signalling proteins required for PDGF-stimulated glucose transport. In this thesis, it has been shown that ANF (which will

generate cGMP, and is capable of inhibiting PDGF-stimulated glucose transport) does not affect PDGF's ability to stimulate p38 or p42/44 activity, therefore cGMP is not inhibiting PDGF-stimulated glucose transport at this level. The only other signalling molecule that has been shown to be involved in PDGF-stimulated glucose transport is PI3' kinase. The effects of cGMP on PI3' kinase activity in VSMCs have not yet been studied, and this would be a logical protein to investigate.

Although several difficulties were encountered in using the GLUT-1/GFP chimeras, with more time better use could have been made of these. For example, one of the biggest problems in using the N-terminal GLUT-1/GFP was that the degree of chimera associated with the plasma membrane was very variable. If the cells were expressing high levels of chimera there tended to be a higher degree of plasma membrane association. One way in which this problem may be overcome is if cells were stably transfected to express the chimera. This way cells could be selected that express a more moderate level of chimera and show an even intracellular distribution of chimera in basal/untreated cells, and the movement of the chimera would be more easy to follow and quantify.

## REFERENCES

- Aass H., Skomedal T. & Osnes J. *Molecular and Cellular Cardiology* **20**, 847-860 (1988).
- Backer J.M., Myers M.G., Sun X. *et al.* *Journal of Biological Chemistry* **268**, 8204-8212 (1993).
- Baldwin J.M., Baldwin J.M. & Leinhard G.E. *Biochemistry* **21**, 3837-3842 (1982).
- Barrett M.P., Walmisley A.R. & Gould G.W. *Current Opinion in Cell Biology* **11**, 496-502 (1999).
- Barros L.F., Marchant R.B. & Baldwin S.A. *Biochemical Journal* **309**, 731-736 (1995).
- Battagay E.J., Raines E.W., Seifert R.A., Bowen-Pope D.F. & Ross R. *Cell* **63**, 515-524 (1990).
- Benzakour O., Kanthou C., Kanse S.M., Scully M.F., Kakkar V. V., & Cooper D.N. *Thrombosis and Haemostasis* **75**, 854-858 (1996).
- Bobik A. & Campbell J.H. *Pharmacological Reviews* **45**, 1-42 (1993).
- Bolger G.B. *Cellular Signalling* **6**, 851-859 (1994).
- Bolger G.B., McPhee I. & Houslay M.D. *Journal of Biological Chemistry* **271**, 1065-1071 (1996).
- Bos J.L. *Trends in Biochemical Science* **20**, 441-442 (1995).

- Brant A.M., McCoid S.C., Thomas H.M., Davies A., Baldwin S.A., Parker J.C., Gibbs E.M. & Gould G.W. *Cellular Signalling* **4**, 641-650 (1992).
- Brüggermann A., Prado L.A., Stühmer W. & Pongs O. *Nature* **365**, 445-448 (1993).
- Burant C.F., Takeda J., Brot-Laroche E., Bell G.I. & Davidson G.Q. *Journal of Biological Chemistry* **267**, 14523-14526 (1992).
- Campbell G.R. & Campbell J.H. *Experimental Molecular Pathology* **42**, 139-162 (1985).
- Canos E. & Mahadevan L.C. *TIBS* **20**, 117-122 (1995).
- Carpenter C.L., Auger K.R., Chanudhuri M. *et al.* *Journal of Biological Chemistry* **268**, 9478-9483 (1993).
- Chamley-Campbell J.H., Campbell G.R. & Ross R. *Physiol. Reviews* **59**, 1-61 (1979).
- Chiche J., Schlutsmeier S.M., Bloch D.B., de la Monte S.M., Roberts Jr. J.D., Filippov G., Janssens S.P., Rosenzweig A. & Bloch K.D. *The Journal of Biological Chemistry* **273**, 34263-34271 (1998).
- Chinkers M., & Wilson E.M. *Journal of Biological Chemistry* **267**, 18589-18597 (1992).
- Chuang L.M., Hausdorff S.F., Myers M. Jr. *et al.* *Journal of Biological Chemistry* **269**, 27645-27649 (1994).
- Clarke J.F., Young P.W., Yonezawa K. *et al.* *Biochemical Journal* **300**, 631-635 (1994).
- Coffer P.J., Jing J., Woodgett J.R. *Biochemical Journal* **335**, 1-13 (1998).

- Colledge M. & Scott J.D. *Trends in Cell Biology* **9**, 216-221 (1999).
- Cornelius P., Marlowe M., Call K. & Pekala P.H. *Journal of Cellular Physiology* **146**, 298-308 (1991).
- Cornwell T.L., Soft G.A., Traynor A.E. & Lincoln T.M. *The Journal of Vascular Research* **31**, 330-337 (1994).
- Corvera S., & Czech M.P. *Trends in Cell Biology* **8**, 442-427 (1998).
- Cushman S.W. & Wardzala L.J. *Journal of Biological Chemistry* **255**, 4758-4762 (1980).
- Czech M.P., Clancy B.M., Pessino *et al.* *Biochemical Science* **17**, 197-201 (1992).
- Davidson N.O., Hausman A.M.L., Ifkovits C.A., Buse J.B., Gould G.W., Burant C.F. & Bell G.I. *Journal of Physiology* **262**, C795-C800 (1992).
- Davis R.J. *Trends in Biological Science* **19**, 470-473 (1994).
- de Jonge H.R. *Advances in Cyclic Nucleotide Research* **14**, 315-333 (1981).
- De Rooij J., Zwartkruis F.J.T., Verheijen M.H.G., Cool R.H., Nijman S.M.B., Wittinghofer A. & Bos J.L. *Nature* **396**, 474-477 (1998).
- Dell'Acqua M.L. & Scott J.D. *The Journal of Biological Chemistry* **272**, 12881-12884 (1997).
- DiFrancesco D. & Tortora P. *Nature* **351**, 145-147 (1991).
- Edelmann A.M., Blumenthal D.K. & Krebs E.G. *Annual Review of Biochemistry* **56**, 567-613 (1987).

- Egan S.E., Giddings B.W., Brooks M.W., *et al.* *Nature* **363**, 45-51 (1993).
- Evans J.L., Honer C.M., Wolmelsdorf B.F. *et al.* *Cellular Signalling* **0007**, 365-376 (1995).
- Fantl W.J., Johnson D.E. & Williams L.T. *Annual Review of Biochemistry* **62**, 453-481 (1993).
- Farese R.V., Rosic N., Standaert M. *et al.* *Diabetes* **35**, 951-957 (1986).
- Faux M.C. & Scott J.D. *Cell* **85**, 9-12 (1996).
- Fischer Y., Kamp J., Thomas J., Pöpping S., Rose H., Carpené C. & Kammermeier H. *American Journal of Physiology* **270**, C1211-1220 (1996).
- Fisher D.A., Smith J.F., Pillar J.S., St. Denis S.H. & Cheng J.B. *The Journal of Biological Chemistry* **273**, 15559-15564 (1998).
- Flier J.S., Muecklar M., McCall A. & Lodish H.F., *Journal of Clinical Investigation* **79**, 657-661 (1987).
- Francis S.H. & Corbin J.D. *Advances in Pharmacology* **26**, 115-170 (1994).
- Frost S.C. & Lane M.D. *Journal of Biological Chemistry* **260**, 2646-2652 (1985).
- Fujiwara R. & Nakai T. *Atherosclerosis* **127**, 49-57 (1996).
- Fukamoto H., Seino S., Imura H., Seino Y. & Bell G.I., *Diabetes* **37**, 647-661 (1988).
- Fukamoto H., Seino S., Imura H., Seino Y., Eddy R.L., Fukushima Y., Byers M.G., Shows T.B. & Bell G.I. *Proceedings of the National Academy of Science U.S.A.* **85**, 5434-5438 (1988).

- Gamm D.M., Francis S.H., Angelotti T.P., Corbin J.D. & Uhler M.D. *The Journal of Biological Chemistry* **270**, 27380-27388 (1995).
- Garbers D.L. & Lowe D.G. *The Journal of Biological Chemistry* **269**, 30741-30744 (1994).
- Garcia-Mata R., Bebok Z., Sorscher E.J. & Sztul E.S. *Journal of Cell Biology* **146**, 1239-1254 (1999).
- Gibbs A.F., Chapman D. & Baldwin S.A. *Biochemical Journal* **256**, 421-427 (1988).
- Gibbs E.M., Lienhard G.E. & Gould G.W. *Biochemistry* **27**, 6681-6685 (1988).
- Girotti M. & Banting G. *Journal of Cell Science* **109**, 2915-2926 (1996).
- Gonzales-Crussi F. *American Journal of Anatomy* **130**, 441-460 (1971).
- Gould G.W., Brant A.M., Kahn B.B., Shepherd P.R., McCoid S.C. & Gibbs E.M. *Diabetologia* **35**, 304-309 (1992).
- Gould G.W. & Holman G.D. *Biochemical Journal* **295**, 329-341 (1993).
- Gould G.W., Jess T.J., Andrews G.C., Herbst J.J., Plevin R.J. & Gibbs E.M. *Journal of Biological Chemistry* **269**, 26622-26625 (1994).
- Gould G.W., Cuenda A., Thomson F.J., Cohen P. *Biochemical Journal* **311**, 735-738 (1995).
- Gould G.W. In: *Facilitative Glucose Transporters, Molecular Biology Intelligence Unit*. pp10-12 (1997).

- Heil W.G., Landgraf W. & Hofmann F. *European Journal of Biochemistry* **168**, 117-121 (1987).
- Hempel C.M., Vincent P., Adams S.R., Tsien R.Y. & Selverston A.I. *Nature* **384**, 166-169 (1996).
- Hiraki Y., Rosen O.M. & Birnbaum M.J. *Journal of Biological Chemistry* **263**, 13655-13662 (1988).
- Hobbs A.J. *Trends in Pharmacological Science* **18**, 484-491 (1997).
- Holman G.D. & Kasuga M. *Diabetologia* **40**, 2990-1003(1997)
- Horowitz A., Menice C.B., Laporte R. & Morgan K.G. *Physiological Reviews* **76**, 967-1003 (1996).
- Hosaka Y., Tawata M., Kurihara A., Ohtaka M., Endo T. & Onaya T. *Endocrinology* **131**, 159-165 (1992).
- Houslay M.D. and Milligan G. *Trends in Biological Sciences* **22**, 217-224 (1997).
- Hurley J.H. *Current Opinion in Structural Biology* **8**, 770-777 (1998).
- Iyengar R. *FASEB Journal* **7**, 768-775 (1993).
- Jarchau T., Hausler C., Markert T., Pohler D., Vandekerckhove J., de Jonge H.R., Lohmann S.M. & Walter U. *Proceedings of the National Academy of Sciences U.S.A.* **91**, 9426-9430 (1994).
- Johnson R.A., Alvarez R. & Salomon Y. *Methods in Enzymology* **238**, 31-56 (1994).
- Johnston J.A., Ward C.L. & Kopito R.R. *Journal of Cell Biology* **143**, 1883-1898 (1998).



Jung C.Y. *Journal of Membrane Biology* **5**, 200-214 (1971).

Jurevičius J. & Fischmeister R. *Proceedings of the National Academy of Science U.S.A.* **93**, 295-299 (1996).

Kacther C. & Gerdes H. *FEBS Letters* **369**, 267-271 (1995).

Katsura T., Gustafson C.E., Ausiello D.A. & Brown D. *American Journal of Physiology* **272**, F816-F822 (1997).

Kayano T., Burant C.F., Fukumoto II., Gould G.W., Fan Y.S., Eddy R.L., Byers M.G., Shows T.B., Seino S. & Bell G.I. *Journal of Biological Chemistry* **265**, 13276-13282 (1990).

Kemp B.E. & Pearson R.B. *Trends in Biological Science* **15**, 342-347 (1990).

Kihara S., Ouchi N., Funahashi T., Shinohara E., Tamura R., Yamashita S. & Matsuzawa Y. *Atherosclerosis* **136**, 163-168 (1998).

Kitagawa K., Nishino H. & Iwashima A. *Biochim. Biophys. Acta.* **887**, 100-104 (1986).

Kitagawa T., Tanaka M. & Akamatsu Y. *Biophys. Acta.* **980**, 100-108 (1989).

Klussmann E., Maric K., Wiesner B., Beyermann M. & Rosenthal W. *The Journal of Biological Chemistry* **274**, 4934-4938 (1999).

Kohn A.D., Summers S.A., Birnbaum M.J. & Roth A. *Journal of Biological Chemistry* **271**, 31372-31378 (1996).

Komalavilas P. & Lincoln T.M. *The Journal of Biological Chemistry* **269**, 8701-8707 (1994).

Komalavilas P. & Lincoln T.M. *The Journal of Biological Chemistry* **271**, 21933-21938 (1996).

Kronemann N., Nockher W.A., Busse R. & Schini-Kerth V.B. *British Journal of Pharmacology* **126**, 349-357 (1999).

Kuhne M.R., Pawson T., Leinhard G.E. *et al.*, *Journal of Biological Chemistry* **268**, 21478-21481 (1993).

Kumar R., Cartledge W.A., Lincoln T.M. & Pandey K.N. *Hypertension* **29**, 414-421 (1997).

Landgraf W., Ruth P., Keilbach A., May B., Welling A. & Hofmann F. *Journal of Cardiovascular Pharmacology* **20**, S18-S22 (1992).

Lazar D.F., Wiese R.J., Brady M.J. *et al.* *Journal of Biological Chemistry* **270**, 20801-20807 (1995).

Ledoux S., Dussaule J., Chatziantoniou C., Ardaillou N., Vandermiersch S. & Ardaillou R. *American Journal of Physiology* **272**, C82-C89 (1997).

Leevers S.J., Vanhaesbroeck B. & Waterfield M.D. *Current Opinion in Cell Biology* **11**, 219-225 (1999).

Lemmon M.A., Falasca M., Ferguson K.M. & Schlessinger J. *Trends in Cell Biology* **7**, 237-242 (1997).

Libby P., Warner S.J.C., Salomon R.N. & Birinyi L.K. *New England Journal of Medicine* **318**, 1493-1498 (1988).

Lin M.C., Almus-Jacobs F., Chen H.H. *et al.* *Journal of Clinical Investigation* **99**, 737-744 (1997).

- Lönnroth P., Davies J.I., Lönnroth I. & Smith U. *Biochemical Journal* **243**, 789-795 (1987).
- MacEwan D.J., Kim G.D. & Milligan G. *Molecular Pharmacology* **48**, 316-325 (1995).
- MacEwan D.J. & Milligan G. *Molecular Pharmacology* **50**, 1479-1486 (1996).
- Magun R., Burgering B.M., Coffey P.J., Pardasani D., Lin Y., Charbot J. & Sorisky A. *Endocrinology* **137**, 3590-3593 (1996).
- Manganiello V.C., Murata T., Taira M., Belfrage P. & Degerman E. *Archives of Biochemistry and Biophysics* **322**, 1-13 (1995).
- McPhee I., Pooley L., Lobban M., Bolger G. & Houslay M.D. *Biochemical Journal* **310**, 965-974 (1995).
- Merrall N., Wakelam M.J.O., Plevin *et al.* *Biochim. Biophys. Acta.* **1117**, 191-198 (1993).
- Merrall N.W., Plevin R.J., Stokoe D. *et al.* *Biochemical Journal* **295**, 351-355 (1993).
- Milligan G. *TIPS* **14**, 239-243 (1993).
- Mosse P.R.L., Campbell G.R., Wang Z.L. & Campbell J.H. *Laboratory Investigation* **53**, 556-562 (1985).
- Moughal N., Stevens P.A., Kong D., Pyne S. & Pyne N.J. *Biochemical Journal* **306**, 723-726 (1995).
- Moule S.K. & Denton R.M. *FEBS Letters* **439**, 287-290 (1998).

Mukhopadhyay S., Webster C.R.L., Anwer M.S. *The Journal of biological Chemistry* **273**, 30039-30045 (1998).

Muekler M., Caruso C., Baldwin S.A. *et al.Science* **229**, 941-945 (1985).

Muñiz M., Alonso M., Hidalgo J. & Velasco A. *The Journal of Biological Chemistry* **271**, 30935-30941 (1996).

Murray K.J. *Pharmacol. Ther.* **47**, 329-345 (1990).

Murthy K.S., Severi C., Griders J.R. & Makhlouf G.M. *American Journal of Physiology* **264**, G967-G974 (1993).

Murthy K.S.& Makhlouf G.M. *American Journal of Physiology* **286**, C171-180 (1995).

Myers M.J., Backer J., Sun X. *et al. Proceedings of the National Academy of Science U.S.A.* **89**, 10350-10354 (1992).

Myers M,Jr., Wang L.M., Sun X.J. *et al. Cellular Biology* **14**, 3577-3587 (1994).

Nagamatsu S., Kornhauser J.M., Burant C.F., *et al. Journal of Biological Chemistry* **267**, 467-472 (1992).

Nakashima Y., Raines E.W., Plump A.S., Breslow J.L., Ross R. *Arterioscler Thromb Vasc Biol* **18**, 842-851 (1998).

Napoli C., D'Armiento F.P., Mancini F.P., *et al.Journal of Clinical Investigation* **100**, 2680-2690 (1997).

Nave B.T., Haigh R.J., Hayward A.C., Siddle K. & Shepherd P.R. *Biochemical Journal* **318**, 55-60 (1996).

Niwa H., Inouye S., Hirano T., Matsuno T., Kojima S., Kubota M., Ohashi M. & Tsui F.I. *Proceedings of the National Academy of Science U.S.A.* **93**, 13617-13622 (1996).

O'Connell J.C., McCallum J.F., McPhee I., Wakefield J.M., Houslay F.S., Wishart W., Bolger G., Frame M. & Houslay M.D. *Biochemical Journal* **318**, 255-262 (1996).

Patki V., Lawe D.C., Corvera S., Virbasius J.V. & Chawla A. *Nature* **394**, 433-434 (1998).

Pawson T. & Gish G.D *Cell* **71**, 359-362 (1992).

Piper R.C., James D.E., Slot J.W., Puri C. & Lawrence Jr. J.C. *The Journal of Biological Chemistry* **268**, 16557-16563 (1993).

Polson J.B. & Strada S.J. *Annual Review of Pharmacology and Toxicology* **36**, 403-27 (1996).

Pyne N. J., Moughal N., Stevens P.A., Tolan D. & Pyne S. *Biochemical Journal* **304**, 611-616 (1994).

Pyne N.J. & Pyne S. *Cell Signalling* **10**, 363-369 (1998).

Quinn L.A. & McCumbee W.D. *Journal of Cellular Physiology* **177**, 94-102 (1998).

Quinn M.T., Parthasarathy S., Fong I.G. & Steinberg D., *Proceedings of the National Academy of Science U.S.A* **84**, 2995-2998 (1987).

Resnick N., Collins T., Atkinson W., Bonthron D.T., Dewey C.F. Jr., Gimbrone M.A. Jr. *Proceedings of the National Academy of Science USA* **90**, 4591-4595 (1993).

Rizzuto R., Brini M., Pizzo P., Murgia M. & Pozzan T. *Current Biology* **5**, 635-642 (1995).

- Rollins B.J., Morrison E.D., Usher P., *et al.* *Journal of Biological Chemistry* **263**, 16523-16526 (1988).
- Rönnstrand L., Mori S., Arridsson A-K., *et al.* *EMBO* **11**, 3911-3919 (1992).
- Ross R. & Glomset J.A. *Science* **180**, 1332-1339 (1973).
- Ross R. & Glomset J.A. *New England Journal of Medicine* **296**, 369-377 and 420-425 (1976).
- Ross R. *Nature* **362**, 801-809 (1993).
- Ross R. *New England Journal of Medicine* **340**, 115-126 (1999).
- Rubin C.S., *Biochimica et Biophysica Acta* **1224**, 467-479 (1994).
- Sakaue M., Bowtell D. & Kasuga M. *Molecular and Cellular Biology* **15**, 379-388 (1995).
- Saxena M., Williams S., Tasken K. & Mustelin T. *Nature Cell Biology* **1**, 305-311 (1999).
- Schmidt W., Poll-Jordon G. & Löffler G. *The Journal of Biological Chemistry* **265**, 15489-15495 (1990).
- Schwartz S.M., Heimark R.L. & Majesky M.W. *Physiology Review* **70**, 1177-1209 (1990).
- Shanahan M.F. & Edwards B.M. *Endocrinology* **125**, 1074-1081 (1989).
- Shepherd P.R., Gibbs E.M., Waslau C. *et al.* *Diabetes* **41**, 1360-1365 (1992).
- Shimizu Y., Satoh S., Yano H., Minokoshi Y., Cushman S.W. & Shimazu T. *Biochemical Journal* **330**, 397-403 (1998).

- Sjölund M., Hedin U., Sejersen T., Heldin C-H. & Thyberg J. *Journal of Cellular Biology* **106**, 403-413 (1988).
- Skolnik F. Y., Batzer A., Li N. *et al. Science* **260**, 1953-1955 (1993).
- Smit M.J. & Iyengar R. *Advances in Second Messenger and Phosphoprotein Research* **32**, 1-21 (1998).
- Smit M.J., Verzijl D. & Iyengar R. *Proceedings of the National Academy of Science U.S.A.* **95**, 15084-15089 (1998).
- Soderling S.H., Bayuga S.J. & Beavo J.A. *Proceedings of the National Academy of Sciences U.S.A.* **95**, 8991-8996 (1998).
- Soderling S.H., Bayuga S.J. & Beavo J.A. *The Journal of Biological Chemistry* **273**, 15553-15558 (1998).
- Soderling S.H., Bayuga S.J. & Beavo J.A. *Proceedings of the National Academy of Sciences U.S.A.* **96**, 7071-7076 (1999).
- Sorbara L.R., Davies-Hill T.M., Koehler-Stec E.M., Vannucci S.J., Horne M.K. & Simpson I.A. *Biochemical Journal* **328**, 511-516 (1997).
- Sowers J.R. *Diabetes* **45**, supp.3, S47-S51 (1996).
- Stanley P.R., Ram J.L. & Sowers J.R. *Endocrinology* **133**, 1693-1699 (1993).
- Stary H.C., Chandler A.B., Glagov S., *et al. Circulation* **89**, 2462-2478 (1994).
- Stenmark H. Aasland R., Toh B.H. & D'Arrigo A. *Journal of Biological Chemistry* **271**, 24048-24054 (1996).

- Sternweis P.C. *Current Opinion in Cell Biology* **6**, 198-203 (1994).
- Suhasini M., Li H., Lohmann S.M., Boss G.R., Pilz R.B. *Molecular and Cellular Biology* **18**, 6983-6994 (1998).
- Sun X.J., Rothenberg P., Kahn C.R., *et al.*, *Nature* **352**, 73-77 (1991).
- Sun X.J., Wang L-M., Zhang Y. *et al.* *Nature* **377**, 173-177 (1995).
- Suzuki K. & Kono T. *Proceedings of the National Academy of Science U.S.A.* **77**, 2542-2545 (1980).
- Taylor S.S., Buechler J.A. & Yonemoto W. *Annual Review of Biochemistry* **59**, 971-1005 (1990).
- Tesmer J.J.G. & Sprang S.R. *Current Opinion in Structural Biology* **8**, 713-719 (1998).
- Thomson F.J., Moyes C., Scott P.H., Plevin R. & Gould G.W. *Biochemical Journal* **316**, 161-166 (1996).
- Thomson F. & Gould G.W. *In: Facilitative Glucose Transporters, Molecular Biology Intelligence Unit*. Pp197-217 (1997).
- Thorens B., Sarker H.K., Kaback H.R. *et al.* *Cell* **55**, 281-290 (1988).
- Thorens B., Dériaz N., Bosco D., DeVos A., Pipeleers D., Schuit F., Meda P. & Porret A. *The Journal of Biological Chemistry* **271**, 8075-8081 (1996).
- Toyoshima H., Nasa Y., Hashizume Y., Koscki Y., Isayama Y., Kohsaka Y., Yamada T. & Takeo S. *Journal of Cardiovascular Pharmacology* **32**, 543-551 (1998).



- Tsien R.Y. *Annual Review of Biochemistry* **67**, 509-544 (1998).
- Verhey K.J., Hausdorf S.F. & Birnbaum M.J. *Journal of Biological Chemistry* **123**, 137-147 (1993).
- Waddell I.D., Zomerschoe A.G., Voice M.W. & Burchell A. *Biochemical Journal* **286**, 173-177 (1992).
- Walmsley A.R., Barrett M.P., Bringaud F. & Gould G.W. *Trends in Biological Sciences* **23**, 476-480 (1998).
- Walter U. *Rev. Physiol. Biochem. Pharmacol.* **113**, 42-85 (1989).
- Watson S. & Arkinstall S. *In: The G-protein Linked Receptor*, Academic Press Ltd. (1994).
- Wiese R.J., Mastick C.C., Lazar D.F. *et al. Journal of Biological Chemistry* **270**, 3442-3446 (1995).
- Witters L.A., Vater C.A. & Leinhard G.E. *Nature* **315**, 777-778 (1985).
- Wolfe L., Corbin J.D. & Francis S.H. *Journal of Biological Chemistry* **264**, 7734-7741 (1989).
- Wong Y.H. *Methods in Enzymology* **238**, 81-94 (1994).
- Wusmer A.E., Gary J.D. & Emr S.D. *The Journal of Biological Chemistry* **274**, 9129-9132 (1999).
- Yao H., York R.D., Misra-Press A., Carr D.W. & Stork P.J.S. *The Journal of Biological Chemistry* **273**, 8240-8247 (1998).

Yarwood S.J., Anderson N.G. & Kilgour E. *Biochemical Society Transactions* **23**, S175 (1995).

Yarwood S.J., Kilgour E. & Anderson N.G. *Biochemical and Biophysical Research Communications* **224**, 734-739 (1996).

